

# **Role of Pathogenic Antibodies in Rheumatic Diseases**

## **Dissertation**

zur Erlangung des akademischen Grades eines

Doktors der Naturwissenschaften

an der Universität Konstanz

Fakultät für Biologie



Vorgelegt von

**Subhasis Mohanty**

Konstanz, im Januar 2003

**Dissertation Referees:**

Prof. Dr. Rolf Knippers (Chair, Molecular Genetics)

Priv. Doz. Dr. Harald Illges (Immunology)

Faculty of Biology, University of Konstanz, Germany

**Date of Oral Examination: 14th May 2003**

Prof. Dr. Rolf Knippers (Molecular Genetics)

Prof. Dr. Wolfram Welte (Biochemistry)

Priv. Doz. Dr. Harald Illges (Immunology)

*In Memory of “Baba & Mama”*

## ACKNOWLEDGEMENTS

It was a unique opportunity to come to Germany for my Doctoral work at University of Konstanz. I am grateful to my research supervisor PD Dr. Harald Illges for inviting me to carry out research in his group and providing me financial support throughout this study. I am thankful to him for his guidance, constant encouragement and most importantly his confidence in me without which this thesis would not have been possible. His interest and enthusiasm in organizing summer and winter retreats to “Wild Haus”, “Tanheimer Taal” and “Hoch Ybrig” will be always remembered.

I take this opportunity to extend my special thanks to Prof. Dr. Rolf Knippers for being my doctoral father and for his guidance and care through this study.

My sincere thanks to Prof. Dr. Marcus Groettrup for his support and advice.

I am grateful to Prof. Dr. Wolfram Welte for his kind consent to take my oral examination.

I am grateful to Prof. Dr. Peter Kroneck and Prof. Dr. Sandro Ghisla for their guidance and encouragement during spectroscopic measurements. My sincere thanks are due to members of AG Ghisla for their help and cooperation.

I would like to take this opportunity to thank Dr. Cornelia Kolb for her excellent suggestions and guidance for transgenic mice experiments.

My special thanks to Brigitte Schanze for her help, assistance and excellent office management.

I thank Elisabeth Naidoo and Ulrike Beck for their cooperation and technical support.

My special thanks to Dr. Andreas Richter, Atef Allam, Alex Tiz, Radek, Markus, Torsten, Birgit, Tanya, Dr. Hua Sen and Joerg, all former members of the Lab.

I would like to thank my Lab colleagues at University of Konstanz, Joerg Schwab, Samuel Solomon, Dr. Madhan Masilamani, Lawrence, Narendiran Rajasekaran, Daniela Kassahn and at BiTg, Thurgau, Switzerland, Annette Aichem, Eva Maria Boneberg, Melanie Hofer, Vera Klett, Elisabeth von Seydlitz and Elvira Jeisy for their company and cooperation.

Finally I take this opportunity to thank members of TFA, University of Konstanz for excellent animal facility. My special thanks to Andrea who took care of all the transgenic mice lines, I used for my research.

---

---

## CONTENTS

<b>CHAPTER I: Introduction</b> .....	<b>1</b>
1.1. Autoimmune rheumatic diseases .....	1
1.1.1. Rheumatoid arthritis .....	4
1.1.2. Cryoglobulinemic vasculitis .....	9
1.1.3. Cryoglobulinemia .....	10
1.2. Self and Non- self: Immunological tolerance .....	11
1.3. Regulation of immunity by complement and complement receptors .....	13
1.3.1. Generation of C3b from C3 .....	14
1.3.2. Initiation alternative pathway .....	15
1.3.3. Initiation of classical pathway .....	15
1.3.4. Initiation of lectin pathway .....	16
1.3.5. Formation of C5 convertase .....	17
1.3.6. Regulation of complement activation .....	17
1.3.7. Complement receptor 1 (CR1 or CD35) .....	18
1.3.8. Complement receptor 2 (CR2 or CD21) .....	19
1.4. Pain in Arthritis: A neuroendocrine connection .....	19
1.4.1. Substance P and related neuropeptides in joint inflammation .....	20
<b>CHAPTER II: Materials and Methods</b> .....	<b>22</b>
2.1. Mouse strains .....	22
2.1.1. KRN Transgenic mouse strain .....	22
2.1.2. C57BL/6 (B6) mouse strain .....	22
2.1.3. NOD/Lt mouse strain .....	23
2.1.4. Cr2 <sup>-/-</sup> mouse strain .....	23
2.1.5. Balb/c mouse strain .....	23
2.1.6. K/BxN and BxN mouse strain .....	24
2.1.7. SP <sup>-/-</sup> Mouse strain .....	24
2.2. Breeding experiments .....	24
2.3. Ankle thickness measurement .....	25
2.4. Locomotor activity measurement .....	25
2.5. Immunological methods .....	26

---

---

2.5.1. Fluorescence Activated Cell Sorting (FACS) .....	26
2.5.2. ELISA .....	27
2.5.3. Immunoblot .....	28
2.5.3.1. Western blot .....	28
2.5.3.2. Dot blot .....	30
2.6. Histology .....	30
2.6.1. Tissue fixation .....	30
2.6.2. Decalcification .....	31
2.6.3. Hematoxylin and Eosin staining .....	31
2.6.4. Toluidine Blue staining .....	32
2.7. Skeletal preparation .....	32
2.8. Survival frequency test .....	33
2.9. Chemical sympathectomy .....	33
2.9.1. Transient sympathectomy .....	33
2.9.2. Permanent sympathectomy .....	34
2.10. Induction of arthritis by K/BxN serum transfer .....	34
2.11. Protein purification .....	35
2.11.1. Purification of cryoglobulin .....	35
2.11.2. Protein G affinity chromatography .....	35
2.11.3. Fast Performance Liquid Chromatography .....	36
2.11.4. SDS PAGE .....	37
2.12. Spectroscopy .....	38
2.12.1. UV/Vis- Spectroscopy .....	38
2.12.2. Kinetics experiments .....	39
<b>CHAPTER III: Results .....</b>	<b>41</b>
3.1. Contribution of <i>Cr2</i> gene in murine autoimmune arthritis .....	41
3.1.1. Generation of mice lines .....	41
3.1.1.1. Generation of $Cr2^{-/-}$ KRN mouse line .....	42
3.1.1.2. Generation of $Cr2^{-/-}$ NOD mouse line .....	44
3.1.1.3. Generation of $Cr2^{-/-}$ K/BxN and $Cr2^{-/-}$ BxN mouse lines .....	46

---

---

3.1.2. Emergence of auto-reactive CD4 <sup>+</sup> Vβ6 <sup>+</sup> T cell clones in Cr2 <sup>-/-</sup> K/BxN mouse strain .....	47
3.1.3. High levels of anti-GPI antibodies in Cr2 <sup>-/-</sup> K/BxN mouse strain .....	49
3.1.4. The Cr2 <sup>-/-</sup> K/BxN mouse strain is susceptible to arthritis development ..	50
3.1.4.1. Clinical onset of arthritis: Ankle swelling in Cr2 <sup>-/-</sup> K/BxN mouse strain .....	51
3.1.4.2. Locomotor Activity of Cr2 <sup>-/-</sup> K/BxN mouse strain .....	52
3.1.4.3. Histological assessment of joint destruction in the Cr2 <sup>-/-</sup> K/BxN mouse strain .....	54
3.1.4.4. Growth in Cr2 <sup>-/-</sup> K/BxN mouse strain is impaired due to arthritis ..	59
3.1.5. Cr2 <sup>-/-</sup> K/BxN mouse strain has decreased survival in acute phase of arthritis .....	61
3.1.6. Transient Sympathectomy partially protects Balb/c mice from antibody-induced arthritis .....	62
3.1.7. Permanent sympathectomy protects Balb/c mice from antibody-induced arthritis .....	64
3.1.8. SP <sup>-/-</sup> mouse strain is partially protected from antibody-induced arthritis .....	66
3.2. Molecular analysis of cryoglobulins .....	68
3.2.1. Purification of cryoglobulins .....	68
3.2.2. Immunoblot analysis of cryoglobulins .....	70
3.2.3. Gelfiltration analysis of Type I cryoglobulins .....	72
3.2.4. Protein sequence analysis of type I cryoglobulin .....	75
3.2.5. Temperature induced reversible precipitation of cryoglobulins .....	77
3.2.6. Cryoprecipitation is concentration dependent .....	78
3.2.7. Osmolytes lower the threshold temperature for cryoprecipitation .....	80
3.2.7.1. Effect of Sarcosine on cryoprecipitation .....	81
3.2.7.2. Effect of TMAO on cryoprecipitation .....	82
3.2.8. Chemical chaperone “Cyclodextrin” protects Immunoglobulins from cryoprecipitation .....	84

---

---

<b>CHAPTER IV: Discussion</b> .....	<b>89</b>
4.1. Emergence of auto reactive T cells in the periphery of K/BxN and Cr2 <sup>-/-</sup> K/BxN mice .....	89
4.2. Lack of or incomplete tolerance results in high levels of GPI specific auto antibodies in Cr2 <sup>-/-</sup> K/BxN mice serum .....	90
4.3. Rapid and aggressive destruction of joints in Cr2 <sup>-/-</sup> K/BxN mice .....	92
4.4. Growth retardation in Cr2 <sup>-/-</sup> K/BxN Mice .....	93
4.5. Sympathetic Nervous System and antibody-induced arthritis .....	95
4.6. IgG1/IgG3 Cryoglobulin suggesting lack of allelic exclusion .....	97
4.7. Cryoprecipitation is the outcome of a cooperative intermolecular interaction .....	100
4.8. Osmolytes and the chemical chaperon cyclodextrin prevent cryoprecipitation .....	100
<b>CHAPTER V: Summary</b> .....	<b>102</b>
<b>CHAPTER VI: ZUSAMMENFASSUNG</b> .....	<b>105</b>
<b>CHAPTER VII: References</b> .....	<b>109</b>

---

## FIGURES

<b>Figure 1.</b> A graphic presentation of the normal joint (A) and RA joint (B)	5
<b>Figure 2.</b> Schematic representation of immunopathological processes in Rheumatoid Arthritis. Obtained from “Autoimmune Rheumatic Diseases”, by Morrow J. et al., second edition, Oxford University Press .....	6
<b>Figure 3.</b> Peripheral blood lymphocytes from KRN TCR transgene positive and negative mouse stained for CD4 and Vb6 .....	42
<b>Figure 4.</b> Breeding scheme for the generation of the <b>Cr2<sup>-/-</sup> KRN<sup>+/-</sup></b> mouse line .	43
<b>Figure 5.</b> Peripheral blood lymphocytes from Cr2 <sup>+/+</sup> and Cr2 <sup>-/-</sup> mouse stained for B220 and CD21 .....	43
<b>Figure 6.</b> Breeding scheme for generation of <b>Cr2<sup>-/-</sup>-NOD (Cr2<sup>-/-</sup> H-2g<sup>7+/+</sup>)</b> mouse line .....	45
<b>Figure 7.</b> Peripheral blood lymphocytes from Cr2 <sup>-/-</sup> H-2g <sup>7+/+</sup> and Cr2 <sup>-/-</sup> H-2g <sup>7+/-</sup> mice with B220-PE & I-A <sup>d</sup> -FITC as well as B220-PE & I-AbAβ -FITC .....	45
<b>Figure 8.</b> Breeding scheme for the generation of <b>Cr2<sup>-/-</sup>-K/BxN and Cr2<sup>-/-</sup>-BxN</b> mouse lines .....	46
<b>Figure 9.</b> Peripheral blood lymphocytes of Cr2 <sup>-/-</sup> -K/BxN (upper row) and Cr2 <sup>-/-</sup> -BxN (lower row) mice stained for CD4 and Vβ6 .....	48
<b>Figure 10.</b> Peripheral blood lymphocytes of K/BxN (upper row) and BxN (lower row) mice stained for CD4 and Vβ6 .....	49
<b>Figure 11.</b> Anti-GPI IgG levels in the sera of Cr2 <sup>-/-</sup> -K/BxN and K/BxN mouse at different ages .....	50
<b>Figure 12.</b> Average ankle thickness (A) and Clinical Index (B) of sick Cr2 <sup>-/-</sup> -K/BxN, sick K/BxN mice and their healthy litter mate controls at different ages .....	52
<b>Figure 13.</b> Assessment of locomotor activity of sick Cr2 <sup>-/-</sup> -K/BxN, sick K/BxN mice and their healthy littermate controls. (A) shows walking and (B) shows climbing behavior .....	53

---

<b>Figure 14.</b> Eosin and Hematoxylin stained sections of ankle joints at different ages of K/BxN and Cr2 <sup>-/-</sup> K/BxN mice. Sections (a-c under 10x) & (d-f under 40x) of K/BxN mice and sections (A-C under 10x) & (D-F under 40x) of Cr2 <sup>-/-</sup> K/BxN mice show joint structure at different stages of disease. Sections (g-i under 40x) of K/BxN and (G-I under 40x) of Cr2 <sup>-/-</sup> K/BxN mice show chondrocytes at growth plate region at different stages of disease.....	56
<b>Figure 15.</b> Toluidine blue staining of ankle joints at different ages of K/BxN and Cr2 <sup>-/-</sup> K/BxN mice. Sections (a-c) of K/BxN and sections (A-C) of Cr2 <sup>-/-</sup> K/BxN mice show proteoglycan staining in articular cartilage at different stages of disease. Sections (d-f) of K/BxN and sections (D-F) of Cr2 <sup>-/-</sup> K/BxN mice show proteoglycan staining in growth plate region .....	58
<b>Figure 16.</b> Eosin and Hematoxylin stained sections showing infiltrating neutrophils and pannus formation in late stage of disease in K/BxN and Cr2 <sup>-/-</sup> K/BxN mice .....	59
<b>Figure 17.</b> Skeletal preparation of hind limbs of K/BxN, Cr2 <sup>-/-</sup> K/BxN and control mice at six months of age. Paw, ankle and knee joints are mostly affected. Small size hind limb of Cr2 <sup>-/-</sup> K/BxN mouse represents growth retardation .....	60
<b>Figure 18.</b> Survival Plot of K/BxN, Cr2 <sup>-/-</sup> K/BxN and their healthy litter mates. Cr2 <sup>-/-</sup> K/BxN mice have reduced survival during acute phase of Arthritis .....	61
<b>Figure 19.</b> Western Blot analysis of Tyrosine Hydroxylase in spleen of 6-OHDA treated mice and control mice. Lane (1) permanently sympathectomised mice, lane (2) vehicle (ascorbate) treated mice and lane (3) transiently sympathectomised mice .....	63
<b>Figure 20.</b> Average ankle thickness (a) and clinical Index (b) of transiently sympathectomised Balb/c and control Balb/c mice. A & B represents Balb/c mice treated with PBS, C & D represent transiently sympathectomized Balb/c mice treated with 100µl of K/BxN serum and E & F represents control Balb/c mice treated with 100µl of K/BxN serum .....	64

---

---

<b>Figure 21.</b> Average ankle thickness (a) and clinical Index (b) of permanently sympathectomized Balb/c and control Balb/c mice. A & B represents Balb/c mice treated with PBS, C & D represents permanently sympathectomized Balb/c mice treated with 100µl of K/BxN serum and E &F represents control Balb/c mice treated with 100µl of K/BxN serum .....	65
<b>Figure 22.</b> Average ankle thickness (a) and clinical Index (b) of SP <sup>-/-</sup> mice, C57BL/6 mice control mice .....	66
<b>Figure 23.</b> SDS-PAGE analysis of type I cryoglobulin KCR purified from human serum. The Coomassie stained gel shows bands under non-reducing and reducing conditions .....	69
<b>Figure 24.</b> SDS-PAGE analysis of type I cryoglobulin NCR purified from human serum (lane 2) and Human myeloma protein IgG1 (lane 1). Coomassie stained gels show bands under reducing condition .....	69
<b>Figure 25.</b> Immunoblot analysis of type I cryoglobulin KCR. 65 kDa and 51 kDa bands corresponding to two IgG heavy chains detected by anti-human IgG antibody (lane a) and all three bands detected by anti-human whole Ig antibody (lane b) .....	70
<b>Figure 26.</b> Immunoblot analysis of the type I cryoglobulin KCR in comparison with purified human myeloma protein IgG1 and normal human serum. Gamma 1 chain of cryoglobulin detected by anti-human IgG1 antibody (lane a), human myeloma protein IgG1 detected by the same anti-human IgG1 antibody (lane b), cryoglobulin IgG3 chain detected by anti-human IgG3 antibody (lane c) and IgG3 chain detected in normal human serum by the same anti-human IgG3 antibody (lane d) .....	71
<b>Figure 27.</b> Immunoblot analysis of type I cryoglobulin NCR in comparison with human myeloma protein IgG1. Myeloma protein IgG1 (lane1) and cryoglobulin (lane 2) stained with anti-human IgG1 antibody. Cryoglobulin (lane 3) and myeloma protein IgG1 (lane 4) stained with anti-human IgG3 antibody .....	72

---

---

<b>Figure 28.</b> FPLC profile of the type I cryoglobulin KCR. Superdex-200HR gel filtration column splits the cryoglobulin complex (A) into major peak and a minor peak (shoulder) and the later shows the same mobility as purified myeloma IgG3-kappa (B) and IgG1-kappa (C) control proteins .....	73
<b>Figure 29.</b> FPLC profile of the type I cryoglobulin KCR after treatment with 6M guanidinium hydrochloride (A). Immunoblot analysis of the samples collected from peak 1 and peak 2 in serial dilution using isotype specific antibodies against human IgG3 and IgG1 (B) .....	74
<b>Figure 30.</b> Peptide sequencing of the cryoglobulin KCR chains. Alignment of the peptide sequences of IgG3 heavy chain with that C-region V <sub>H</sub> 4 germline gene sequences (A), of the IgG1 heavy chain with the C-region and the V <sub>H</sub> 3 germline sequences (B) and of Igκ light chain with that of VκIII-L2 germline sequences (C). Dashes indicate identities .....	76
<b>Figure 31.</b> Effect of temperature on cryoprecipitation. Optical density measured at 600nm in a spectrophotometer while incubating the sample alternating at 37°C and 4°C. Y-axis represents the change in O.D <sub>600nm</sub> value due to turbidity in the medium upon cryoprecipitation .....	77
<b>Figure 32.</b> Effect of cryoglobulin KCR concentration on cold induced precipitation. Change in O.D <sub>600nm</sub> as a function of temperature (A). Threshold temperature (T <sub>m</sub> ) versus concentration (B) .....	78
<b>Figure 33.</b> Effect of cryoglobulin NCR concentration on cold induced precipitation. Change in O.D <sub>600nm</sub> as a function of temperature (A). Threshold temperature (T <sub>m</sub> ) versus concentration (B) .....	79
<b>Figure 34.</b> Effect of Sarcosine on Cryoprecipitation. Change in O.D <sub>600nm</sub> of Cryoglobulin KCR at increasing concentrations of Sarcosine (A). Threshold temperature (T <sub>m</sub> ) as function of sarcosine concentration (B) .....	81
<b>Figure 35.</b> Effect of Sarcosine on Cryoprecipitation. Change in O.D <sub>600nm</sub> of Cryoglobulin (NCR) at increasing concentrations of Sarcosine (A). Threshold temperature (T <sub>m</sub> ) as function of sarcosine concentration (B) .....	82

---

---

<b>Figure 36.</b> Effect of TMAO on Cryoprecipitation. Change in O.D <sub>600nm</sub> of Cryoglobulin KCR at increasing concentrations of TMAO (A). Threshold temperature (T <sub>m</sub> ) as function of TMAO concentration (B) .....	83
<b>Figure 37.</b> Effect of TMAO on Cryoprecipitation. Change in O.D <sub>600nm</sub> of Cryoglobulin. NCR at increasing concentrations of TMAO (A). Threshold temperature (T <sub>m</sub> ) as function of TMAO concentration (B) .....	83
<b>Figure 38.</b> Kinetics of cold-induced precipitation of cryoglobulin. A change in absorbance at 600 <sub>nm</sub> as a function of time for various concentrations of cryoglobulin NCR. Straight lines at the origin of the graph indicates observed initial rates of reaction at 2mg/ml (A), 3mg/ml (B) and 4mg/ml (C) of Cryoglobulin NCR. Observed initial rates at 3mg/ml (B) and at 4 mg/ml (C) of cryoglobulin are identical .....	85
<b>Figure 39.</b> Kinetics of cold-induced precipitation of cryoglobulin NCR at various concentrations of cyclodextrin. A change in absorbance at 600 <sub>nm</sub> as a function of time .....	86
<b>Figure 40.</b> Observed Initial rate of the cryoprecipitation as function of cyclodextrin concentration .....	87

---

---

## ABBREVIATIONS

6-OHDA	6-hydroxydopamine
Ab	Antibody
Ag	Antigen
AICD	Activation-Induced Cell Death
APC	Antigen Presenting Cell
APS	Ammoniumpersulfate
BCR	B Cell Receptor
BSA	Bovine Serum Albumin
C1-INA	C1-Inactivator
CLL	Chronic Lymphocytic Leukemia
CR	Complement Receptor
CTD	Connective Tissue disease
CV	Cryoglobulinemic Vasculitis
Cys	Cysteine
DAF	Decay Accelerating Factor
DC	Dendritic Cell
EDTA	Ethylenediaminetetraacetic acid
ELISA	Enzyme-linked Immunosorbent Assay
FACS	Fluorescence Activated Cell Sorter
FDC	Follicular Dendritic Cell
FGF	Fibroblast Growth Factor
FITC	Fluorescein Isothiocyanate
FLS	Fibroblast Like Synoviocytes
FPLC	Fast Performance Liquid Chromatography
GBM	Glomerular Basement Membrane
GC	Germinal Center
GM-CSF	Granulocyte-Macrophage Colony-Stimulating Factor
GN	Glomerulonephritis
GPI	Glucose-6-Phosphate-Isomerase

---

HCV	Hepatitis-C Virus
HEL	Hen Egg Lysozyme
HIV	Human Immunodeficiency Virus
HRP	Horse Radish Peroxidase
i.p	Intra peritoneal
IC	Immune Complex
Ig	Immunoglobulin
IL	Interleukin
k Da	Kilo Dalton
l, ml, $\mu$ l	Liter, Milliliter, Micro liter
M, mM	Molar, Millimolar
mA	Milli ampere
MAC	Membrane Attack Complex
MBL	Mannose Binding Lectin
MC	Mixed Cryoglobulin
MCP	Monocyte Chemoattractant Protein
MCP	Membrane Cofactor Protein
MCTD	Mixed Connective Tissue Disease
MHC	Major Histocompatibility Complex
MMP	Matrix Metalloproteinase
NOD	Nonobese Diabetic
O.D	Optical Density
PAGE	Polyacrylamide Gel Electrophoresis
PAN	Polyarthritis Nodosa
PBL	Peripheral Blood Lymphocytes
PBS	Phosphate-Buffered Saline
PDGF	Platelet-Derived Growth Factor
PE	Phycoerythrin
PSS	Progressive Systemic Sclerosis
PVDF	Polyvinylidene Fluoride
RA	Rheumatoid Arthritis

---

---

RANKL	Receptor Activator of Nuclear- $\kappa$ B Ligand
RF	Rheumatoid Factor
SCR	Short Consensus Repeat
SDS	Sodium Dodecyl Sulfate
SLE	Systemic Lupus Erythematosus
SP	Substance P
SS	Sjogren's Syndrome
TCR	T Cell Receptor
TEMED	N,N,N',N'-tetramethylethylenediamine
TGF	Transforming Growth Factor
TMAO	Trimethylamine N-Oxide
TNF	Tumor Necrosis Factor
TRANCE	TNF-related Activation-induced Cytokine Receptor
v/v, w/v	volume / volume, weight / volume
VCAM	Vascular Cell Adhesion Molecule
VEGF	Vascular Endothelial Growth Factor
V	Volt

---

## **PRIMARY AIMS OF THE STUDY**

- I. To investigate the effects of *Cr2* gene deficiency in murine autoimmune Arthritis.
- II. To investigate the role of sympathetic nervous system in antibody-induced Arthritis
- III. Molecular characterization of human cryoglobulin

# CHAPTER I

## INTRODUCTION

### 1.1. Autoimmune Rheumatic Diseases

Autoimmune diseases are those in which autoimmunity contributes to or has an association with the pathogenesis of the disease. The immune system comprises of organs and tissues that recruit specialized cells called lymphocytes for the protection of the host against invading pathogens. This system operates in a complex way and executes its functions through a variety of components to provide defense to host. In case of an antigenic challenge the pathogen is picked up by either monocytes or macrophages and the pathogen is processed and finally presented to both B- and T-cells. B-cells circulating in blood and lymphatic system produce antibodies for detection of the antigen and elimination by the other immune cell types. B-cells constitute the humoral immune system. On the other hand T-cells regulate the immune system in two different ways. CD4<sup>+</sup> T-cells or T helper cells recognize antigenic epitopes presented by the MHC class-II molecules on antigen presenting cells (APCs) and then enhance the antibody response by the B-cells. On the contrary the CD8<sup>+</sup> T-cells (T cytotoxic cells) recognize the epitopes (mostly viral) presented by the MHC I molecules on APCs. This binding leads to the activation of the cytotoxic T- cell so that it destroys the diseased cells. Once activated, the B-cells transform into antibody producing plasma cells, which recognize the specific antigen. Antibodies bound to the specific antigen trigger the complement system and then the complement system recruits neutrophils to eliminate the antigen.

---

The production of the antibodies in response to a foreign antigen is part of the normal immune response. The central theme of the immune response is distinction between foreign antigen and self-components of the body tissues. This distinction is always maintained by the clonal deletion of autoreactive T-cells in thymus during perinatal period (self tolerance) and subsequently by the elimination the autoreactive B- and T- Cells in successive stages of the development. Failure of such distinction between self and foreign epitopes leads to the production of autoantibodies, which eventually destroy the self-tissues in the body of the host. Formation of autoantibodies in small quantities may be a normal physiological process but excessive production of autoantibodies leads to pathological conditions. The way in which autoantibodies cause structural damage to the body tissues is varied. Although the exact cause of autoantibody production is not known, the molecular mimicry hypothesis gets some importance. In such a situation, a viral, bacterial or other foreign antigen has antigenic epitope(s) with amino acid sequences similar to a host protein and thus the antibody production is directed against both host as well as the foreign protein.

Autoimmune diseases involving pathological conditions can be broadly divided into two but overlapping groups:

*a.) Organ specific Autoimmune diseases*

In this group local injury, inflammation, or dysfunction are produced by autoantibody- or cell-mediated reactions against a specific target antigen located in a specialized cell, tissue or organ.

Clinical examples include: **autoimmune hemolytic anemia** (erythrocyte autoantibodies); **Hashimoto's thyroiditis** (thyroid autoantibodies and autoreactive T cells); **myasthenia gravis** (acetylcholine receptor autoantibodies); **Grave's**

**disease** characterized by diffuse goiter and hyperthyroidism (thyrotropin receptor autoantibodies); **Goodpasture's syndrome** comprising anti-GBM nephritis and pulmonary intraalveolar hemorrhage (anti-GBM autoantibodies); and type I (insulin-dependent) diabetes (pancreatic beta-cell autoreactive T cells and autoantibodies).

*b.) Systemic Autoimmune diseases*

Contradictory to the former group, in systemic autoimmune diseases, tissue injury and inflammation occur at multiple sites in organs without relation to their antigenic makeup. This is initiated by vascular leakage and tissue deposition of circulating autologous immune complexes (ICs). The immune complexes are formed by immune responses to ubiquitous soluble cellular antigen of nuclear origin and less commonly to the cytoplasmic origin.

The IC mediated diseases can be further grouped into Diffuse Connective Tissue Diseases (CTDs) (Theofilopoulos and Dixon, 1980). Clinical examples of human CTDs are:

- Systemic Lupus Erythematosus (SLE)
- Rheumatoid Arthritis (RA)
- Sjogren's Syndrome (SS)
- Progressive Systemic Sclerosis (PSS)
- Mixed Connective Tissue Disease (MCTD)
- Polyarthritis Nodosa (PAN)
- Glomerulonephritis (GN)
- Infectious diseases:

**Bacterial:** Infective endocarditis, disseminated streptococcal, staphylococcal, meningococcal, gonococcal infections, Lyme disease (borreliosis), syphilis, leprosy

**Viral:** Hepatitis B, cytomegalovirus infection, infectious mononucleosis

**Parasitic:** malaria, toxoplasmosis, trypanosomiasis.

### 1.1.1. Rheumatoid Arthritis

Rheumatoid Arthritis (RA) is one of the best-known autoimmune diseases. It is a chronic inflammatory condition affecting the joints in a symmetrical fashion and subsequently leads to the destruction of the articular cartilage and the bone (Feldmann et al., 1996a; Feldmann et al., 1996b). The general symptoms include marked lethargy, anorexia, weight loss, weakness, aching and stiffness. Morning stiffness is one of the first symptoms of rheumatoid arthritis. The most commonly affected joints are wrists, metacarpophalangeal and proximal interphalangeal joints of the hands, knees, and the small joints in the feet. There are varieties of extra-articular manifestation of the disease like nodules in the skin, vasculitis, uveitis, cataract, nodular lung disease, pericarditis, myocarditis, peripheral neuropathy, spinal cord compression, amyloid deposits, osteopenia, monocytopenia and ulcers. RA has been detected in almost all the populations. The prevalence rate ranges from 0.2% to 1% in an average in almost all populations studied. Synovial inflammation is one of the most conspicuous symptoms observed in RA. The normal synovium consists of a thin layer of so-called lining cells and loose synovial tissue with fenestrated vessels. During chronic joint inflammation

---

considerable thickening of this tissue is a remarkable event and the subsynovial tissue becomes infiltrated by numerous macrophages and lymphocytes (Figure1). During the chronic phase the joint space is filled with only granulocytes (Kouskoff et al., 1996; van den Berg and van Lent, 1996).

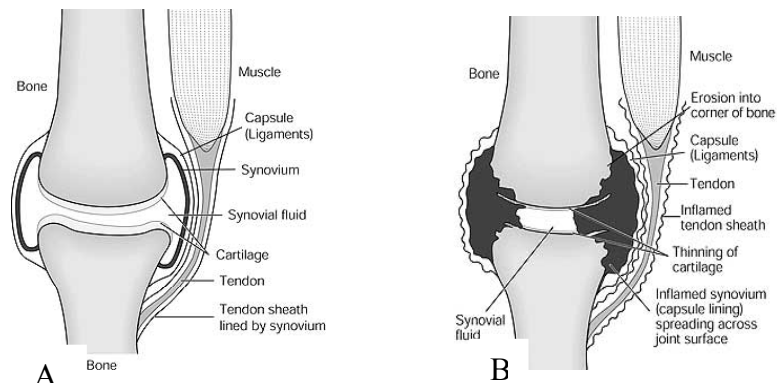


**Figure 1.** A graphic presentation of the normal joint (A) and RA joint (B).

The immunopathogenesis of RA is multifactorial, highly complex and the development of disease is dependent on genetic susceptibility, infection and other environmental factors. The etiology and pathogenesis of RA is still a debatable issue. The concept of exogenous antigen(s) initiating and driving the disease is still under consideration and no such antigen has been categorically detected so far. However it is more likely that endogenous antigen can initiate and drive the disease. One such model (K/BxN mice strain) has been reported in murine RA (Kouskoff et al., 1996). In this model glucose phosphate isomerase (GPI) has been recognized as the potential auto-antigen responsible for the RA pathogenesis (Matsumoto et al., 1999).

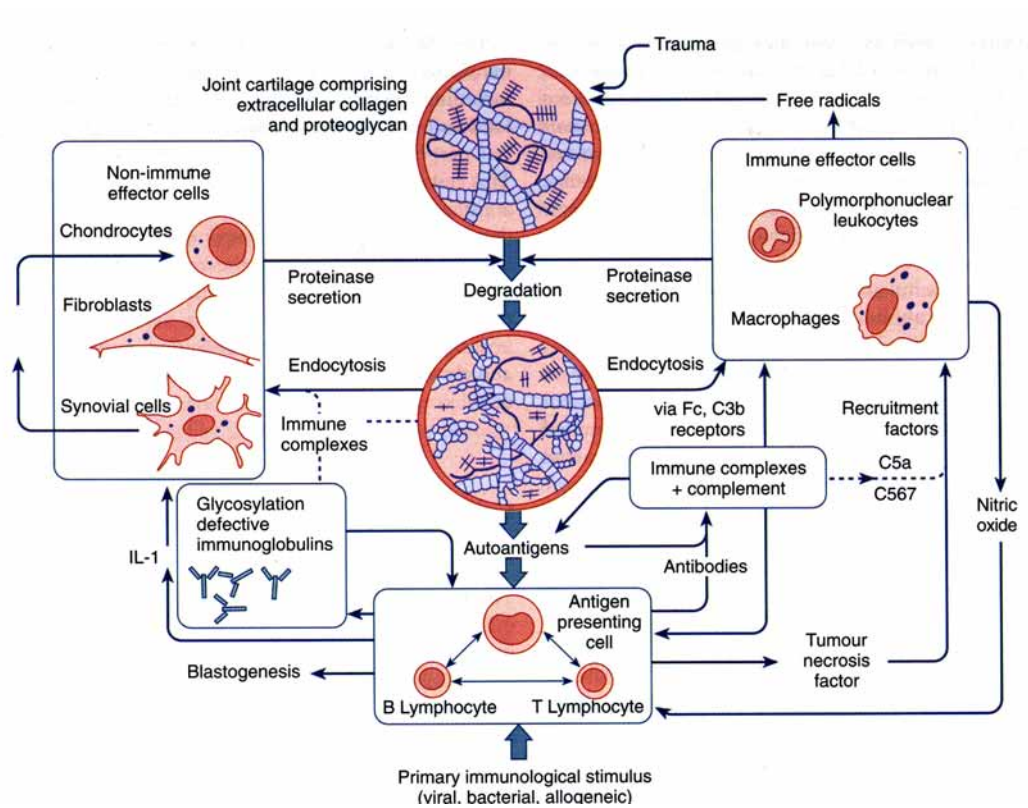


**Figure 2.** Schematic representation of immunopathological processes in Rheumatoid Arthritis. Obtained from “Autoimmune Rheumatic Diseases”, by Morrow J. et al., second edition, Oxford University Press

Current knowledge suggests that the immunopathological processes taking place in joint of rheumatoid arthritis patient are due to the interaction between antigen presenting cells (APC) and CD4<sup>+</sup> T helper cells, macrophage activation and secretion of proinflammatory cytokines. Accumulation of Dendritic cells (DC) the professional APCs, in the synovial tissues have been reported (Zvaifler et al., 1985). These DCs differentiate in the presence of abundant monocytes and fibroblast derived cytokines and express high levels of MHC molecules. Repeated nonspecific stimulation culminating in TNF $\alpha$  and GM-CSF production in the joint may result in DC differentiation and autoreactive T cell activation (Thomas and Lipsky, 1996b). The activated T cells would lead to cytokine production and provide help for B cells. The central role played by T cells in RA pathogenesis has been reported in 1980 (Janossy et al., 1981). It has also been suggested that in chronic disease the T cell response becomes polyclonal due to bystander activation effects (Thomas and Lipsky, 1996a). Many studies suggest that the TCR V $\beta$  chain repertoire is skewed in both the joint and peripheral blood in RA (Gonzalez-Quintial et al., 1996; Goronzy et al., 1994; Hingorani et al., 1996; Struyk et al., 1995).

Ectopic lymphoid tissue regions consisting of follicular B cell areas have been reported in synovitis. Synovial fibroblasts express molecules that favor survival and differentiation of B cells in the joint. A significant proportion of B cell clones produce rheumatoid factors (Rf) and these Rf can aggregate into small and large immune complexes (IC) and can lead to perpetuation of inflammation in the joint (Edwards and Cambridge, 1998).

Macrophages constitute a major part of the synovial lining where they protect the joint from infection. But in RA they are activated and mediate the inflammation by production of TNF $\alpha$  and IL1 (Firestein et al., 1990). In RA synovial macrophages are known to have up regulated levels of Fc $\gamma$  RI and Fc $\gamma$  RIII, both important for the capture of the immune complexes. Recently it has been shown that Fc $\gamma$  RIII has got a predominant role in RA pathogenesis (Edwards et al., 1997). In RA, two different kinds of synoviocytes are seen in the joint. Type A synoviocytes are macrophage-like and the type B synoviocytes are fibroblast-like synoviocytes (FLS). Under normal conditions, the synovial lining provides nutrients for the maintenance of healthy cartilage and the proteoglycans in the synovial fluid provide lubrication for articular surface. But in RA deformative tissue destruction is due to malfunction of cells originating from this lining. Most important enzymes responsible for the tissue destruction are the matrix metalloproteinases (MMP) produced by the FLS (Woessner and Gunja-Smith, 1991).

Cytokines are the dominant players in the pathogenesis of RA. Most cytokines present in synovium or synovial fluid are products of activated macrophage and fibroblast. Cytokines in turn activate the T cells, other leukocytes, endothelium, synoviocytes and chondrocytes to secrete further cytokines, proteolytic enzymes and oxygen free radicals which eventually contribute to the expression of the adhesion molecules. The most prominent players of the cytokine profile in RA are IL1, TNF $\alpha$ , GM-CSF, TGF $\beta$ , PDGF and chemokines as well as proteolytic enzymes generally produced due to macrophage activation. The FLS contribute to the production of IL6, angiogenic factors like fibroblast growth factor (FGF) and vascular endothelial growth factor (VEGF). In a local loop, IL1 and TNF $\alpha$  induce FLS to produce GM-CSF and IL8 together with proteases and small molecule mediators. IL8 and monocyte chemoattractant protein

---

(MCP-1), exacerbate the inflammation by recruiting additional macrophages to the synovium.

### **1.1.2. Cryoglobulinemic Vasculitis**

Vasculitides is a mixed group of diseases characterized by inflammation and necrosis of blood vessels. Vasculitis can be grouped into primary type occurring in the absence of a recognized precipitating cause or disease, or secondary type in which an underlying disease (e.g. rheumatoid arthritis, or SLE) or infection (such as hepatitis or HIV) is associated (Somer and Finegold, 1995). The consequence of vascular inflammation depends on the size, location, and number of blood vessels involved. The lesions can be of segmental (affecting the whole vessel circumference) or focal leading to aneurysm formation. Haemorrhage into vital internal organs is one of the most serious complications of vasculitis.

Cryoglobulinemic vasculitis (CV) results from immune complex deposition on the vascular endothelial wall. The immune complex deposits are nothing but the cryoglobulins, which undergo cold dependent precipitation. CV commonly affects the small vessels (Jennette et al., 1994). Less often medium-sized or large vessels can be affected (Carson et al., 1993; Genereau et al., 1998; Guillevin et al., 1997).

### 1.1.3. Cryoglobulinemia

Cryoglobulinemia is a systemic vasculitis that mainly damages the small and medium-sized arteries and veins. It is thought that deposition of immune complexes on the vessel surfaces activates complement system and leads to serious damages of the tissues.

Cryoglobulins were first reported by Wintrobe and Buell in a multiple myeloma patient in 1933 (Wintrobe and Buell, 1933). Lerner systematically studied the cold-precipitable immunoglobulin and in 1947 Lerner and Watson coined the term “cryoglobulins” (Lerner and Watson, 1947). In normal human serum a small quantity of cryoprecipitable material is detected. However in cryoglobulinemia the cryoprecipitation is caused by intrinsic characteristics of monoclonal or polyclonal Ig components. Current hypothesis of induction of cryoglobulinemia include genetic susceptibility, prolonged antigenic stimulation, polyclonal activation of B lymphocytes, superantigen properties of the infectious agents, reduced clearance of immune complexes in the liver and activation of proto oncogenes (D'Amico, 1998; Ellis et al., 1995; Monti et al., 1995; Wong et al., 1996).

Brouet et al., classified the cryoglobulins in three types according to their composition (Brouet et al., 1974).

**Type I:** Isolated monoclonal Immunoglobulins (IgM, IgG etc.) associated with lymphoproliferative and myeloproliferative diseases.

**Type II:** Mixed cryoglobulins with a monoclonal component (usually IgM) and a polyclonal component (usually IgG) associated with lymphoproliferative diseases, autoimmune diseases, and viral and bacterial infections.

**Type III:** Mixed polyclonal cryoglobulins (MC) (monoclonal IgM or polyclonal IgM) with rheumatoid factor (RF) activity and are usually associated with lymphoproliferative diseases, autoimmune diseases and diseases related to certain viral and bacterial infections.

However, there are some unusual cryoglobulins, which do not fit into the conventional classification. For example MC formed by oligoclonal IgM and traces of polyclonal IgG, have been reported and as per Brouet classification they are described as type II-type III variant (Musset et al., 1992). A higher frequency of subclass IgG3 has been reported (Musset et al., 1994). IgG3s have a peculiar cryogenic potential of their own due to a long hinge region and a high ability to self-aggregate with each other through spontaneous Fc-Fc interaction. Shortly after the discovery of the HCV in 1989 (Choo et al., 1989) several authors reported on the association of HCV with mixed cryoglobulinemia (MC) in 80-90% of the patients. The development of cryoglobulinemia in patients with HCV infection increases with the duration of the infection. One probable hypothesis assumes that the chronic HCV infection of lymphocytes triggers a polyclonal B lymphocyte proliferation and subsequently causes a benign lymphoproliferative disease (Ferri et al., 1993; Hartmann et al., 1995).

### **1.2. Self and Non-self: Immunological Tolerance**

Immunological tolerance is the absence of immunological responsiveness to specific antigens, most importantly to the self-antigens of normal body constituents. Immunological tolerance to foreign antigens can be introduced experimentally in fetal or perinatal animals by exposure to transplanted foreign cells, infectious viruses or appropriately introduced foreign proteins. T cells recognize peptide fragments derived

---

from the protein antigens presented in the context of the major histocompatibility complex molecules (Nossal, 1994; von Boehmer, 1994). In the thymus the MHC molecules predominantly present the self-peptides and therefore positive selection gives rise to T cells, which are inherently self-reactive. Hence a negative selection is required to eliminate the self reactive T cells. Approximately 95% of T cells are eliminated in the thymus due to this process. This process poses a difficult task to discriminate between self and non-self. Again if a particular self-antigen is not expressed in the thymus, then the negative selection is ineffective and that can lead to release of potential self-reactive T cells to the periphery. Another factor for poor selection of self-reactive T cells might be due to the inefficient MHC/peptide interaction.

There are two hypotheses explaining the appearance of the self reactive T cells in the periphery.

First hypothesis suggests that many tissue specific antigens are not expressed in the thymus, thereby precluding any central tolerance to these antigens. It is suggested that lack of such central tolerance leads to the influx of self reactive T cells to the periphery and there by inducing organ specific autoimmunity. However this hypothesis needs further examination as it has been reported that many “tissue specific” self antigens associated with Diabetes, thyroiditis and uvetis are also expressed in thymus. Other possible mechanism that explain the escape of self reactive T cells to the periphery are:

- a.) “Tissue-specific” self-antigens do mediate deletion of high-affinity cells, and the cells that are seeded to the periphery have low affinity for self-antigen compared with their affinity for foreign antigen; (Targoni and Lehmann, 1998)

- b.) Self-reactive cells escape because the form of the self-antigen expressed in the thymus differs from that expressed in the peripheral tissue; (Anderson et al., 2000; Klein et al., 2000).
- c.) “Tissue-specific” self-antigens do not mediate negative selection due to inefficient antigen presentation by the MHC alleles present in the individual (Harrington et al., 1998; Kumar et al., 1995; Liu et al., 1995).

The second hypothesis proposes that inefficient antigen presentation by certain disease-associated MHC alleles results in peripheral repertoire biased towards autoreactivity (Ridgway et al., 1999).

The peripheral tolerance is achieved by two different mechanisms in order to control the self-reactive T cells in the periphery. The first one is clonal deletion of self-reactive T cells by activation induced cell death (AICD) and the second one is the functional silencing (clonal anergy) of T cells without clonal deletion.

### **1.3. Regulation of Immunity by Complement and Complement Receptors**

The complement system is a major humoral component of the innate immune system and functions as the mediator of the inflammation. It consists of 20 different plasma proteins mostly in their inactive form and gets activated upon stimulation through classical or alternative pathway to mediate the effector functions.

An important activity of complement is the formation of the C3b from C3. The three pathways of the complement system are (1) the “Alternative Pathway”, (2) the “Classical Pathway” and (3) the “Lectin Pathway”.

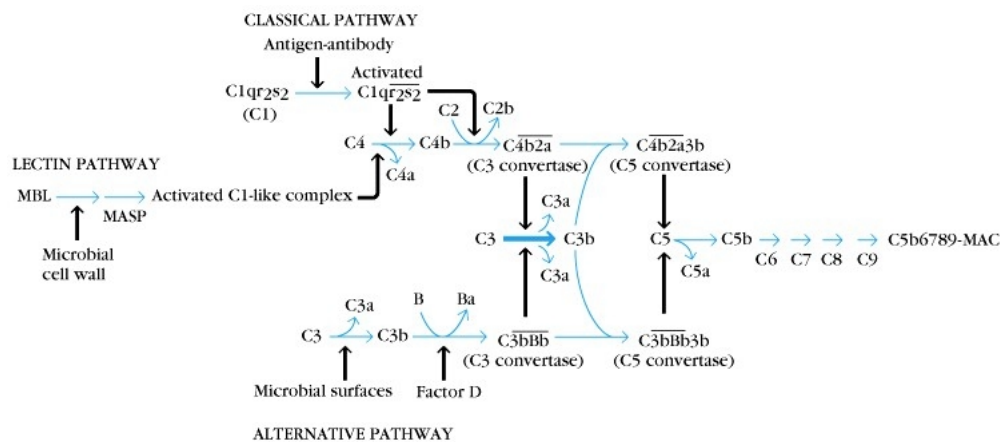


**Figure 3.** Schematic representation of the Complement cascade. Obtained from “Kuby Immunology” Fourth Edition, W.H. Freeman and Company, New York

### 1.3.1. Generation of C3b from C3

C3 is the central component of complement system. In fact C3 and its derivatives have distinct binding sites for a series of molecules including CR1, CR2, CR3, CR4, C3a and factor B, P, H and serum conglutinin. The serum concentration of C3 is about 1 mg/ml in human.

C3 is a 190 kDa heterodimeric glycoprotein with a 110 kDa  $\alpha$ -chain and a 75 kDa  $\beta$ -chain. It has got an internal thioester bond between a cysteine (Cys 1010) and the  $\gamma$ -carboxyl group of a glutamine residue 1013. This thioester bond can be hydrolyzed either by small molecules such as water through a “Tickover mechanism” or it can be hydrolyzed by reactive groups such as amines and hydroxyls on the protein and carbohydrate molecules. Due to the spontaneous and slow hydrolysis of the internal

thioester bond of C3, iC3b is formed all the time. This hydrolysis of thioester bond enhances the binding of factor B (95 kDa zymogen of serine protease) in the presence of  $Mg^{++}$  in the fluid (in plasma) phase. This binding between C3b and factor B leads to conformational change of B resulting in activation of protease activity of factor B (Hourcade et al., 1998). The fluid phase C3b is an unstable C3 convertase, which is recognized by factor D. Factor D cleaves a 30 kDa fragment “Ba” from B and then the C3b becomes the active fluid phase stable C3 convertase, which converts the C3 to C3b.

### **1.3.2. Initiation of Alternative Pathway**

The fluid phase iC3b may bind to the hydrophobic moieties of membranes of self or non-self origin facing the aqueous environment. Commonly hydroxyl groups are present on the microbial carbohydrates such as LPS, zymosan, inulin, dextran sulfate etc. The iC3b thioester can also form covalent amide linkage with amine groups in proteins. The end product of these reactions is the target bound C3b complex, which is more or less similar to the fluid phase C3b-  $H_2O$ . This reaction initiates the cascade to bring in the factor B and then comes the factor D to cleave off the Ba fragment to generate the target bound C3-  $H_2OBb$  ( $Mg^{++}$ ). This keeps on producing more and more C3b by amplification process.

### **1.3.3. Initiation of Classical Pathway**

The prominent players of the classical pathway are the C1, C2, C3 and C4. There is also a regulatory component called C1-inactivator (C1-INA). This pathway is called

---

antibody dependent pathway. Most importantly this pathway always requires the C2 and C4.

The C1 in the serum is a macromolecular complex consisting of C1q, two molecules of each C1r and C1s (serine esterases), stabilized by interaction with the  $\text{Ca}^{++}$ .

The C4 is a 200 kDa heterotrimeric molecule consisting of three subunits  $\alpha$ - (95 kDa),  $\beta$ - (75 kDa) and  $\gamma$ - (33 kDa).

In the initiation process the C1q binds to the antigen-bound antibody of IgG or IgM subclass. The globular heads of the C1q binds to the Fc region of the antibody when bound state with antigen. In order to activate the C1q this binding must involve two or more C1q molecules of a single C1 complex. The activated C1s cleave C4 into C4a and C4b. The C4b has got an exposed thioester bond much like C3b and binds to the target surface via thioester hydrolysis or surface hydroxyls and amines. The hydrolysis signals the C2 to bind to the C4b and then the enzymatically active C4bC2a complex is formed. Upon hydrolysis, C2b (75 kDa) dissociates into fluid phase leaving behind a stable C4bC2aMg<sup>++</sup> complex. This is also called as membrane C3 convertase. Here both the classical and alternative pathway converse.

### **1.3.4. Initiation of Lectin Pathway**

This is similar to the classical pathway but gets activated by the mannose binding lectins (MBLs). The lectin pathway is a subdivision of the classical pathway and it activates classical pathway without using the C1 complex.

### 1.3.5. Formation of C5 Convertase

The covalent association of several hundred C3b molecules with C3 convertase leads to the formation of the C5 convertase. In case of the classical pathway the C3b must bind to the C4 in the region of Ala-1186, to give rise to the C5 convertase. This statistically happens when 100 molecules of C3b are attached to the C3 convertases (Kozono et al., 1990). Once the C5 convertase has been formed, then it has got two biological functions;

- i. Formation of **C5a**, major chemoattractant protein for host leukocytes,
- ii. Initiation of the **membrane attack complex (MAC)** by the formation of C5b.

Once the C5 is cleaved the C5b interacts and remains in contact with the C3b component of C5 convertase. During this transitory condition (about 2 minutes) C5b can bind to C6. Once the C5bC6 complex is formed, it undergoes a conformational change and either binds to C7 or dissociates from C5 convertase. If the C5 convertase-C5bC6 binds to C7, this triggers the irreversible transition of the hydrophilic C5bC6 “precursor” to another conformationally distinct amphiphilic C5bC6C7 complex. The conformational changes result in the exposure of hydrophobic regions, which insert into the target membrane. Then C8 gets attached to the C5bC6C7 complex and undergoes conformational changes. A hydrophobic tail is inserted into lipid bilayer. The final step in MAC formation is the binding of C9 to C5bC6C7C8 complex.

### 1.3.6. Regulation of Complement Activation

The fate of C3b is decided by a set of regulator proteins. The 88 kDa heterodimeric **factor I** is a neutral serine protease with high specificity for C3b and C4b. Regulators

---

like factor H, CR1 and MCP direct factor I to cleave C3f (2-3 kDa) from C3B to generate iC3b (inactive). From iC3b, factor I can generate C3dg. The **factor H** (cofactor to factor I) preferentially inactivates the fluid phase C3b, which have not found a surface (Fearon and Austen, 1977). Factor I also requires C4 binding protein C4Bp or CR1 to hydrolyze C4b.

Membrane cofactor protein (**MCP**) is a 45-70 kDa integral membrane glycoprotein. It acts as a cofactor to factor I. It binds to C3b and thereby factor I cleaves C3b into iC3b and subsequently to C3c and C3dg. The wide distribution of the MCP in all tissue helps to protect the tissues from C3b mediated destruction.

Decay accelerating factor (**DAF**) is a 75-80 kDa intramembrane glycoprotein, distributed widely in all the tissues. It is the primary protection of the host cell from C3 convertase attack. DAF splits C3bBb and C4bC2a (the C3 convertases) complexes apart and binds to the C3b or C4b thus preventing the formation of the C3 convertases.

### **1.3.7. Complement Receptor 1 (CR1 or CD35)**

CD35 is a 190 kDa transmembrane glycoprotein found in phagocytes, B cells, FDCs and erythrocytes. The CR1 is encoded along with CR2 at the single locus Cr2 on chromosome 1 in mice. The CR1 and CR2 consist of multiple repeating structures referred to as short consensus repeats (SCR). The SCR consists of conserved units of 60-70 amino acids. CR2 consists of 16 SCR, a transmembrane region and a 35 amino acid cytoplasmic tail, where as CR1 includes all of CR2 and an additional 6 SCR on its N-terminal region. Just like factor H, CR1 acts as a cofactor and promotes cleavage of C3b to iC3b by factor I (Kinoshita et al., 1985; Molina et al., 1994). CR1 has moderate affinity for C3b but very low affinity for iC3b. It does not bind to the further

---

metabolites of iC3b. CR1 also binds to the C4b. It helps the phagocytes to generate opsonized particles, enhances antigen specific B cell endocytic responses and clearance of antigen-antibody complex by erythrocytes. The erythrocytes inactivate C3b and deliver them to the liver macrophages in humans.

### **1.3.8. Complement Receptor 2 (CR2 or CD21)**

CD21 is a 140 kDa glycoprotein encoded in the RCA gene region, which binds iC3b, C3d, C3dg, and C4d. CR2 is expressed on the surface of B cells, follicular dendritic cells, pharyngeal epithelial cells, thymocytes and some T cells. It does not act as a regulator or cofactor but instead, appears to enhance specific B-cell responses as a co-receptor to the BCR. B cell proliferation and differentiation can occur by cross-linking of CD21 with polymeric C3d or anti-CD21 antibodies in the presence of T cell factors (Nemerow et al., 1985; Wilson et al., 1985) or phorbol esters (Bohnsack and Cooper, 1988). CD21 also plays a synergistic role in the activation of B cells induced by ligation of surface IgM (Fingeroth et al., 1989; Luxembourg and Cooper, 1994a; Luxembourg and Cooper, 1994b). Most of the signaling effects are initiated by physical association of CD21 with CD19 and CD81 (TAPA-1) on the surface of B lymphocytes (Bradbury et al., 1992; Matsumoto et al., 1991; Matsumoto et al., 1993).

### **1.4. Pain in Arthritis: A Neuroendocrine Connection**

The synovial joints are innervated by three different kinds of peripheral nerve fibers: the heavily myelinated A $\beta$  fibers, thinly myelinated A $\delta$  fibers and unmyelinated C fibers. So any kind of twisting or bending of the joints beyond its limit results in pain sensation. In RA there is a striking symmetry in joint involvement. This may explain

---

the involvement of nervous system. The pain in RA is not due to the loss of the articular cartilage rather due to a more complex mechanism. When there is a sustained inflammation in the RA joints, several mechanisms of pain amplification take place. For example, PGE<sub>2</sub>, PGD<sub>2</sub> and PGI<sub>2</sub> activate sensory nerves directly and sensitize the nerve endings to bradykinin. Again the C-fibers become sensitized due to noradrenaline. Neuropeptides like substance P accumulate in the site of inflammation and contribute to the pain amplification. In the acute phase of inflammation redness, heat, swelling, and pain occur in the affected joint secondary to vasodilatation. Increased blood flow and increased permeability of vascular endothelium and post capillary plasma extravasations facilitates access of blood cells and serum to the damaged tissue. Another important aspect of inflammation is the contribution of mast cells. Antidermic activation of peripheral nerves or tissue injury degranulates cutaneous mast cells. Activated mast cells produce a range of inflammatory mediators which casue perivascular edema in synovial membrane and also stimulate chondrocytes and fibroblasts to release proteolytic enzymes, which destroy the cartilage and bone.

### **1.4.1. Substance P and Joint Inflammation**

Substance P is an undecapeptide member of the tachykinin family and therefore related to neurokinin A and B. Substance P is stored in secretory granules of sensory neurons such as unmyelinated C fibers. Once released substance P has been known to be associated with the following activities:

- Activation of macrophages
- Stimulation of human B lymphocyte differentiation
- Degranulation of mast cells with release of histamine

- Proliferation of fibroblasts
- Increase in expression of cytokines, prostaglandins, and metalloproteases.
- Increase in microvascular permeability
- Chemotaxis and activation of neutrophils

The substance P concentration increases in the RA joints (Levine et al., 1984).

## CHAPTER II

### MATERIALS AND METHODS

#### 2.1. Mouse Strains

##### 2.1.1. KRN Transgenic Mouse strain

The KRN transgenic mice strain was propagated in the TFA, University of Konstanz, Germany. The strain harbors a transgene encoding the  $\alpha/\beta$  chains of the T cell receptor (Kouskoff et al., 1996). A T cell hybridoma (R28) originally derived from B10A.4R mouse was designed to recognize bovine pancreas RNase peptide 41-61 in the context of A<sup>k</sup> molecules (Peccoud et al., 1990). To study the R28 specificity a transgenic mice line was generated by using the rearranged T cell receptor hybridoma (Kouskoff et al., 1996). The strain was maintained by serial crossing from heterozygotes against C57BL/6 (B6) background. This transgene has been abbreviated as “K” and is used for identification in different crosses. For example K/B denotes KRN transgenic mice in C57BL/6 background.

##### 2.1.2. C57BL/6 (B6) Mouse strain

Inbred strains of C57BL/6 (B6) KN mice were obtained from the Animal facility University of Konstanz, Germany and were maintained under pathogen free conditions. This mouse line was used for different experiments.

### 2.1.3. NOD/Lt Mouse strain

The nonobese diabetic (NOD) mouse strain (H-2K<sup>d</sup>D<sup>b</sup>) was obtained from the Animal facility, University of Konstanz, Germany. This strain was originally derived from out bred JCL-ICR mice. During this breeding a diabetic mouse was discovered and subsequently three inbred lines were made. The NOD, NON, and CTS. Serological studies indicated NOD mice expressing MHC haplotype : K<sup>d</sup> -A<sup>NOD</sup> -E<sup>-</sup> -D<sup>b</sup> and NON mice K<sup>b</sup> -A<sup>NON</sup> -E<sup>+</sup> -D<sup>b</sup> (Acha-Orbea and McDevitt, 1987; Hattori et al., 1986; Ikegami et al., 1988). This stain serves as an excellent model for the autoimmune disease, insulin dependent diabetes mellitus.

### 2.1.4. Cr2<sup>-/-</sup> Mouse strain

The Cr2<sup>-/-</sup> mouse strain on mixed 129/C57BL/6 background (Ahearn et al., 1996) was obtained from the TFA, University of Konstanz, Germany. The Cr2<sup>-/-</sup> mice lack the expression of complement receptors CR1 (or CD35) and CR2 (or CD21). The CR1 and CR2 are both encoded by the Cr2 locus and CD21 is derived from CD35 by alternate splicing.

### 2.1.5. Balb/c Mouse strain

Inbred strains of Balb/c mice were obtained from the TFA, University of Konstanz, Germany.

### 2.1.6. K/BxN and BxN Mouse strain

The K/BxN mouse strain (Kouskoff et al., 1996) was obtained through a genetic cross between K/B (KRN transgene carrying B6 mice line) and the NOD (N) strain. KRN being heterozygous, the F1 offspring were either carrier or non-carrier of the KRN transgene. The carriers of the KRN transgene were designated as K/BxN and developed arthritis in the third week after birth. The non-carriers were healthy litter mates and were designated as BxN (F1 offspring of B6 and NOD strain)

### 2.1.7. SP<sup>-/-</sup> Mouse strain

SP<sup>-/-</sup> Mouse strain was obtained from Dr. A. Zimmer, University of Bonn, Germany (Bilkei-Gorzo et al., 2002) and propagated in the TFA, University of Konstanz, Germany.

## 2.2. Breeding Experiments

The mouse strains were kept in a pathogen free environment in the TFA, University of Konstanz, Germany. The KRN strain was bred with C57BL/6 (B6) strain to maintain the KRN mouse line in heterozygous condition on B6 background. The mice were screened by FACS analysis of the peripheral blood lymphocytes (PBL) using CD4-PE and TCR-V $\beta$ 6-FITC antibodies (BD-Pharmingen, Heidelberg, Germany). The double positive phenotypes were selected.

NOD/Lt (N) mouse strain was maintained under pathogen free environment and used for breeding with KRN strain and Cr2<sup>-/-</sup> strain. Similarly inbred lines of the B6 strain were maintained under pathogen free conditions. B6 strain was used for wild type

control experiments. Inbred lines of the Cr2<sup>-/-</sup> strain were maintained under pathogen free condition and crossed with KRN as well as NOD strains. The Cr2<sup>-/-</sup> strain was selected using B220-PE and CD21-FITC monoclonal antibodies (BD-Pharmingen, Heidelberg, Germany) in FACS analysis.

### **2.3. Measurement of Ankle Thickness and Clinical Index**

In order to assess disease onset in arthritic mice, ankle swelling of K/BxN and BxN strains were measured on the second week after birth. The mice were fixed and the ankle thickness was measured with the help of caliper. The data were recorded and subsequently plotted in a graph. The clinical Index is the determination of first clinical manifestation of disease in the mice. The clinical index was also measured in a scale varying from 0 to 4. The lowest score 0 was given to a mouse if no leg displayed ankle swelling. A score 1 was given for swelling in one leg only and 2 for swelling in 2 legs only and 3 for swelling in 3 legs and finally 4 for swelling in 4 legs. In a study 10 healthy and 10 sick age matched mice were taken.

### **2.4. Locomotor Activity Measurement**

Abnormality in the locomotor activity of the sick as well as healthy mice was recorded in a simple experiment. The mice were housed in an experiment room with D/L cycles. A single mouse was removed from its littermates and acclimatized to a solitary cage for over night. The following night, the locomotor activity was video taped. Once the data were recorded, the locomotor activity was monitored on a screen. The total surface area of the cage was divided into 16 rectangles for measurement of movement from one to another. A numerical score of 1 was given for movement from one rectangle to another.

---

Thus the total number of movements was recorded. The data obtained from the whole cohort study were represented in a histogram.

In yet another experiment, the climbing ability of the sick as well as healthy mice was measured in a similar fashion. Number of times the mouse climbed the cover of the cage by perching to the metal wires of the cover were recorded. Each time it comes to the top by climbing, a score of 1 was given. Thus the climbing ability of the entire cohort was measured and data were represented in a histogram.

## **2.5. Immunological Methods**

### **2.5.1. Fluorescence Activated Cell Sorting (FACS)**

Mice were bled from the tail vein and blood was directly collected into 1.5ml centrifuge tubes containing 300  $\mu$ l of Alsever's solution (0.42g NaCl, 0.8g tri-Na-citrate-2 H<sub>2</sub>O, 2.05g D-glucose in 100 ml of water). Samples were mixed properly in order to avoid blood coagulation. Samples were centrifuged in Ficoll gradient at 1600 rpm for 20 min at room temperature in 1.5ml centrifuge tubes in a Heraeus Biofuge Pico. The lymphocytes were carefully removed from the interface of the two layers and transferred into a 96 well micro titer plate on ice. The cells were centrifuged at 1200 rpm in a Heraeus multifuge 3 S-R at room temperature for 5 minutes and the supernatant containing Ficoll was removed carefully without disturbing the pellet. The cells were washed by re-suspending them in ice-cold FACS buffer (1x PBS containing 2% FCS, 0.1%NaN<sub>3</sub>, 0.2% Triton X100, 0.1mM EDTA). To the cells were added 20  $\mu$ l of corresponding antibodies diluted in FACS buffer. All antibodies used in the FACS analysis were obtained from BD-PharMingen, Heidelberg Germany. The anti-CD4-PE and anti-B220-PE monoclonal antibodies were diluted 1:320 in FACS buffer. The anti-

---

TCR V $\beta$ 6-FITC monoclonal antibody was used at a dilution factor of 1:100 in FACS buffer. The anti-CD21-FITC, anti-I-A<sup>d</sup>-FITC and anti-I-A<sup>b</sup> A $\beta$ <sup>b</sup> monoclonal antibodies were diluted at a factor of 1:200 in FACS buffer. Cells in the antibody solution were incubated on ice for 1 hour. Cells were washed with 200  $\mu$ l of FACS buffer per well. The cells were centrifuged at 1200 rpm at 4°C for 3 minutes. The unbound antibodies in the supernatant were removed carefully without disturbing the pellet. Finally the pellet was re-suspended in 200  $\mu$ l FACS buffer and transferred to FACS-tubes (BD-Pharmingen, Heidelberg, Germany). Data were collected in a FASCan machine using “Cell Quest” software (BD-PharMingen, Heidelberg, Germany).

### 2.5.2. ELISA

The 96 well flat bottom ELISA plates (Immunomaxi, TPP, Trassadingen, Switzerland) were coated with 0.125 $\mu$ g of GST-GPI fusion protein in 50 $\mu$ l of PBS per well and incubated over night at 4°C. The wells were washed twice with washing buffer (PBS containing 0.1% tween-20) in order to remove unbound GST-GPI fusion protein. Blocking was performed by adding 400  $\mu$ l blocking buffer (PBS containing 1% non-fat milk powder and 0.1% tween-20) to each well and incubated for 2 hours at room temperature. Subsequently the wells were washed with PBS containing 0.1% tween-20. Sick as well as healthy mouse sera were serially diluted starting with 1:10 in the first well. After addition of the sera, plates were incubated overnight at 4°C. The plates were washed four times with wash buffer (PBS containing 0.1% Tween 20). Anti-GPI antibodies present in the sick mouse sera were detected by biotinylated goat anti-mouse IgG1 monoclonal antibodies (Cymbus Technology, Germany) diluted 1:500 from the

stock concentration. The plates were incubated for 2 hours at room temperature and subsequently washed four times with wash buffer (PBS containing 0.1% Tween 20). 100  $\mu$ l of Streptavidin peroxidase (Sigma, Germany) diluted 1:2000 in blocking buffer (PBS containing 1% non-fat milk powder and 0.1% Tween 20) was added to each well and the plates were incubated for 1 hour at room temperature. 100  $\mu$ l of p-nitrophenyl phosphate (1mg/ml) (Sigma, Germany) prepared in substrate buffer (167mM NaHCO<sub>3</sub>, 12mM Na<sub>2</sub>CO<sub>3</sub>, 1mM MgCl<sub>2</sub>, pH 8.6) was added to each well. 1  $\mu$ l of 30% H<sub>2</sub>O<sub>2</sub> was added to the developing solution just before the reaction. The plates were incubated for about 30minutes to see the color change. The reaction was stopped by adding 25  $\mu$ l of 1M H<sub>2</sub>SO<sub>4</sub> to each well. The optical density was measured at 492nm in the ELISA reader.

### **2.5.3. Immunoblot**

#### **2.5.3.1. Western Blot**

Immunoblotting is a technique used for the detection of the macromolecular antigens (usually proteins) using specific antibody (Towbin et al 1979, Burnette 1981). Semi-dry electrophoretic transfer of polypeptides from polyacrylamide gels to a nitrocellulose membrane or polyvinylidene fluoride (PVDF) membrane was performed by use of semi-dry gel transfer apparatus (Biorad, Munich, Germany). Proteins bind to the nitrocellulose chiefly by hydrophobic bonds (van Oss et al 1987) and the PVDF membrane ensures a much stronger hydrophobic interaction (Pluskal et al 1986). Polyacrylamide gels were carefully removed from the electrophoresis chamber and placed on top of an equal size nitrocellulose or PVDF membrane soaked in transfer

buffer (50mM Tris, pH 8.8, 250mM Glycine, pH 8.3, 20% Methanol). Six pieces of Whatmann 3mm paper of equal size were also soaked in the transfer buffer to saturation. Three pieces Whatmann 3mm paper saturated with transfer buffer were placed on the bottom of the gel-membrane sandwich and three on the top. The complete sandwich was placed on the bed of the transfer apparatus in such a way that the membrane faces the anode. Transfer was carried out for 1 hour at 20 V and 200mA. Soon after transfer the membrane was carefully taken out of the sandwich and stained with Ponceau S solution for detection of the transferred polypeptide bands. The band pattern was scanned electronically and stored for future reference.

The membrane containing the polypeptide bands were placed in a tank containing the blocking buffer (10mM Tris pH 7.6, 100mM NaCl, 0.05% Tween 20 and 5% non-fat Milk Powder) for 1 hour at room temperature while rocking on a flat bed rocker. Soon after blocking the membrane was incubated in primary antibody solution (diluted in blocking buffer according to the manufacturers instructions) for 1 hour at room temperature. The unbound antibodies were removed by washing the membrane three times with wash buffer (10mM Tris pH 7.6, 100mM NaCl, 0.05% Tween 20) for 20 minutes each. After the last wash the membrane was incubated with Horse Radish Peroxidase (HRP) conjugated secondary antibody (diluted in blocking buffer according to the manufacturer's instructions) for 1 hour at room temperature. Then the membrane was washed three times in wash buffer (as mentioned above).

SuperSignal chemiluminescent substrate (Pierce, Rockford, Illinois, USA) was prepared by mixing equal volumes of solution A and solution B. The cocktail was added to the membrane and incubated for five min at room temperature. The X-ray film was carefully placed on the membrane in the dark and subsequently developed.

---

For immunoblotting of the cryoglobulins, anti-human-IgG (H+L) and -IgM were obtained from Dianova, Hamburg, Germany, anti-human IgG2, IgG3 and IgG4 were from Pharmingen, Heidelberg, Germany and anti-human IgG1 was from HyTest, Finland. The secondary antibody HRP conjugated goat anti-mouse IgG (H+L) was from Pierce, Rockford, Illinois, USA.

For immunoblot analysis of the tyrosine hydroxylase in spleen lysates of the chemically sympathectomised mice and control mice, affinity purified rabbit polyclonal anti-tyrosine hydroxylase (Chemicon International, CA, USA) was used. The secondary antibody was HRP conjugated goat anti-rabbit IgG (Pierce, Rockford, Illinois, USA).

### **2.5.3.2. Dot Blot**

Instead of running a SDS PAGE, protein samples were spotted directly on to a nitrocellulose or PVDF membrane. The membrane was blocked with blocking buffer as described above in 2.5.3.1. The antibody staining was carried out as described above.

## **2.6. Histology**

### **2.6.1. Tissue Fixation**

Ankle and knee joints of the mice were carefully dissected out without damage to the joints. Skin and soft tissues were removed surgically and the complete joints were fixed overnight in 4% formaldehyde solution. Then the joints were kept for dehydration in 50% ethanol until further processing.

### 2.6.2. Decalcification

Decalcification of formaldehyde fixed joints was carried out for two weeks in 10% ethylenediaminetetraacetic acid (EDTA) solution pH 7.2. The EDTA solution was prepared by dissolving 100gm of EDTA in 200ml of distilled water. The solution was warmed and stirred with the help of magnetic bead and to it 50ml NaOH (40%) was added drop by drop. The final pH was adjusted to 7.2 with concentrated HCl. Finally the volume was adjusted to 1 liter. The decalcification was checked with the help of a scalpel for softening of the hard tissues. Soon after decalcification the joints were kept for dehydration in 50% ethanol until needed. The dehydrated joints were embedded in paraffin for sectioning. About 5 to 10  $\mu\text{m}$  thick sagittal serial sections were cut. The sections were carefully placed on the glass slides and quality of the tissue was observed microscopically.

### 2.6.3. Hematoxylin and Eosin Staining

The paraffin embedded sections were deparaffinised by three xylol washes for five minutes each. Excess xylol was removed by washing with 100% ethanol twice for 1 min each. The sections were placed in 70% ethanol for 1 minute and finally washed with double distilled water. After washing the sections were placed in Mayer's hematoxylin solution (Sigma-Aldrich Chemie GmbH, Steinheim, Germany) for 10 minutes. The sections were washed in running water and then placed in 1% eosin solution (Sigma-Aldrich Chemie GmbH, Steinheim, Germany) for 1 minute. Then the sections were rinsed with double distilled water and subsequently dehydrated by placing the sections in 70% ethanol for 1 minute followed by two changes in 100%

ethanol for 1 minute each. The sections were placed three times in xylol for 5 minutes each. The sections were mounted with cover slips and evaluated by light microscopy.

### **2.6.4. Toluidine Blue Staining**

Adjacent sections were taken for the proteoglycan staining with toluidine blue. The sections were deparaffinised first by xylol treatment as described in 2.6.3. Then the sections were rehydrated with double distilled water for 10 minutes. Rehydrated sections were placed in toluidine blue solution (0.1% toluidine blue, 2.5% NaCO<sub>3</sub> in H<sub>2</sub>O) (Sigma-Aldrich Chemie GmbH, Steinheim, Germany). Sections were rinsed with double distilled water four times and then transferred to 70% ethanol for 1 minute followed by two changes in 100% ethanol for 1 minute each. Finally the sections were placed thrice in xylol for 1 minute each. Sections were mounted and evaluated with light microscopy.

### **2.7. Skeletal Preparation**

Mice were sacrificed by cervical dislocation and dissected open to harvest the organs. The hindlimbs and forelimbs were surgically removed. The skin and muscles were carefully dissected out. Then the limbs were fixed overnight in 1% glacial acetic acid and 95% ethanol. Cartilage was stained with freshly prepared Alcian blue (15mg Alcian blue dissolved in 80ml 95% ethanol, 20ml glacial acetic acid) for 48 hours. The limbs were dehydrated in 95% ethanol for a day and then dissolved in 2% KOH for one day at 37°C. Bones were stained overnight with Alizarin red solution (75mg/ml of Alizarin red dissolved in 1% KOH). Limbs were put in destaining solution (20% glycerol and 1% KOH) for 15 days. The remaining loose tissues were surgically removed and finally the limbs were preserved in 50% ethanol and 50% glycerol.

## 2.8. Survival Frequency Test

Ten mice from each strain such as Cr2<sup>-/-</sup>K/BxN, Cr2<sup>-/-</sup>BxN, K/BxN and BxN were observed for 500 days for terminal illness and severity of the disease under pathogen free environment. The death resulting out of terminal illness was recorded and finally represented in survival percentage curve.

## 2.9. Chemical Sympathectomy

Balb/c mice (8 weeks old) were obtained from the TFA, University of Konstanz, Germany. Chemical sympathectomy was performed by injecting 6-OHDA (6-hydroxydopamine hydrochloride, (Sigma-Aldrich Chemie GmbH, Steinheim, Germany) in two different methods (see 2.9.1 and 2.9.2). 6-OHDA was dissolved in 0.8% NaCl containing  $1 \times 10^{-3}$  M Ascorbate as antioxidant. The solution was stored in dark at  $-20^{\circ}\text{C}$ .

### 2.9.1. Transient Sympathectomy

In this method eight weeks old Balb/c mice were injected weekly once with 6-OHDA (150mg/kg of body weight) for seven weeks. The control mice were injected with the vehicle alone (0.8% NaCl containing  $1 \times 10^{-3}$  M Ascorbate as antioxidant). Mice were observed carefully and maintained in a pathogen free environment. At the end of the last injection mice were taken for the arthritis induction by serum transfer.

### **2.9.2. Permanent Sympathectomy**

For permanent sympathectomy, pups were injected with 6-OHDA (50mg/kg of body weight) at postnatal day 1. The control pups were injected with the vehicle alone (0.8% NaCl containing  $1 \times 10^{-3}$  M Ascorbate as antioxidant). At 8 weeks of the age the mice in this group were taken for the serum transfer experiments for arthritis induction.

### **2.10. Induction of Arthritis by K/BxN Serum Transfer**

The K/BxN mice (F1 offspring of KRN transgenic mice on B6 background crossed with NOD) develop arthritis at about the third week after birth. K/BxN mice produce anti-GPI antibodies during the course of the disease. A serum pool was prepared by collecting blood samples from sick (K/BxN) mice as well as healthy BxN mice. Blood samples were allowed to clot at room temperature for 1 hour. Samples were centrifuged for 10 min at 1600 rpm in a Heraeus Biofuge pico and the clear serum was separated carefully. The serum samples were pooled together and used for arthritis induction.

Arthritis was induced in the recipient mice by intraperitoneal (ip) injection of 100  $\mu$ l of pooled K/BxN serum. The mice received one injection at day 0 and the disease onset was monitored until day 12. Transiently sympathectomised Balb/c mice were divided into two groups; one received pooled K/BxN serum and the other received PBS as control group. Development of arthritis was monitored carefully in both the groups. Similarly the vehicle alone treated control Balb/c mice were divided into two groups. One group received pooled K/BxN serum injection intraperitoneally and the other received PBS as control. Permanently sympathectomised Balb/c mice and their control mates (vehicle alone recipients) were also given intraperitoneal injection of pooled K/BxN serum for arthritis induction and PBS as control in a similar fashion as

---

discussed above. Arthritis was scored by measurement of ankle swelling and clinical index.

### **2.11. Protein Purification**

#### **2.11.1. Purification of Cryoglobulin**

Peripheral venous blood was taken at least 12 hours after the last meal from patients and transported at 37°C to the laboratory. After clotting and centrifugation at 37°C, serum was removed. The cryoglobulin was precipitated from serum after incubation for 24 hours at 4°C and isolated by centrifugation at 1400 rpm for 20 min at 4°C in a Haraeus Multifuge 3 S-R. The cryoglobulin fraction remained at the bottom of the tube as a precipitate. The supernatant was taken out and kept at 4°C for 24 to 36 hours to remove any cryoprecipitate. The partially purified cryoglobulin present in the form of a precipitate was washed with ice-cold phosphate buffered saline (PBS), pH 7.2. The sample was re-solubilized by incubating at 37°C and again precipitated at 4°C. The cycle of cryo-precipitation and re-solubilization was carried out for 6 times in order to remove unspecific serum proteins possibly trapped in the precipitate. The purity of the samples was checked by SDS polyacrylamide gel electrophoresis (PAGE).

#### **2.11.2. Protein G Affinity Chromatography**

The supernatant obtained from the above purification was subjected to affinity chromatography using Hi Trap Protein-G columns (Amersham-Pharmacia Biotech, Freiburg, Germany) for purification of IgG molecules present in the sample which did not cryoprecipitate. The supernatant was centrifuged at 1400 rpm for 10 minutes in

a Haraeus Multifuge 3 S-R and then filtered through a 0.45  $\mu\text{m}$  filter. The Hi Trap Protein G column (1ml) and buffers were warmed to room temperature. The column was connected to AEKTA Prime (Amersham-Pharmacia Biotech, Freiburg, Germany) and equilibrated with five column volumes of de-gassed distilled water followed by 3 column volumes of binding buffer (0.02M Sodium Phosphate buffer, pH 7.0) at a flow rate of 0.7 ml per minute. Then the supernatant was applied to the column for binding IgGs with the column matrix. The column was washed with binding buffer until no protein was observed in the eluent. The eluent was checked for protein by measuring the OD at 280nm. The elution was carried out with 3 ml of elution buffer (0.1M Glycin-HCl, pH 2.7) and the fractions were collected into tubes containing 200  $\mu\text{l}$  neutralizing buffer (1.0M Tris-Cl, pH 9.0). Soon after elution, the column was re-equilibrated with 10 ml of binding buffer (0.02M Sodium Phosphate buffer, pH 7.0). The eluted IgG fractions constitute the non-pathogenic immunoglobulins, which do not cryoprecipitate. IgG concentration was determined by measuring the OD at 280 nm.

### **2.11.3. Fast Performance Liquid Chromatography**

The samples were dissolved in Phosphate Buffered Saline (PBS) pH 7.2 (137mM NaCl, 2.7mM KCl, 10mM  $\text{Na}_2\text{HPO}_4$ , 2mM  $\text{KH}_2\text{PO}_4$ ) at 37°C and were filtered through a 0.45 $\mu\text{m}$  filter paper prior to loading onto a Superdex-200 HR gel filtration column attached to AEKTA Prime (Amersham Pharmacia Biotech, Freiburg, Germany). The elution buffer PBS pH 7.2 was filtered through a 0.45 $\mu\text{m}$  filter paper and degassed for 1 hour. The degassed buffer was used for calibrating the column prior to the sample loading. The column was washed with degassed buffer over night at a flow rate of 0.2

ml per minute. The base line was established to make sure the column is clean. The AEKTA Prime was connected to a chart recorder for plotting the curves.

Standard Molecular weight marker (Amersham Pharmacia Biotech, Freiburg, Germany) mix was prepared as per the manufacturers instructions and loaded to the column for calibration. The elution profiles of the standard molecular weight markers were noted from the chart recorder and subsequently used for the generation of the standard curve. The elution profile of the sample protein was noted down and then the molecular weight was deduced from the standard curve. The flow rate of the column was set to 0.7ml per minute and the chart recorder speed was set at 1cm per minute. Samples from specific elution peaks were collected separately in fractions and used for SDS PAGE and isotype specific immunoblotting.

### **2.11.4. SDS PAGE**

30% acrylamide mix solution (29%(w/v) acrylamide and 1%(w/v) N,N'-methylene-bis-acrylamide), electrophoresis grade sodium dodecyl sulfate (SDS), Tris base, ammonium persulfate (APS), N,N,N',N'-tetramethylethylenediamine(TEMED) and Glycine were purchased from Roth, Karlsruhe, Germany.

For SDS-PAGE under non-reducing condition, gels with 6% acrylamide in the resolving part and 5% acrylamide in the stacking part were prepared in the laboratory as per standard protocol. For SDS-PAGE under reducing condition, gels with 10% acrylamide in the resolving part were prepared. Gels were placed in the electrophoresis tank (Biorad, Munich, Germany) filled up to the mark with the electrophoresis buffer (25mM Tris base, 250mM glycine pH 8.3 and 0.1% SDS). Protein samples were boiled with the 1x SDS gel-loading buffer (50mM Tris-Cl pH 6.8, 100mM DTT, 2%(w/v)

---

SDS, 0.1% bromophenol blue, 10%(w/v) glycerol) for 5 minutes at 90°C. After cooling, the samples were centrifuged for 5 minutes at high speed on a tabletop centrifuge and then the supernatants were loaded on to the gel. The apparatus was connected to the power supply and electrophoresed for 2 hours at 50V and 200mA.

The Coomassie Brilliant Blue R-250 is an aminotriarylmethane dye that forms strong complexes with proteins and is used widely for staining the protein bands on polyacrylamide gels. Separated Polypeptides on the gel matrix were stained with staining solution (0.25g of Coomassie Brilliant Blue R-250 in 100 ml of methanol:water:acetic acid (45:45:10 (v/v)) by rocking gently on a platform for 4 hours at room temperature. Destaining of the gel was done by slowly rocking the gel in 5 volumes of the de-staining solution (45ml methanol + 45 ml water + 10 ml acetic acid) for 4 to 8 hours. The stained protein bands were visualized on a gel illuminator.

## **2.12. Spectroscopy**

### **2.12.1. UV/Vis- Spectroscopy**

Spectrophotometric analysis of the FPLC-purified cryoglobulin complex was done using a double beam UV/Vis- Spectrophotometer equipped with a jacketed cell holder (Lambda 16, Perkin Elmer, Weiterstadt, Germany). The cryoglobulin (1mg/ml) was filled in a 1ml rectangular quartz cuvette with a magnetic stirrer in it. The temperature in both the cuvettes was maintained using a circulating water bath and constantly monitored with calibrated thermistor. A base line was established between 600 nm and 250 nm at 37°C and subtracted from all subsequent spectra. After obtaining the spectra at 37°C, the temperature was lowered to 4°C progressively and again brought back to 37°C. The change in absorbance was recorded as evidenced by the light scattering at

---

600 nm. Four cycles were repeated to establish the reproducibility of the spectral changes with respect to temperature.

The effect of osmolytes on cryoprecipitation was studied in a different assay using an UV/Vis- spectrophotometer fitted with six peltier controlled jacketed cell holders (Perkin Elmer, Weiterstadt, Germany). Samples at different concentrations were kept at a time for measurement and the temperature melt was carried out from 37°C to 4°C while monitoring the changes in optical density at 600 nm. Each experiment was for four consecutive cycles of cooling and heating. Hence the spectra were obtained for cold induced precipitation followed by resolubilization due to heating to 37°C. Data were collected at an interval of 0.1°C and finally analyzed by using Sigma Plot software. The Cryoglobulins were dissolved in PBS pH 7.0 and incubated at 37°C for one hour prior to the actual experiment. For concentration dependent studies, four different concentrations (0.125mg/ml, 0.25mg/ml, 0.5mg/ml and 1.0mg/ml) of cryoglobulins were taken. Osmolytes like Sarcosine and TMAO (Sigma-Aldrich Chemie GmbH, Steinheim, Germany) were prepared in PBS pH 7.0. Cryoglobulins at a concentration of 1 mg/ml were incubated with 1M, 2M and 3M Sarcosine solution in a final volume of 2 ml in different tubes and incubated at 37°C. Similarly the TMAO concentrations were 1M, 1.5M and 2M. The Chaperon like effect of Cyclodextrin was studied in a similar experimental set up.

### **2.12.2. Kinetics Experiments**

The time dependent kinetics of cryoprecipitation was studied in UV/Vis- Spectrophotometer (Kontron Instruments, Germany) fitted with jacketed cell holders. The temperature of the cuvette holder was maintained by a circulating water bath. The

---

cuvette chamber was flushed with nitrogen gas while the experiment was on progress in order to avoid condensation. Cryoglobulin was dissolved in PBS pH 7.0 at stock concentration of 9 mg/ml. For concentration dependent study, samples of three different concentrations (2.0 mg/ml, 3.0 mg/ml and 4.0 mg/ml) were prepared and incubated at 37°C for 1 hour. Initially, only buffer (PBS pH 7.0) was taken in the cuvette and the cuvette temperature was maintained at 4°C. After establishing a base line, cryoglobulin was added to cuvette containing cold buffer with the help of a syringe from the top without disturbing temperature set up. Change in optical density was recorded as a function of time and the data was collected with the help of UVIKON software. Similarly, for chaperon assisted refolding study, cryoglobulin (3.0mg/ml) was incubated with different cyclodextrin (Sigma-Aldrich Chemie GmbH, Steinheim, Germany) concentration (0.25mM, 0.5mM, 1.0mM, 1.3mM, 1.5mM, 2.0mM and 2.5mM) at 37°C prior to the experiment. Data was collected with the help of the UVIKON software finally analyzed with the help of Sigma Plot software.

---

## CHAPTER III

### RESULTS

#### 3.1. Contribution of *Cr2* Gene in Murine Autoimmune Arthritis

The *Cr2* gene encodes both complement receptors CD21 (CR2) and CD35 (CR1) while the former is a splice variant of the later (Kurtz et al., 1990; Molina et al., 1990). The role of the CD21 in humoral immune response has been studied in different inflammation models soon after the availability of mice genetically deficient for the *Cr2* gene (Ahearn et al., 1996). The critical role of complement in maintenance of self-tolerance has been investigated in immunoglobulin transgenic models and in the lupus-like murine model of CD95 (*fas*) deficiency (Prodeus et al., 1998). The role of CD21/CD35 has been studied in an antibody-induced model of arthritis (Solomon et al., 2002). However, we have attempted to study the genetic deficiency of *Cr2* gene in the K/BxN (Kouskoff et al., 1996) murine model of chronic rheumatoid arthritis.

##### 3.1.1. Generation of Mice Lines

K/BxN mice strain, which develops arthritis spontaneously at about the third week after birth, is the F1 generation of the TCR- $\alpha\beta$ -transgenic KRN mouse strain crossed with the NOD mouse strain. The KRN transgenic TCR (originally designed to detect bovine pancreatic ribonuclease (RNase peptide 41-61) recognizes a glycolytic enzyme, Glucose-6-phosphate isomerase (GPI) (Basu et al., 2001; Matsumoto et al., 1999) in the context of NOD MHC class II A<sup>g7</sup> molecule in the K/BxN model of RA. The KRN TCR transgene is kept heterozygous in the KRN mouse strain (B6 background). So the resulting cross between KRN and NOD strain gives rise to two types of F1 mice:

K/BxN sick (carrier of TCR transgene) and BxN healthy mice (lack TCR transgene). Our aim was to generate a mouse line, which carries KRN TCR transgene but lacks *Cr2* gene by crossing *Cr2*<sup>-/-</sup> mouse strain with KRN strain. Similarly we generated a NOD mouse line lacking *Cr2* gene.

### 3.1.1.1. Generation of *Cr2*<sup>-/-</sup>KRN Mouse Line

The KNR strain was maintained by back crossing with the C57BL/6 strain. KRN TCR transgene positive mice were screened by FACS analysis of peripheral blood lymphocytes using CD4-PE and Vβ6-FITC antibodies (Figure 3).

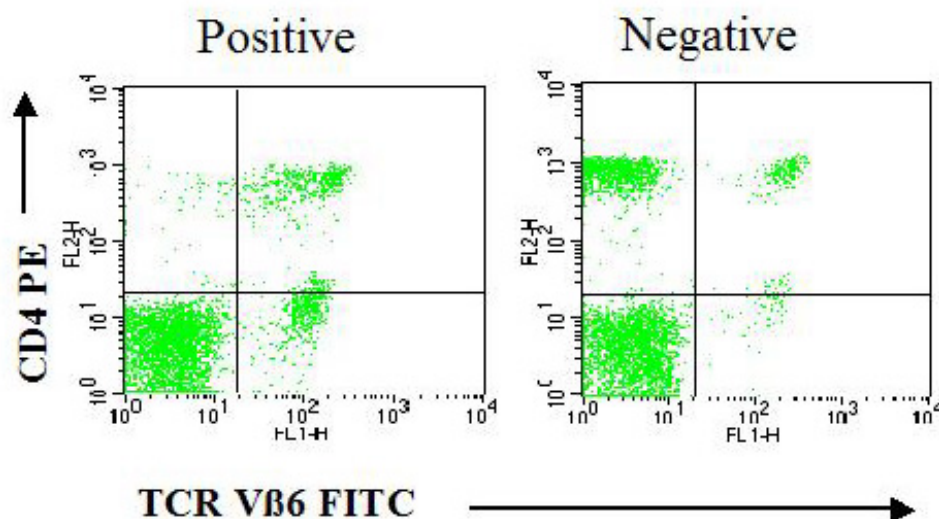


**Figure 3.** Peripheral blood lymphocytes from KRN TCR transgene positive and negative mouse stained for CD4 and Vβ6

The KRN TCR transgene positive mice (*Cr2*<sup>+/+</sup>KRN<sup>+/+</sup>) were crossed with the *Cr2*<sup>-/-</sup> mice (*Cr2*<sup>-/-</sup>KRN<sup>-/-</sup>) resulting in two types of F1 offspring: one heterozygous for the *Cr2*<sup>-/-</sup> locus and KRN TCR<sup>+</sup> (*Cr2*<sup>+/-</sup>KRN<sup>+/-</sup>) and the other heterozygous for the *Cr2*<sup>-/-</sup>



---

In order to screen mice deficient for the *Cr2* gene, the expression of the CD21 molecule on peripheral B-lymphocytes were analyzed by FACS using B220-PE and CD21-FITC antibodies (Figure 5). Four different phenotypes were produced in the backcross. Out of the four only the mice carrying the KRN TCR transgene and lacking both *Cr2* alleles ( $Cr2^{-/-}KRN^{+/-}$ ) were selected for further breeding. The strain was maintained by backcrossing with ( $Cr2^{-/-}KRN^{-/-}$ ) mice for further experiments.

### 3.1.1.2. Generation of $Cr2^{-/-}$ NOD Mouse Line

The NOD mice carrying the MHC haplotype H2-K<sup>d</sup> were crossed with the *Cr2* mice to generate a phenotype, which lack *Cr2* gene but carries the NOD MHC haplotype. The mouse strains were screened for the surface expression of MHC molecules by FACS analysis. The breeding scheme was followed as represented in figure 6. The F1 offspring of the cross between  $Cr2^{-/-}H-2^{g7/-}$  ( $Cr2^{-/-}$  mouse strain) and  $Cr2^{+/+}H-2^{dg7+/+}$  (NOD mouse strain) was backcrossed with the  $Cr2^{-/-}$  mouse strain to generate mice, lacking *Cr2* gene but were heterozygous for the NOD MHC allele. The Phenotype ( $Cr2^{-/-}H-2^{g7+/-}$ ) was screened by FACS analysis of peripheral blood lymphocytes using B220-PE, I-A<sup>d</sup>-FITC and I-A<sup>b</sup>A $\beta$ -FITC antibodies (Figure 7). Inbreeding of the phenotype ( $Cr2^{-/-}H-2^{g7+/-}$ ) resulted in the desired  $Cr2^{-/-}$ NOD ( $Cr2^{-/-}H-2^{g7+/+}$ ) mouse line (Figure 6).



### 3.1.1.3. Generation of $Cr2^{-/-}$ K/BxN and $Cr2^{-/-}$ BxN Mouse Line

In order to study possible effects of *Cr2* deficiency in murine rheumatoid arthritis we crossed the  $Cr2^{-/-}$ KRN mouse line with  $Cr2^{-/-}$ NOD line. The original arthritic K/BxN mice were the F1 offspring of KRN and NOD cross. In this experiment we obtained two kinds of mice depending on the inheritance of KRN TCR transgene as well (Figure 8). The clinical onset of arthritis in the  $Cr2^{-/-}$ K/BxN mice was studied in comparison with original K/BxN mice.

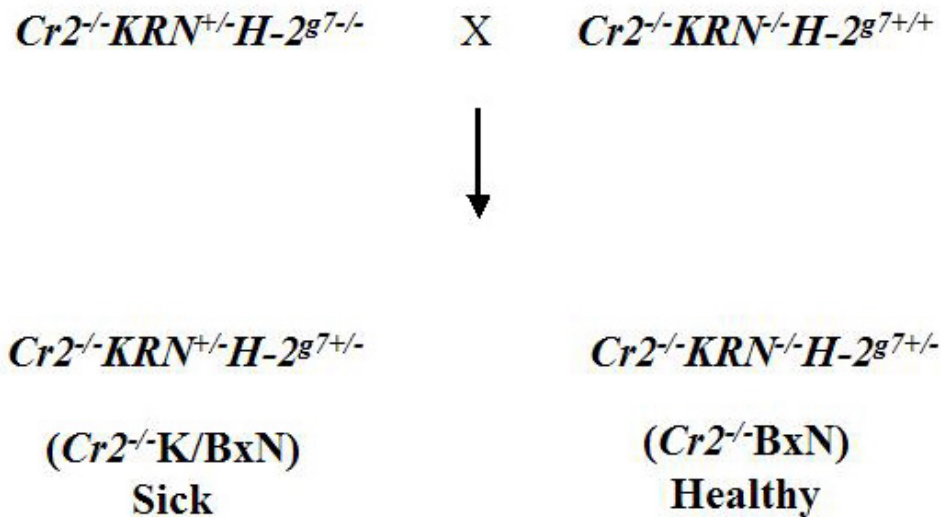


*Figure 8. Breeding scheme for the generation of  $Cr2^{-/-}$ K/BxN and  $Cr2^{-/-}$ BxN mouse lines*

---

### 3.1.2. Emergence of Auto-reactive CD4+ V $\beta$ 6+ T cell Clones in Cr2<sup>-/-</sup>

#### K/BxN Mouse strain

The first and most important requirement for arthritis development in K/BxN mice is the emergence of autoreactive CD4+V $\beta$ 6+ T cells in the periphery. These auto reactive T cells provide help to B cells and eventually the T and B collaboration leads to the organ specific disease onset at about third week of birth (Korganow et al., 1999; Kouskoff et al., 1996). The transgene encoded KRN T cell receptor recognizes glucose 6-phosphate isomerase as the autoantigen in the context of H-2<sup>g7</sup> MHC class II molecule (Matsumoto et al., 1999). In this respect we asked the question at which time after birth the autoreactive KRN T cells escape from the Thymus. We made a fluorimetric analysis of the peripheral blood lymphocytes from K/BxN, BxN, Cr2<sup>-/-</sup> K/BxN, and Cr2<sup>-/-</sup>BxN mice at different ages using CD4-PE and V $\beta$ 6-FITC antibodies (Figure 9 and 10). About the second week of age the autoreactive KRN T cells appeared in the periphery. In second week the percentage of CD4+ V $\beta$ 6+ T cells in PBLs of Cr2<sup>-/-</sup>K/BxN mice was about 4.12% whereas the percentage of CD4+ T cells was 6.12%. At the same time the percentage of CD4+ V $\beta$ 6+ T cells in PBLs of K/BxN was 4.56% where as the percentage of CD4+ T cells was 6.08%. In case of Cr2<sup>-/-</sup>BxN mice the percentage of CD4+ V $\beta$ 6+ T cells in PBLs was 3.12% and that of the BxN mice was 3.61% at the second week. At the same time the percentage of CD4+ T cells in PBLs of Cr2<sup>-/-</sup>BxN and BxN mice were 33.93% and 50.61% respectively. The number progressively increased with age and at about third week of age the mice showed considerable enrichment of the autoreactive KRN T cell in the periphery. At about the third week after birth the relative percentage of autoreactive KRN T cells in

---

the periphery of  $Cr2^{-/-}K/BxN$  and  $K/BxN$  were 20.12% and 18.26% respectively. At the same time the percentage of  $CD4^{+}$  T cells in the periphery of  $Cr2^{-/-}K/BxN$  and  $K/BxN$  were 22.56% and 20.46% respectively. Similarly in the third week after birth the percentage of  $CD4^{+} V\beta6^{+}$  T cells in the periphery of  $Cr2^{-/-}BxN$  and  $BxN$  mice were 5.42% and 5.24% respectively. At the same time the percentage of  $CD4^{+}$  T cells in the periphery of  $Cr2^{-/-}BxN$  and  $BxN$  were 53.32% and 47.84% respectively. So it seems that the thymocytes expressing the potentially autoreactive KRN TCR escaped clonal deletion much before the onset of the disease. The most plausible reason could be the incomplete allelic exclusion.

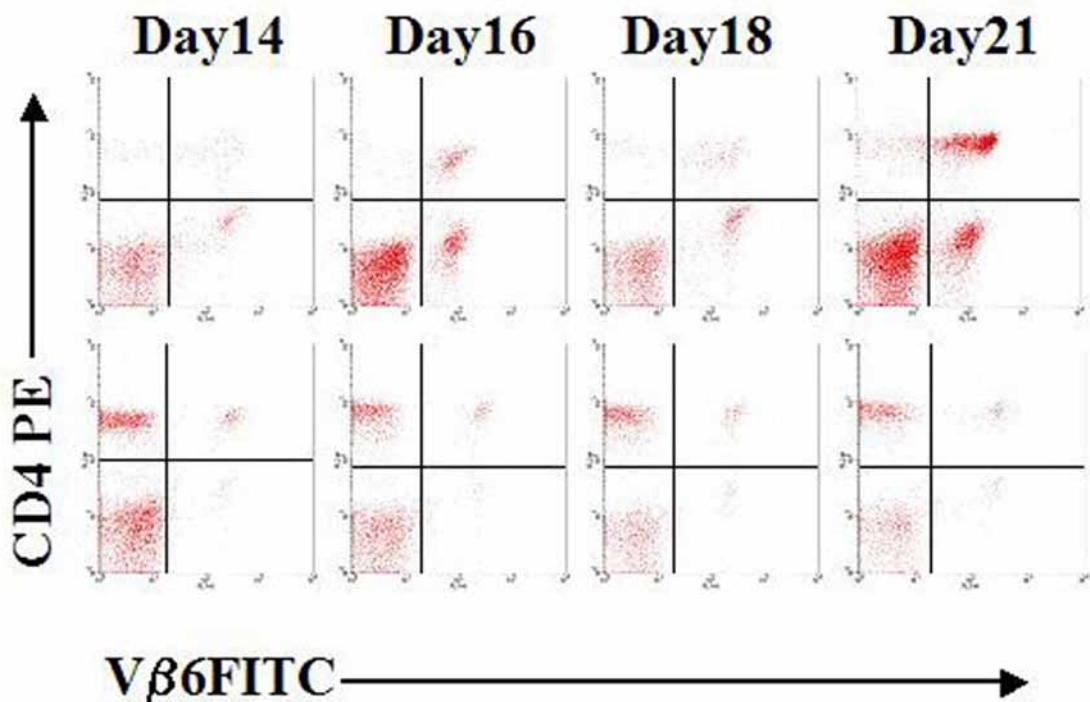


**Figure 9.** Peripheral blood lymphocytes of  $Cr2^{-/-}K/BxN$  (upper row) and  $Cr2^{-/-}BxN$  (lower row) mice stained for CD4 and Vβ6.

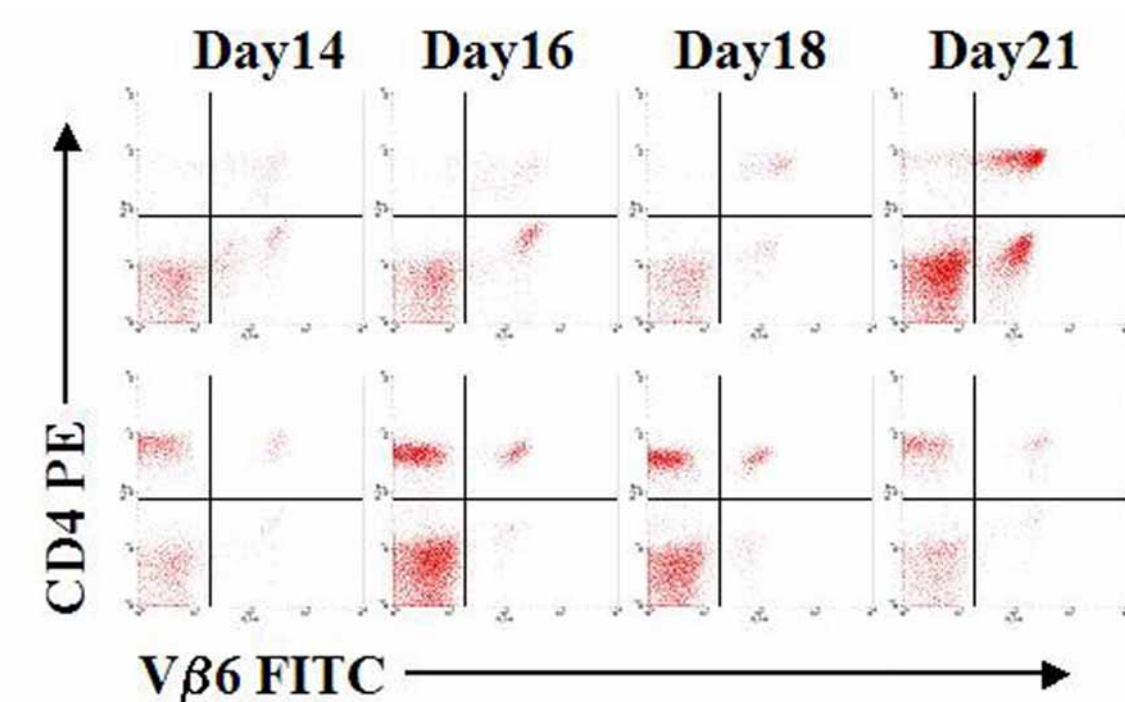


*Figure 10. Peripheral blood lymphocytes of K/BxN (upper row) and BxN (lower row) mice stained for CD4 and Vβ6*

### 3.1.3. High levels of Anti-GPI antibodies in Cr2<sup>-/-</sup>K/BxN Mouse strain

The most striking observation in the K/BxN model is the occurrence of autoantibodies against the ubiquitously expressed glycolytic enzyme glucose 6-phosphate isomerase (GPI). B cells producing anti-GPI antibodies in K/BxN mice receive help from the T cell clones expressing KRN TCR (Korganow et al., 1999; Maccioni et al., 2002). We measured the anti-GPI antibody level in the serum of Cr2<sup>-/-</sup>K/BxN and K/BxN mice at different ages. Mice were periodically bled for serum preparation starting at 16 days of age until 32 days of age. The levels of anti-GPI antibodies in sera of Cr2<sup>-/-</sup>K/BxN and

K/BxN mice were measured by ELISA at different time points during ontogeny (Figure 11). The  $Cr2^{-/-}$ K/BxN mice showed much higher levels of anti-GPI antibodies in the serum starting from day 16 of age compared to K/BxN mice. The serum concentration of the anti-GPI antibodies constantly increased with age reaching the highest level at about 36 days of age. Thus, loss of *Cr2* resulted in early onset of autoantibody production in  $Cr2^{-/-}$ K/BxN mice, which is in agreement with the findings of Prodeus et al., (Prodeus et al., 1998) implying the role of *Cr2* in protection against auto reactive B cells.

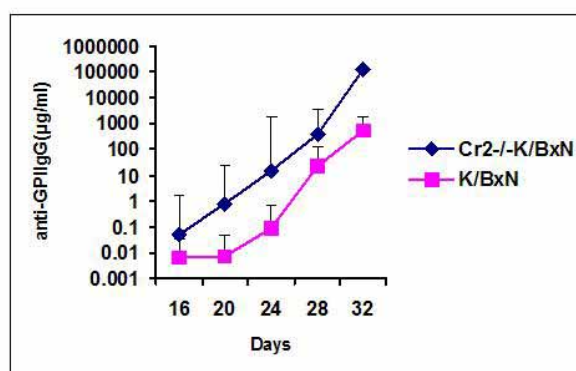


**Figure 11.** Anti-GPI IgG levels in the sera of  $Cr2^{-/-}$ K/BxN and K/BxN mouse at different ages

#### **3.1.4. The $Cr2^{-/-}$ K/BxN Mouse strain is Susceptible to Arthritis Development**

The most easily visible symptom in murine arthritis is the joint swelling. We monitored the disease in  $Cr2^{-/-}$ K/BxN mice starting at day 14 after birth. Quite interestingly the mice developed arthritis at about day 18 of age. So it was quite evident from our

observation that Cr2<sup>-/-</sup>K/BxN mouse strain is not protected rather susceptible to arthritis development.

#### **3.1.4.1. Clinical onset of Arthritis: Ankle Swelling in Cr2<sup>-/-</sup>K/BxN Mouse strain**

As joint swelling is the first clinical manifestation of the arthritis, we measured the joint swelling periodically. The disease was assessed by caliper measurement of the joint in Cr2<sup>-/-</sup>K/BxN and K/BxN mice in comparison to their transgene-negative littermate controls. The data were presented as the average ankle thickness and clinical index as shown in figure 12 (A) and (B). The disease started with slight reddening of the paws and ankles. The ankle swelling was symmetrical that is all the four limbs were involved and hence the clinical index was always four at the onset of the disease. The first clinical onset of disease was about day 19 of age in case of Cr2<sup>-/-</sup>K/BxN mice whereas K/BxN mice showed first signs of ankle swelling at about day 21. The ankle swelling increased swiftly in case of Cr2<sup>-/-</sup>K/BxN mice compared to K/BxN mice. The average ankle thickness reached about 4 mm in both the groups of animal and showed a slight decrease in the ankle swelling at about day 36 of age and thereafter. The disease showed proximal to distal severity. The paws were maximally affected.

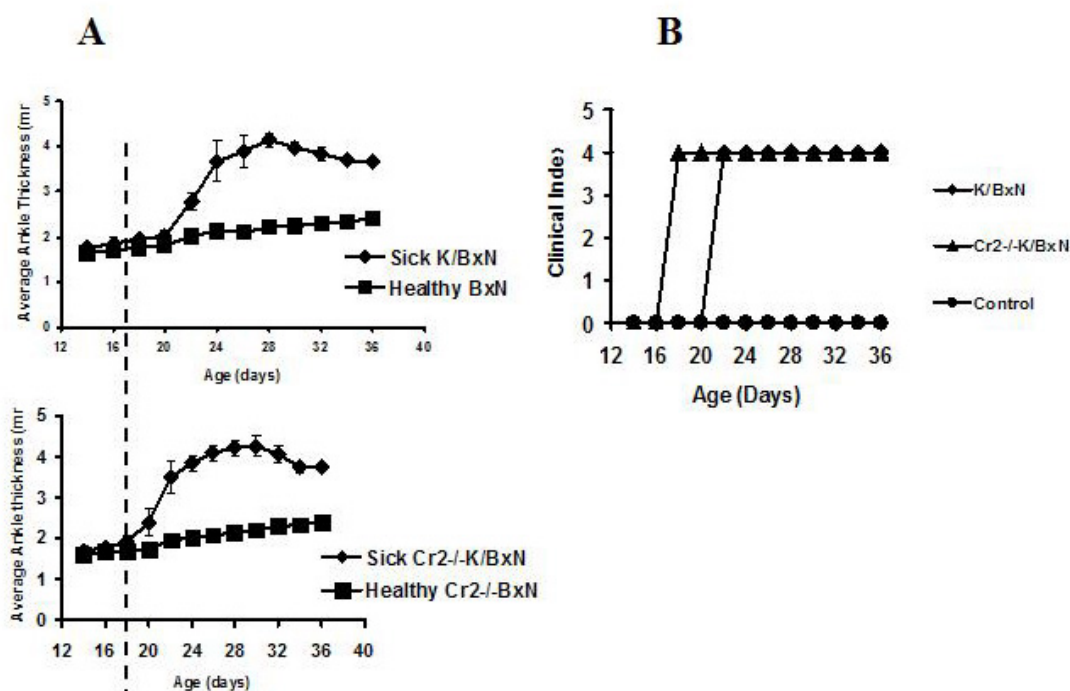


**Figure 12.** Average ankle thickness (A) and Clinical Index (B) of sick Cr2<sup>-/-</sup>K/BxN, sick K/BxN mice and their healthy litter mate controls at different ages

### 3.1.4.2. Locomotor Activity of Cr2<sup>-/-</sup>K/BxN Mouse strain

Morning stiffness is an important parameter in the diagnosis of human RA (Arnett et al., 1988). In order to assess the ability of the animals to move and climb inside the cage, we measured the locomotor activity during acute phase of the disease. Along with the early onset and fast progression of RA in case of the Cr2<sup>-/-</sup>K/BxN mice we observed a dramatically decreased walking behavior (Figure 13, A). Since the phalanges were the most damaged structures in the acute phase of the disease, we observed less perching and climbing ability in case of both the mice strains (Figure 13, B). The climbing and walking ability of Cr2<sup>-/-</sup>K/BxN mice was most compromised as compared to the K/BxN mice. Mice analyzed in this set of experiments were age and sex matched.

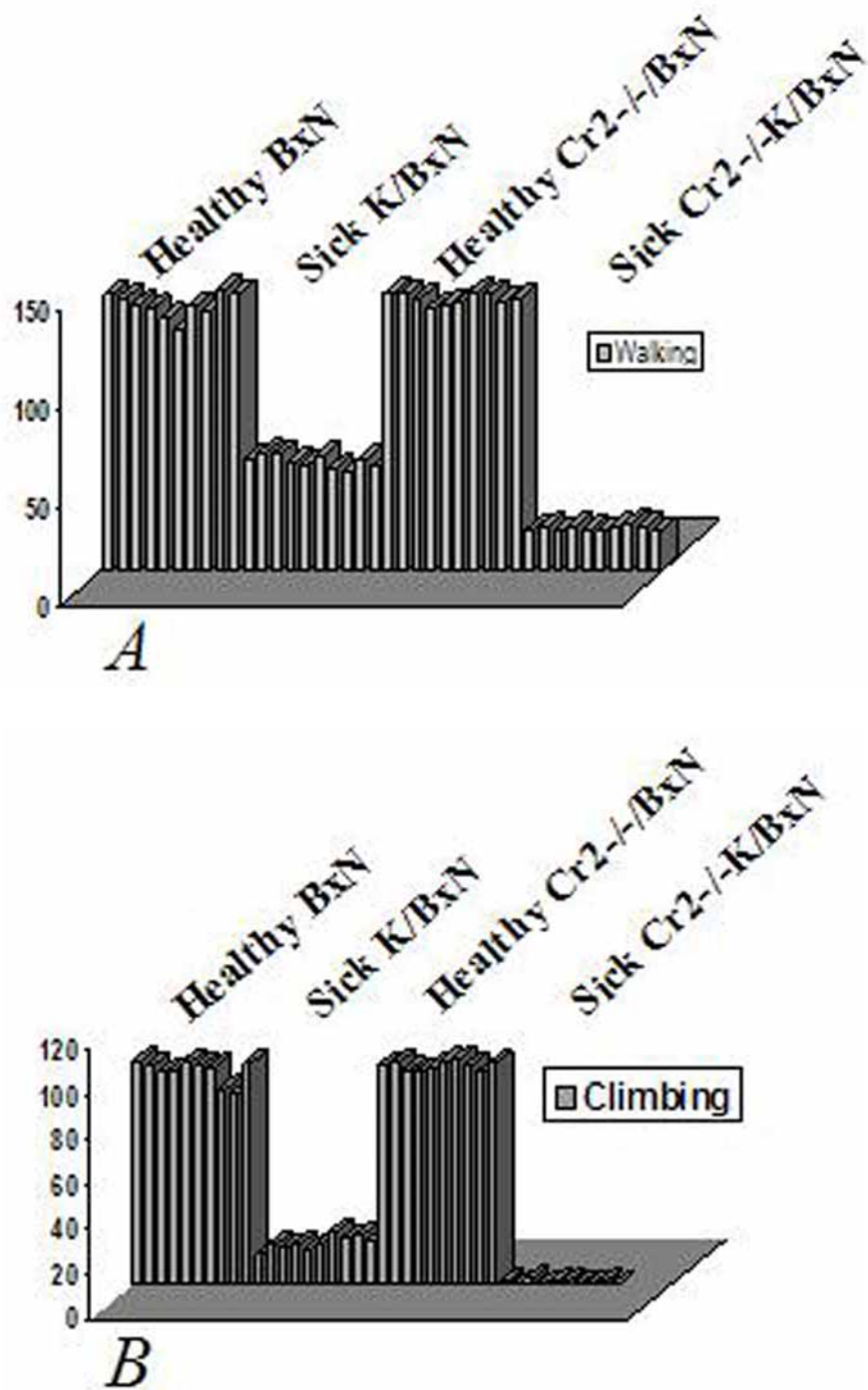
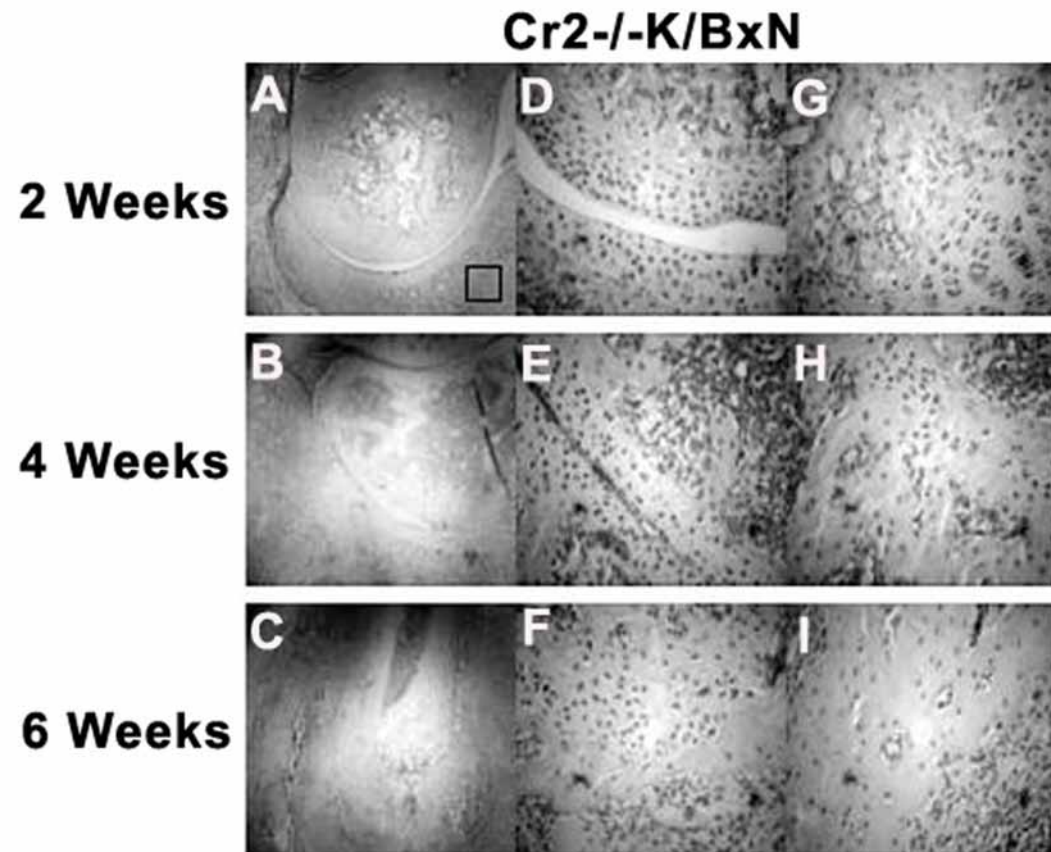
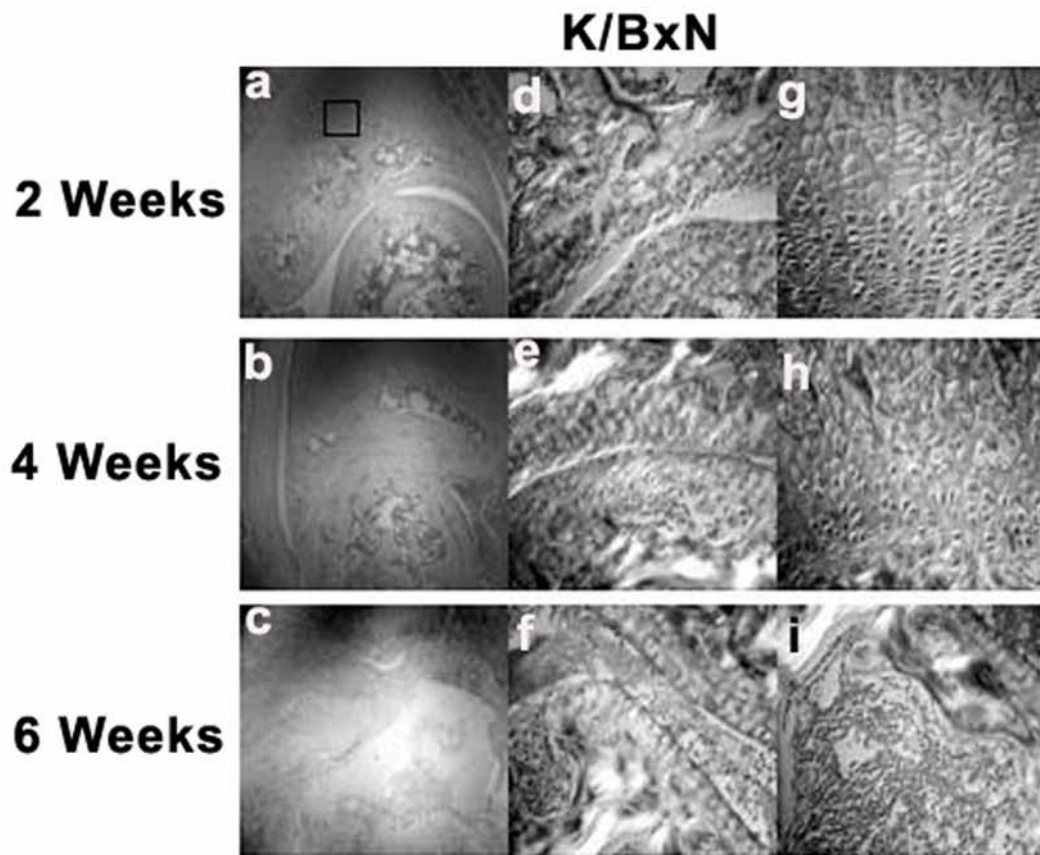


**Figure 13.** Assessment of locomotor activity of sick  $Cr2^{-/-}K/BxN$ , sick  $K/BxN$  mice and their healthy littermate controls. (A) shows walking and (B) shows climbing behavior

---

### 3.1.4.3. Histological Assessment of Joint Destruction in the Cr2<sup>-/-</sup> K/BxN Mouse strain

In order to assess the damage in the joint architecture of Cr2<sup>-/-</sup>K/BxN and K/BxN mice we prepared joint sections at different ages. Ankle sections were prepared from animals sacrificed at two weeks of age (prior to onset of disease), four weeks of age (soon after the onset of disease) and six weeks of age (acute phase of the disease). The Hematoxylin and Eosin stained sections (Figure 14) showed quite normal joint architecture at two weeks of age. The synovial cavity was free from infiltrates, the synovial membrane showed no signs of inflammation and cartilage and bone were not affected. The epiphyseal growth plate region of the tibia showed columnar stalks of normally dividing chondrocytes in K/BxN mice but the epiphyseal growth plate chondrocytes of Cr2<sup>-/-</sup>K/BxN mice showed signs of poor division and elongation. The chondrocytes in epiphyseal growth plate play a crucial role in elongation of the long bones at day 14 of age. The cells in the epiphyseal growth plate remain active during childhood. These cells stop differentiating when the animal stops to grow. The epiphyseal growth plate has got two ends one facing the articular cavity of the joint made up of a layer of stratified cartilage and the other end facing the bone is called growing cartilaginous end. In between these two ends, fast dividing tall columnar chondrocytes are present (Figure 14, g & G). The chondrocytes in the growth plate region stained with toluidine blue, showed no signs of damage in K/BxN mice. To the contrary chondrocytes in the growth plate region appeared abnormal in Cr2<sup>-/-</sup>K/BxN mice (Figure 15, d & D).



---

**Figure 14.** Eosin and Hematoxylin stained sections of ankle joints at different ages of K/BxN and Cr2<sup>-/-</sup>K/BxN mice.

Sections (a-c under 10x) & (d-f under 40x) of K/BxN mice and sections (A-C under 10x) & (D-F under 40x) of Cr2<sup>-/-</sup>K/BxN mice show joint structure at different stages of disease. Sections (g-i under 40x) of K/BxN and (G-I under 40x) of Cr2<sup>-/-</sup>K/BxN mice show chondrocytes at growth plate region at different stages of disease

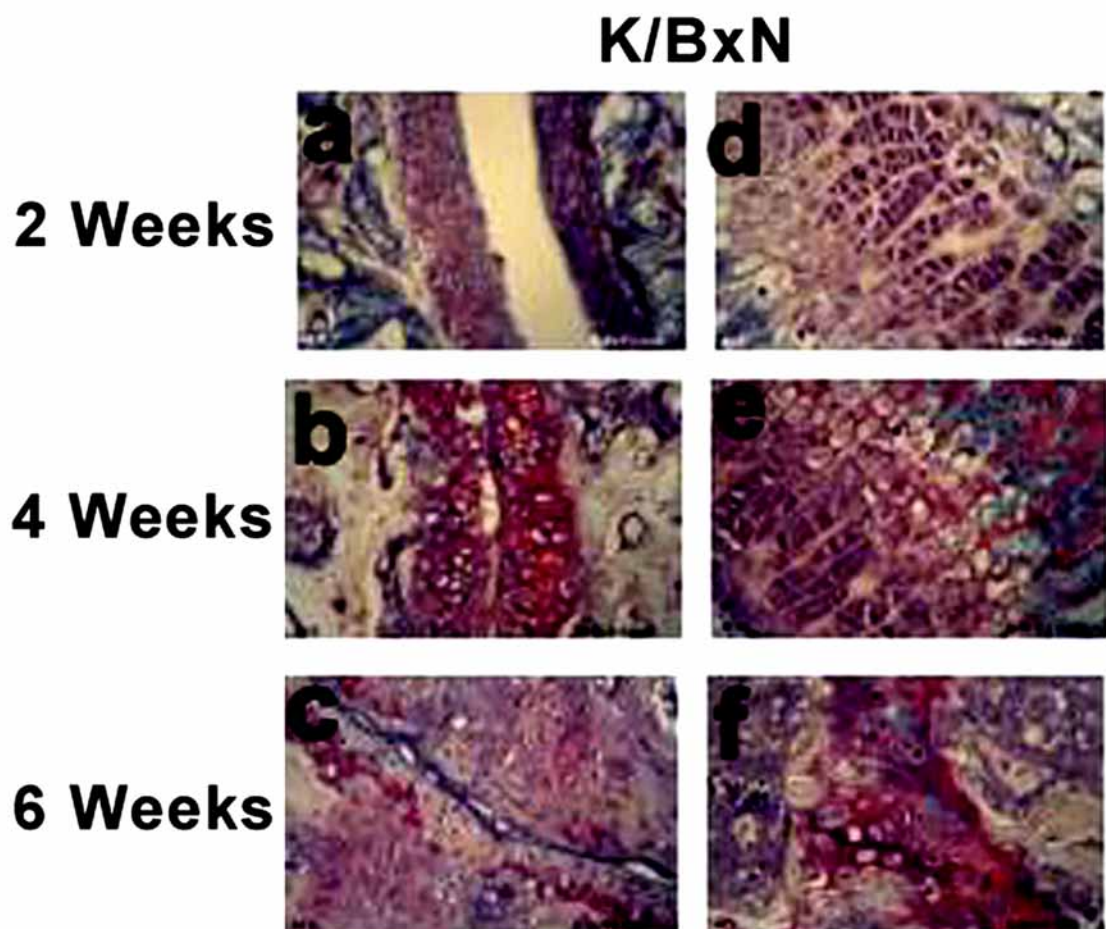
Ankle joint sections from four weeks old animals showed hyperplastic synovia, with massive infiltration of inflammatory cells and the beginning of fibrosis. Considerable hypertrophy of the articular cartilage was clearly visible in K/BxN (Figure 14, b & e) and (Figure 15 b) as well as Cr2<sup>-/-</sup>K/BxN mice (Figure 14, B & E) and (Figure 15 B). Toluidine blue stains the proteoglycans present in chondrocytes. The chondrocytes are mostly present in the lining of the articular cavity (Figure 15 a & b) and (Figure 15 A & B) as well as in the epiphyseal growth plate region of long bones (Figure 15 d & e) and (Figure 15 D & E). In the 4<sup>th</sup> week there are less toluidine blue positive chondrocytes in the growth plate region of Cr2<sup>-/-</sup>K/BxN mice (Figure 15 E) compared to K/BxN mice (Figure 15 e). The articular cavity visible in 2<sup>nd</sup> week (Figure 15 a & A) gets constricted in the 4<sup>th</sup> week due to synovial hyperplasia (Figure 15 b & B).

At the 6<sup>th</sup> week the joint architecture was completely lost in K/BxN mice (Figure 14 c & f) as well as Cr2<sup>-/-</sup>K/BxN mice (Figure 14 C & F). There was massive infiltration of neutrophils. Synovitis had extended all over the cartilage forming clearly defined pannus (Figure 16). At this stage there were a few toluidine blue positive chondrocytes in the epiphyseal growth plate region of Cr2<sup>-/-</sup>K/BxN mice (Figure 15 C & F) compared to K/BxN mice (Figure 15 c & f). Since epiphyseal growth plate chondrocytes were

---

---

more affected in Cr2<sup>-/-</sup>K/BxN mice, this strain showed retarded growth upon development of arthritis.



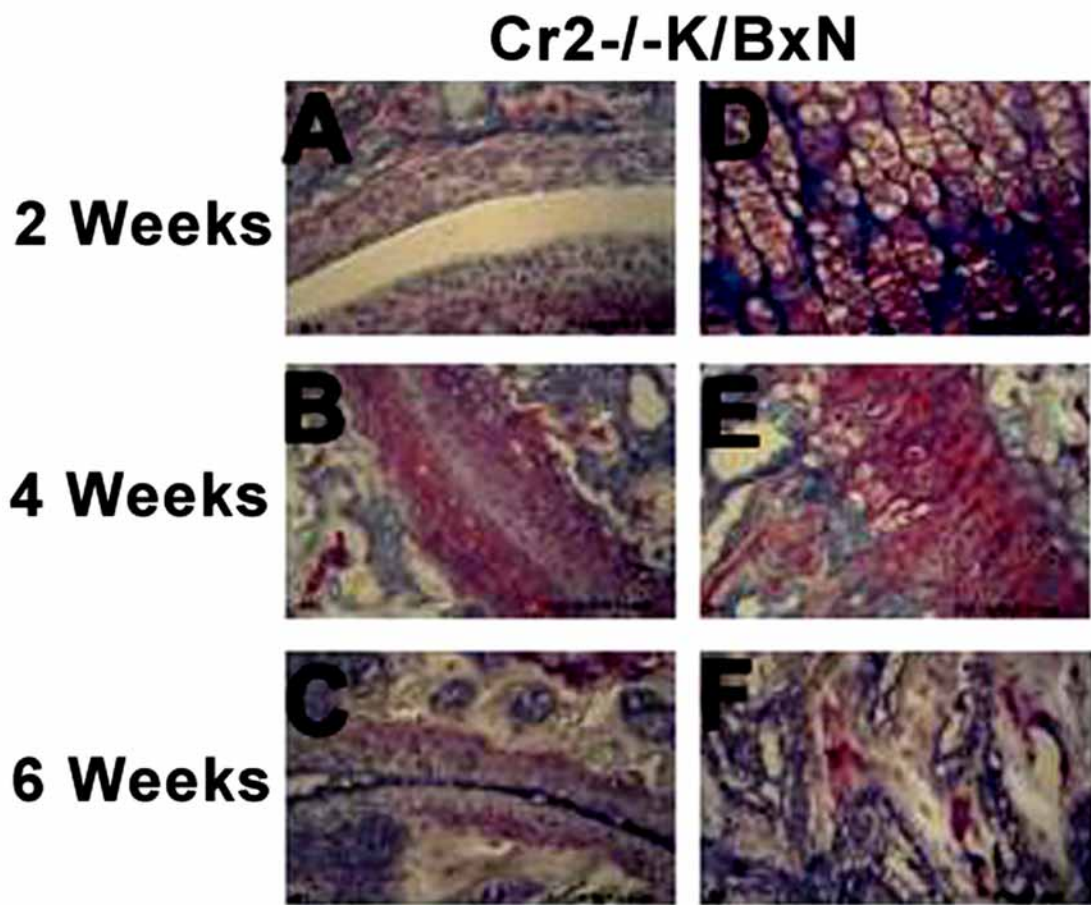


**Figure 15.** Toluidine blue staining of ankle joints at different ages of K/BxN and Cr2<sup>-/-</sup>-K/BxN mice.

Sections (a-c) of K/BxN and sections (A-C) of Cr2<sup>-/-</sup>-K/BxN mice show proteoglycan staining in articular cartilage at different stages of disease. Sections (d-f) of K/BxN and sections (D-F) of Cr2<sup>-/-</sup>-K/BxN mice show proteoglycan staining in growth plate region

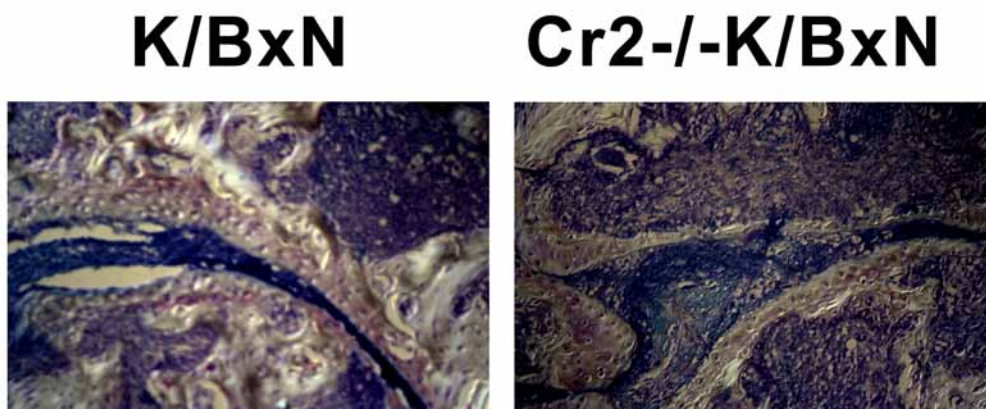


*Figure 16. Eosin and Hematoxylin stained sections showing infiltrating neutrophils and pannus formation in late stage of disease in K/BxN and Cr2<sup>-/-</sup>K/BxN mice*

#### **3.1.4.4. Growth in Cr2<sup>-/-</sup>K/BxN Mouse strain is impaired due to Arthritis**

The long bones increase in length during childhood through adolescent period by a mechanism called endochondral ossification. This ossification center lies in the inner end of epiphyseal growth plate of cartilage. The outer end is not ossified but remains as the articular cartilage and the inner end is constantly replaced with bone cells or osetoblasts. Also at the same time the bone undergoes constant remodeling by two parallel but interdependent activities called osteoblastogenesis (formation of new bone) and osteoclastogenesis (resorption of bone). Both the process act in concert and thus the size and shape of the bone remains in order. The cell types giving rise to new bones are

called osteoblasts and the cell types involved in bone resorption are called osteoblasts. Disturbance in the functioning of these cells results in abnormal growth. In order to assess the growth pattern of the  $Cr2^{-/-}$ K/BxN and K/BxN mice during arthritis development, skeletal preparation of hind limb bones were made. The size considerably differed from each other, the smallest being the  $Cr2^{-/-}$ K/BxN mice (Figure 17). The average length of the femur bone of the  $Cr2^{-/-}$ K/BxN mice was 1.4 cm, that of K/BxN mice was 1.7 cm and that of control mice was 1.9 cm. Similarly average size of the tibiofibula bone was 1.9 cm, 2.3 cm and 2.7 cm in  $Cr2^{-/-}$ K/BxN, K/BxN and control mice respectively. It was quite evident from these observations that the growth of the  $Cr2^{-/-}$ K/BxN mice was retarded due to arthritis development.

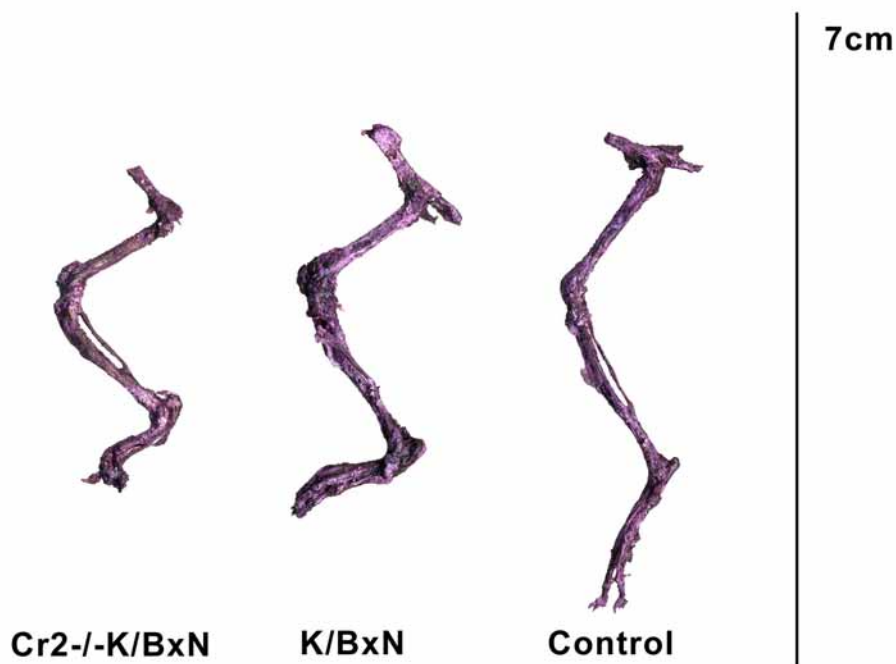


**Figure 17.** Skeletal preparation of hind limbs of K/BxN,  $Cr2^{-/-}$ K/BxN and control mice at six months of age.

*Paw, ankle and knee joints are mostly affected. Small size hind limb of  $Cr2^{-/-}$ K/BxN mouse represents growth retardation.*

### 3.1.5. Cr2<sup>-/-</sup>K/BxN Mouse strain has decreased Survival in Acute Phase of Arthritis

Having observed the severity of the disease in Cr2<sup>-/-</sup>K/BxN mice, we monitored the survival percentage of this strain in a stipulated period in comparison with the Cr2<sup>-/-</sup>BxN, K/BxN and BxN strains. Twenty mice from each strain were taken into study for a period of 16 months and death was recorded. The data were presented in a survival plot (Figure 18). No mice from Cr2<sup>-/-</sup>BxN, K/BxN or BxN strains died during the period of observation. But quite surprisingly, already 10% death was recorded at six months in Cr2<sup>-/-</sup>K/BxN mice. This percentage reached 50% at the end of one year and finally at the end of the study there was 90% death in Cr2<sup>-/-</sup>K/BxN mice. So the pathophysiological consequences of the disease are quite different in Cr2<sup>-/-</sup>K/BxN compared to K/BxN and healthy mice of the same genetic background.

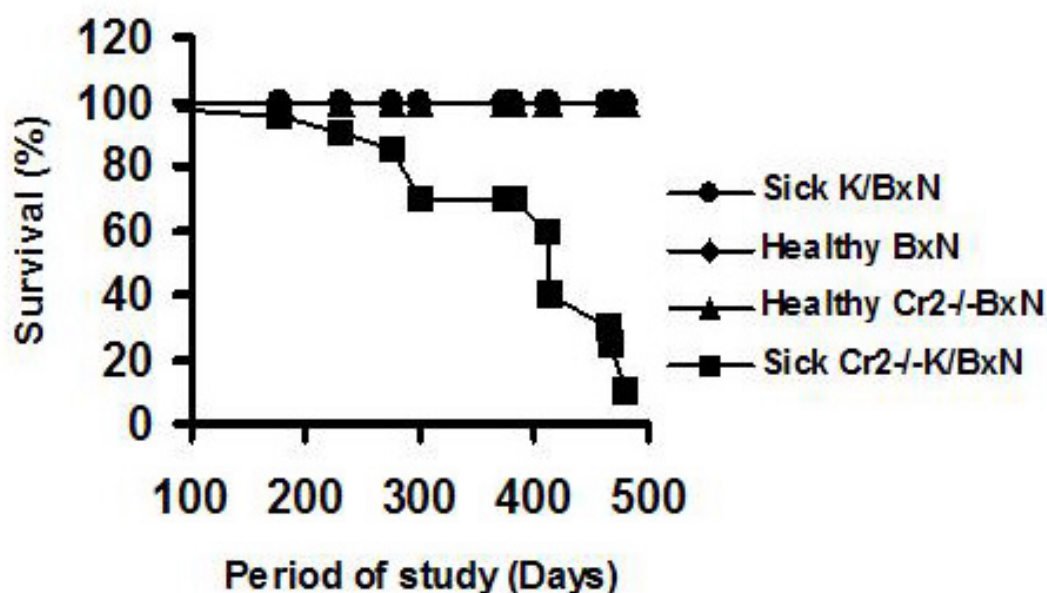


**Figure 18.** Survival Plot of K/BxN, Cr2<sup>-/-</sup>K/BxN and their healthy litter mates. Cr2<sup>-/-</sup>K/BxN mice have reduced survival during acute phase of arthritis

---

### **3.1.6. Transient Sympathectomy partially protects Balb/c Mice from Antibody-induced Arthritis**

Arthritis being a joint specific inflammatory disease is characterized by pain swelling and limited movement of the joint. The localized inflammatory response is characterized by swelling, heat, redness, pain and loss of function. In the acute phase response there is additional fever and synthesis of acute phase proteins by lymphocytes. In a chronic inflammatory response such as arthritis there is always joint specific accumulation of macrophages and cytokine production by activated fibroblasts. In any kind of inflammatory response there is always neutrophil infiltration. In addition there occurs mast cell degranulation and release of histamines and proteases that cause tissue damage. Symmetry of affected joints is one of the criteria to diagnose RA in humans. However no immunological explanation is given so far to this fact. In order to evaluate the role of the sympathetic nervous system in RA pathogenesis, we performed chemical sympathectomy of mice followed by induction of arthritis by K/BxN sera injection.

Sympathectomy was done using 6-OHDA and the depletion of sympathetic nerves was checked by western blot. Since lymphoid organs are richly supplied with sympathetic nerve fibers, we selected spleen for western blot analysis of Tyrosine Hydroxylase, a marker for sympathetic nerve fibers innervating lymphoid organs. The denervation of sympathetic nerve fibers in spleen was significant but not complete as presented in western blot analysis in Figure 19.

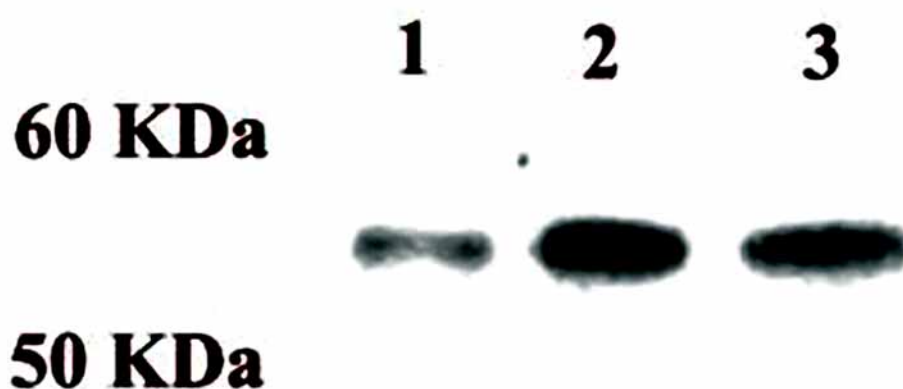


**Figure 19.** Western Blot analysis of Tyrosine Hydroxylase in spleen of 6-OHDA treated mice and control mice. Lane (1) permanently sympathectomised mice, lane (2) vehicle (ascorbate) treated mice and lane (3) transiently sympathectomised mice

Balb/c mice were taken for antibody-induced arthritis study because of their highest susceptibility (Solomon et al., 2002). When transiently sympathectomised mice were injected with K/BxN serum, joint swelling was observed in all the cases and hence the mice were not protected from antibody-induced arthritis. However, the onset of disease was on day two compared to the control mice (not treated with 6-OHDA), which showed first signs of arthritis on day 1 after injection of serum. So there was a delay in the onset of arthritis in transiently sympathectomised mice (Figure 20 a). The disease was evaluated by measurement of average ankle thickness and clinical index. In transiently sympathectomised mice the average ankle thickness reached maximum value of 2.7 mm on day three and the swelling decreased slowly from day four and finally reached an average ankle thickness of about 2.2 mm by day eighteen. In case of control mice the average ankle thickness reached maximum value of 3.1 mm on day

one, persisted until day four and thereafter reduced slowly to reach the normal value of 2.2 mm by day eighteen. Again the clinical index in case of control mice was four, which means all the four limbs were affected. To the contrary in case of transiently sympathectomised mice the clinical index was two, meaning only two limbs were affected (Figure 20 b).

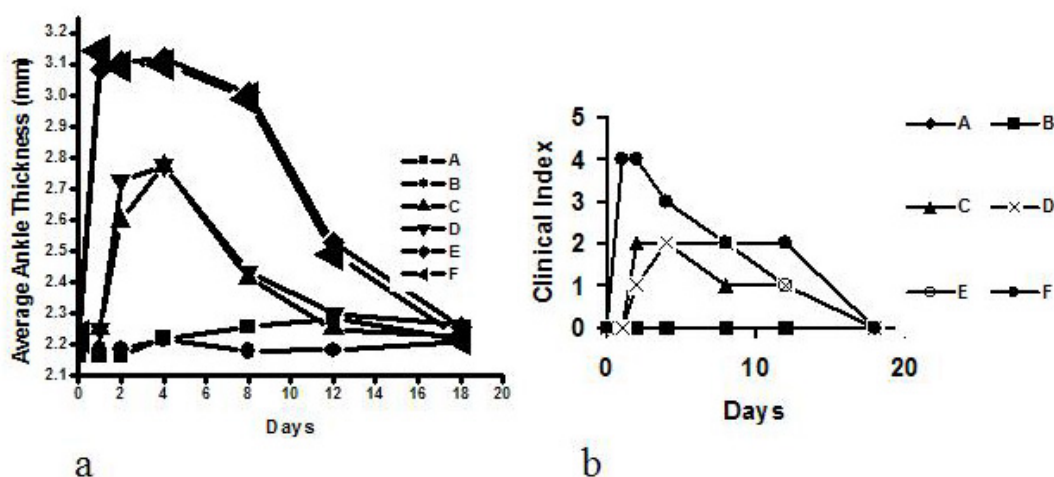


**Figure 20.** Average ankle thickness (a) and clinical Index (b) of transiently sympathectomised Balb/c and control Balb/c mice. A & B represents Balb/c mice treated with PBS, C & D represent transiently sympathectomized Balb/c mice treated with 100 $\mu$ l of K/BxN serum and E & F represents control Balb/c mice treated with 100 $\mu$ l of K/BxN serum.

### 3.1.7. Permanent Sympathectomy protects Balb/c Mice from Antibody-induced Arthritis

Permanent sympathectomy of Balb/c mice was done by injection of 6-OHDA on postnatal day one. The control mice received the vehicle (ascorbate) only. The sympathectomy was significant but not complete (Figure 19). The permanently sympathectomised mice were injected with K/BxN serum at 6 weeks of age. The ascorbate treated mice developed arthritis on day one as seen in previous experiments

(3.1.6). However the permanently sympathectomised mice did not develop the disease. The clinical index in case of the sick Balb/c mice were four (all the four limbs were affected) (Figure 21 a & b). There has been considerable debate regarding the role of sympathetic nerves in chronic inflammatory diseases (Fitzgerald, 1989; Levine et al., 1988; Levine et al., 1986; Nakamura and Ferreira, 1987). Usually pain is associated with stress, which increases the sympathetic activity. Drugs to block adrenoceptors are sometimes used in RA treatment. Sympathetic terminals terminate near blood vessels and mast cells in the synovium and therefore it is conceivable that neurotransmitters released from sympathetic nerves would influence vascular permeability and mast cell activity in joints. ATP released from the adrenergic terminals influence mast cells to degranulate.

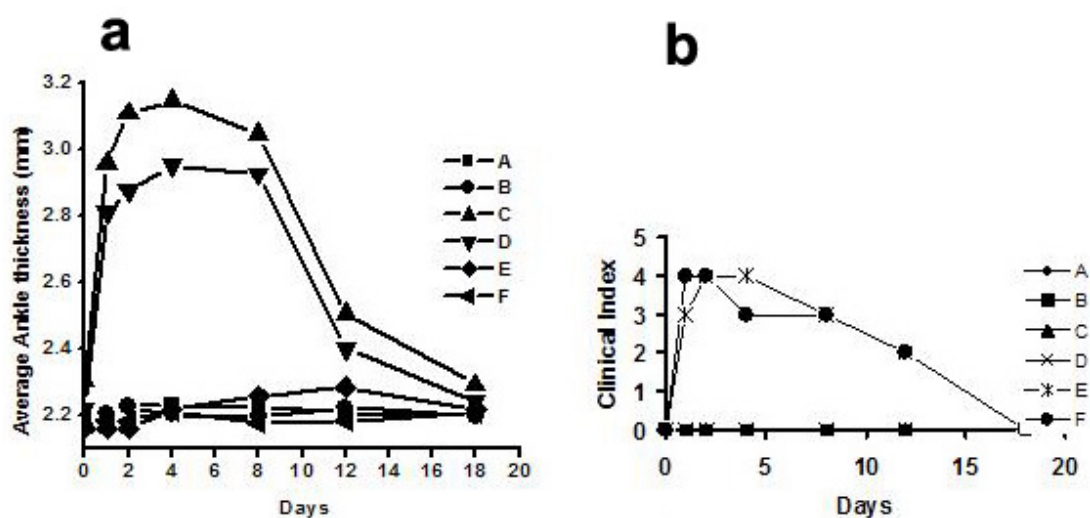


**Figure 21.** Average ankle thickness (a) and clinical Index (b) of permanently sympathectomized Balb/c and control Balb/c mice. A & B represents Balb/c mice treated with PBS, C & D represents permanently sympathectomized Balb/c mice treated with 100 $\mu$ l of K/BxN serum and E & F represents control Balb/c mice treated with 100 $\mu$ l of K/BxN serum.

### 3.1.8. SP<sup>-/-</sup> Mouse strain is partially protected from Antibody-induced Arthritis

In order to specifically observe the influence of the nervous system in arthritis, we investigated the role of peptide neurotransmitter substance P. Substance P is released from unmyelinated C fibers innervating ankle and knee joints. The role of substance P has been studied in adjuvant-induced arthritis (Levine et al., 1984). The concentration of substance P increases in the joints affected by arthritis. Joints having dense innervations display more severe inflammation and tissue destruction in adjuvant- or collagen-induced arthritis (Mitchell and Fries, 1982).

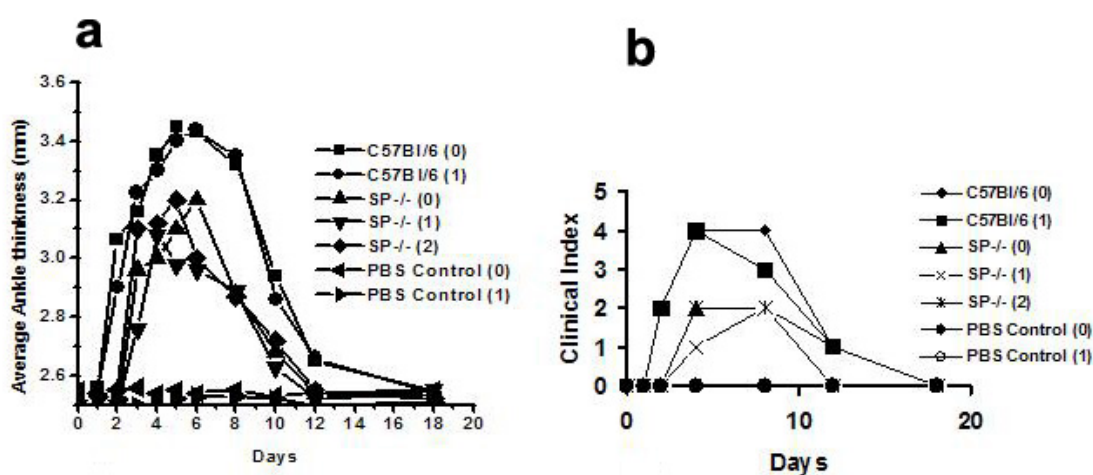


**Figure 22.** Average ankle thickness (a) and clinical Index (b) of SP<sup>-/-</sup> mice, C57BL/6 mice control mice.

The substance P knockout mice (SP<sup>-/-</sup>) mice and genotype matched C57BL/6 control mice were injected with K/BxN serum. The disease was evaluated by measurement of average ankle thickness and clinical index. The disease was partially protected in substance P knockout mice. Ankle swelling was observed in C57BL/6 mice on day two

after injection of K/BxN serum where as in case of SP<sup>-/-</sup> mice the disease started on day three after injection of K/BxN serum. The average ankle thickness of diseased C57BL/6 mice reached its maximum value of 3.4 mm on day five after K/BxN serum injection. The average ankle thickness of SP<sup>-/-</sup> mice reached maximum value 3.2 mm on day six after injection of K/BxN serum. In both the strains the ankle swelling gradually decreased from day seven and reached normal value on day twelve (Figure 22 a). Again the clinical index in C57BL/6 mice was four where as the clinical index in SP<sup>-/-</sup> mice was two. Therefore the role of substance P in vasodilatation and lymphocyte migration to the site of inflammation is extremely important. Substance P plays a crucial role in the acute phase of the inflammation. RA patients show high levels of substance P in the knee joints so also osteoarthritis patients. However the origin of substance P in joints is one of the important questions to be addressed in inflammation research. Substance P plays a pivotal role in both the periphery and central nervous system (CNS) during inflammatory disease like RA.

## **3.2. Molecular analysis of Cryoglobulins**

### **3.2.1. Purification of Cryoglobulins**

Type I cryoglobulins from sera of two patients were purified by reversible precipitation. The first patient was suffering from chronic vasculitis (KCR). The second type I cryoglobulin was isolated from the serum of a plasmacytoma patient undergoing plasmapheresis (NCR).

The cryoglobulins were purified by six cycles of cryoprecipitation and resolubilization. The serum void of cryoglobulins was loaded onto a Protein-G column for purification of non-pathogenic immunoglobulins. After purification, the cryoglobulin concentration was determined by measuring the O.D at 280nm. The cryoglobulin of patient KCR was 2 mg/ml and the Cryoglobulin of patient NCR was 8 mg/ml.

SDS PAGE analysis of cryoglobulin KCR revealed a complex of 210 kDa under non-reducing conditions. The same 210 kDa complex resolved into three different bands of 65 kDa, 51 kDa and 25 kDa under reducing conditions (Figure 23). On the contrary, cryoglobulin NCR resolved into two bands under reducing condition of 65 kDa and 25 kDa (Figure 24).

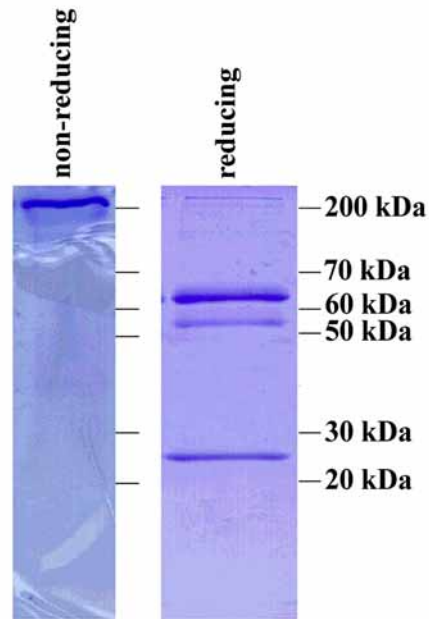


**Figure 23.** SDS-PAGE analysis of type I cryoglobulin KCR purified from human serum. The Coomassie stained gel shows bands under non-reducing and reducing conditions.

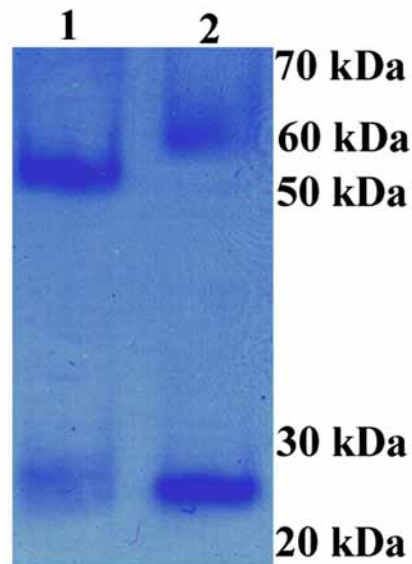


**Figure 24.** SDS-PAGE analysis of type I cryoglobulin NCR purified from human serum (lane 2) and Human myeloma protein IgG1 (lane 1). Coomassie stained gels show bands under reducing condition.

### 3.2.2. Immunoblot Analysis of Cryoglobulins

Cryoglobulins are classified as Type I, II or III (Brouet et al., 1974) depending on their immunoglobulin composition. So immunoblot analysis of the cryoglobulins was performed using anti-human IgG and IgM antibodies. Both the cryoglobulins were turned out to be type I. There was no IgM molecule involved in the cryoprecipitate, as revealed by the immunoblot analysis.

The 65 kDa and 51 kDa bands of cryoglobulin KCR were detected by the anti-human IgG-HC antibodies. But all the three bands including the 25 kDa band were detected by the anti-human whole Ig antibodies (Figure 25). Thus the 25 kDa band was found out to be IgG-LC.

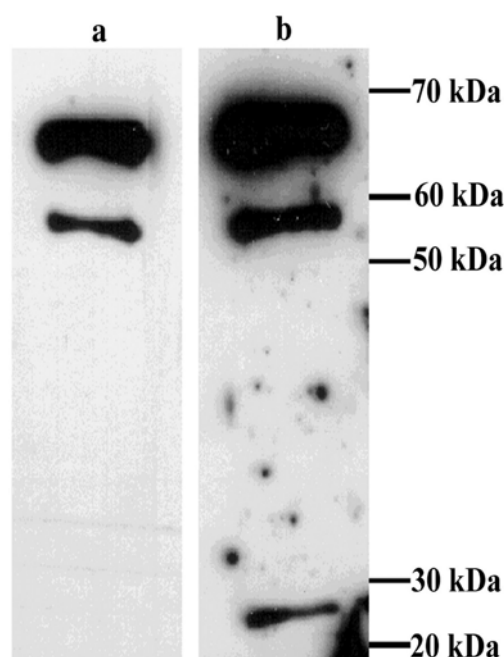


**Figure 25.** Immunoblot analysis of type I cryoglobulin KCR. 65 kDa and 51 kDa bands corresponding to two IgG heavy chains detected by anti-human IgG antibody (lane a) and all three bands detected by anti-human whole Ig antibody (lane b).

In order to further analyze the heavy chain composition of the cryoglobulin KCR complex, monoclonal antibodies specific for human IgG3 and human IgG1 were used. This analysis revealed that the 65 kDa band was IgG3 and 51 kDa band was IgG1 (Figure 26).

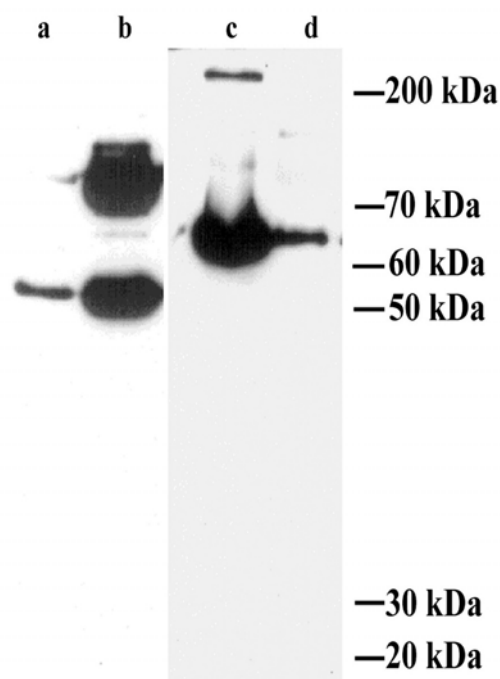


**Figure 26.** Immunoblot analysis of the type I cryoglobulin KCR in comparison with purified human myeloma protein IgG1 and normal human serum. Gamma 1 chain of cryoglobulin detected by anti-human IgG1 antibody (lane a), human myeloma protein IgG1 detected by the same anti-human IgG1 antibody (lane b), cryoglobulin IgG3 chain detected by anti-human IgG3 antibody (lane c) and IgG3 chain detected in normal human serum by the same anti-human IgG3 antibody (lane d).

Immunoblot analysis of the cryoglobulin NCR using anti-human monoclonal antibodies against heavy chains showed that IgG3 was the only Ig heavy chain present in cryoprecipitate (Figure 27).

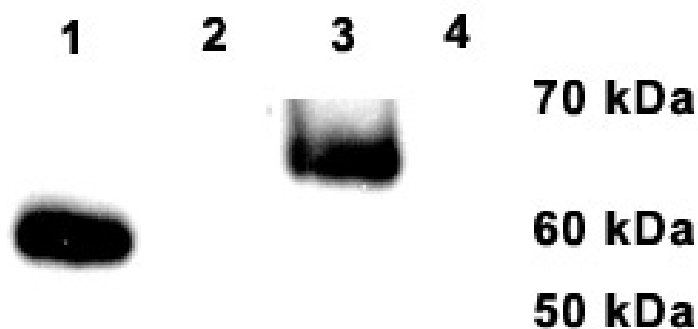


**Figure 27.** Immunoblot analysis of type I cryoglobulin NCR in comparison with human myeloma protein IgG1. Myeloma protein IgG1 (lane 1) and cryoglobulin (lane 2) stained with anti-human IgG1 antibody. Cryoglobulin (lane 3) and myeloma protein IgG1 (lane 4) stained with anti-human IgG3 antibody.

### 3.2.3. Gel Filtration Analysis of Type I Cryoglobulins

Having been confronted with the unusual size (210 kDa) of the type I cryoglobulin KCR, gel filtration analysis of the complex was performed. A major and a minor peak were observed in size exclusion chromatography (Figure 28 A). The elution profile of the commercially available IgG3-kappa and IgG1-kappa myeloma proteins closely coincided with the minor peak (Figure 28 B, C).

Molecular weight determination using standard proteins such as Ferritin (440 kDa), Catalase (232 kDa), Aldolase (158 kDa) and ovalbumin (43 kDa) revealed that the major peak and minor peak correspond to 219 kDa and 160 kDa respectively. It seems that the major peak consisted of IgG3 molecule complexed with a single IgG1 heavy chain. The average size of a human IgG3 molecule is 170 kDa and that of IgG1 molecule is 164 kDa.

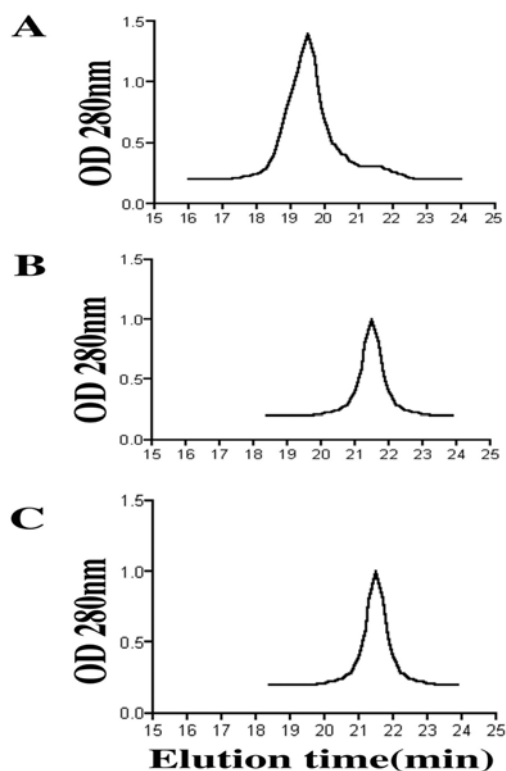


**Figure 28.** FPLC profile of the type I cryoglobulin KCR. Superdex-200HR gel filtration column splits the cryoglobulin complex (A) into major peak and a minor peak (shoulder) and the later shows the same mobility as purified myeloma IgG3-kappa (B) and IgG1-kappa (C) control proteins.

Again to specifically determine the composition of the two peaks, dot blot analysis of the samples eluted from major and minor peaks was performed. The sample was first treated with 6 M guanidinium hydrochloride at 37°C and then subjected to gel filtration chromatography. A similar profile but a change in the elution time was noticed (Figure 29 A). The samples were collected separately from the major peak and minor peak and

spotted on to a nitrocellulose membrane and blotted using monoclonal anti-human IgG3 and anti-human IgG1 antibodies. The sample obtained from major peak (219 kDa) was positive for IgG3 as well as IgG1 in dot blot (Figure 29 B). Samples obtained from minor peak were mostly positive for IgG3 with trace amounts of IgG1. Taken together, all the results obtained from SDS PAGE, immunoblot and chromatography suggested that the IgG3 and IgG1 were in a complex in case of the type I cryoglobulin KCR.

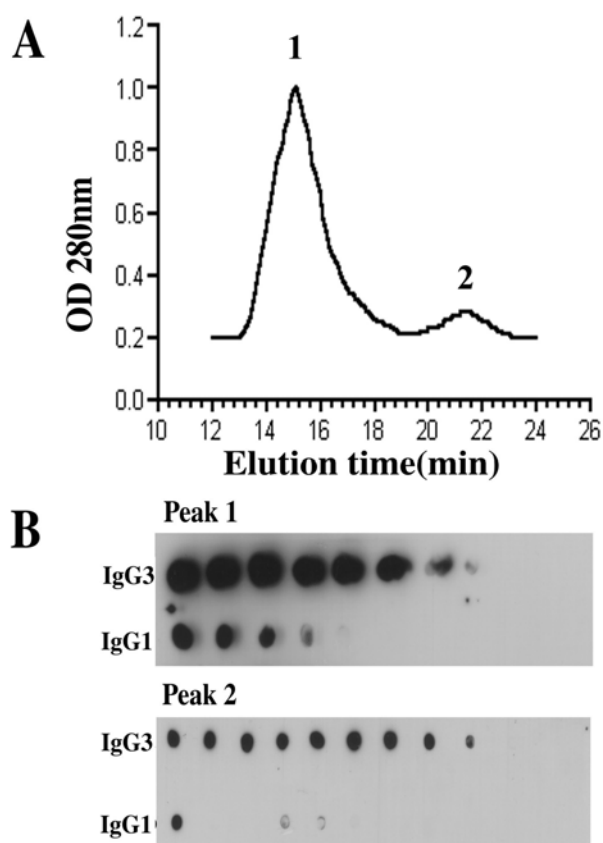


**Figure 29.** FPLC profile of the type I cryoglobulin KCR after treatment with 6 M guanidinium hydrochloride (A). Immunoblot analysis of the samples collected from peak 1 and peak 2 in serial dilution using isotype specific antibodies against human IgG3 and IgG1 (B).

---

### 3.2.4. Protein Sequence Analysis of Type I Cryoglobulin KCR

In order to further identify the immunoglobulin chains (65 kDa, 51 kDa and 25 kDa) involved in the complex of type I cryoglobulin KCR, peptide sequencing of the resolved bands was carried out.

Three peptides obtained from the 65 kDa band matched to the human IgG3 heavy chain sequence (accession number AJ390237). One peptide CPEPK allowed to discriminate among IgG isotypes. Two peptides matched best to the V<sub>H</sub>4-4 germline gene ([www.ncbi.nlm.nih.gov/igblast](http://www.ncbi.nlm.nih.gov/igblast)). One peptide showed a single amino acid change in the FWR2 indicating somatic mutations or allelic differences in the genetic pool (Figure 30 A).

The 51 kDa band was found to be IgG1 heavy chain. The first peptide derived from 51 kDa band showed homologies to c-region. In order to exclude the truncation of the IgG1-HC, we performed the N-terminal sequencing and the resulting peptides matched to the V<sub>H</sub>-gene of the V<sub>H</sub>-3 family without any truncation (Figure 30 B).

Peptides obtained from 25 kDa band matched to sequences of an Igκ light chain. Peptides obtained from the N-terminus showed alignment to IgVκ L2 germline sequence. There were seven amino acid changes suggesting somatic mutations. The peptides derived from the CDR3-region showed similarities to JκII-elements (accession number UO7443). Further four peptides matched to the human Igκ-c-region (Figure 30 C).

---

A

VH4-4 germline  
 <-----FWR1-----> <CDR1<-----FWR2-----> <-----CDR2- ----><----->

1 QVQLQESGPG LVKPSETLSL TCTVSGGSIS SYYWSWIRQP AGKGLEWIGR IYTSGSTNYN PSLKSRVTMS 70  
 A----- -- --

--FWR3----->

71 VDTSKNQFSL KLSSVTAADT AVYYCAR 97

IgG3 c-region

1 QMQGVNCTVS SELKTPLGDT THTCPRCPEP KSCDTPPPCP RCPEPKSCDT PPPCPRCPEP KSCDTPPPCP 70  
 -----

71 RCPAPELLGG PSVFLFPPKP KDTLMISRTP EVTCVVVDVS HEDPEVQFKW YVDGVEVHNA KTKPREQQFN 140  
 -----

141 STFRVSVLT VLHQNWLDGK EYKCKVSNKA LPAPIEKTIS KTKGQPREPQ VYTLPPSRDE MTKNQVSLTC 210  
 -----

211 LVKGFYPSDI AVEWESSGQP ENNYNTTPPM LDSDGSFFLY SKLTVDKSRW QQGNIFSCSV MHEALHNRFT 280  
 -----

QKSLSLSPGK 290

---

B

VH3 germline  
 <---FWR1  
 EVQLVES  
 -----

- IgG1 c-region

1 ASTKGPSVFP LAPSSKSTSG GTAALGCLVK DYFPEPVTVS WNSGALTSKV HTFPAVLQSS GLYSLSSVVT 70  
 -----

71 VPSSSLGTQT YICNVNHKPS NTKVDKKEP KSCDKHTTCP PCPAPELLGG PSVFLFPPKP KDTLMISRTP 140  
 -----

141 EVTCVVVDVS HEDPEVKFNW YVDGVEVHNA KTKPREEQYN STYRVSVLT VLHQDWLNGK EYKCKVSNKA 210  
 -----

211 LPAPIEKTIS KAKGQPREPQ VYTLPPSRDE LTKNQVSLTC LVKGFYPSDI AVEWESNGQP ENNYKTTPPV 280  
 -----

281 LDSDGSFFLY SKLTVDKSRW QQGNVFCV MHEALHNHYT QKSLSLSPGK 330  
 -----

---

C - IGK

VkIII-L2 germline  
 <-----FWR1-----> <CDR1<-----FWR2-----> <CDR2-><----->

1 EIVLTOSPAT LSLSPGERAT LSCRASQSVS SMLAWYQQKPGAPRLIYG ASTRATGIPA RFSGSGSGTE 70  
 -----V- -----G DN-----R- -- ----D --Y-

-----FWR3-----> <-----CDR3----->

71 FTLTISSLQS EDFAVYQCQ YNNWP 95  
 -S--LTFKQGTR

JKII SWPLTFG

C-REGION

1 GGGTKVEIKR TVAAPSVFIF PPSDEQLKSG TASVVCLLNN FYHREAKVQW KVDNALGSGN SQESVTEQDS 70  
 -----

71 KDSTYLSLST LTLK 85  
 -----

**Figure 30.** Peptide sequencing of the cryoglobulin KCR chains. Alignment of the peptide sequences of IgG3 heavy chain with that C-region  $V_{H4}$  germline gene sequences (A), of the IgG1 heavy chain with the C-region and the  $V_{H3}$  germline sequences (B) and of Ig $\kappa$  light chain with that of  $V_{kIII-L2}$  germline sequences (C). Dashes indicate identities.

### 3.2.5. Temperature Induced Reversible Precipitation of Cryoglobulins

Cryoprecipitation is a temperature dependent process. To better understand the exact nature of cryoprecipitation and to determine the threshold temperature at which the cryoprecipitation occurs, spectroscopic experiments were performed. FPLC purified samples were used in this experiment. Change in optical density of the sample was monitored with temperature changes from 37°C to 4°C. Rapid change in absorbance at 600nm was observed due to cold-induced precipitation of cryoglobulins. Results obtained from four consecutive cycles of cryoprecipitation and resolubilization was represented in a histogram (Figure 31). At the end of each cycle there was complete recovery of samples from the precipitate, indicating the process was fully reversible.

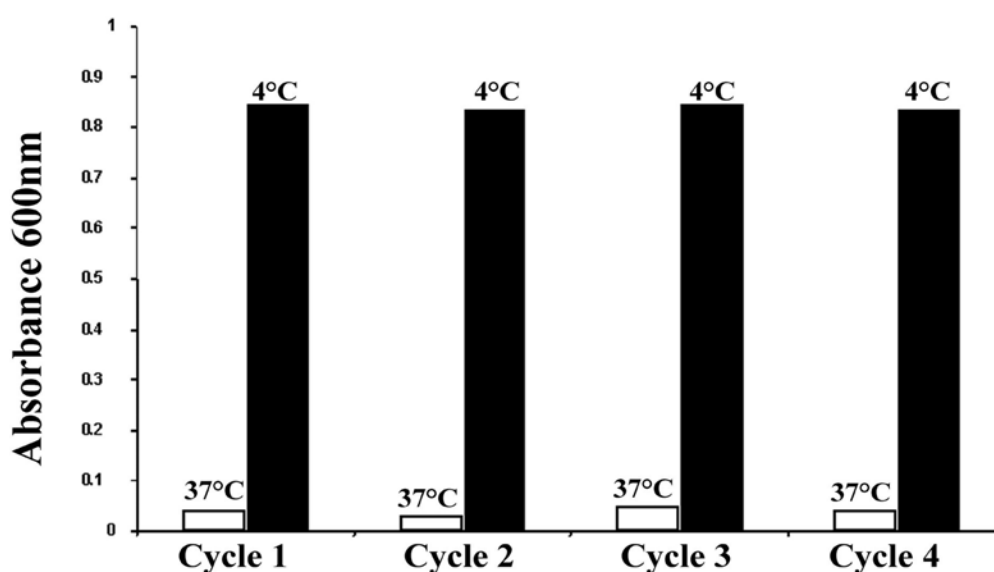


*Figure 31. Effect of temperature on cryoprecipitation. Optical density measured at 600nm in a spectrophotometer while incubating the sample alternating at 37°C and 4°C. Y-axis represents the change in  $O.D_{600nm}$  value due to turbidity in the medium upon cryoprecipitation.*

### 3.2.6. Cryoprecipitation is Concentration Dependent

Cryoprecipitation is an event in which the pathogenic immunoglobulins associate with each other at a certain temperature. This threshold temperature depends upon immunoglobulin isotypes involved and the nature of the environment such as pH and salt concentration. IgG3 molecules have a large hinge region. IgG3 molecules undergo aggregation due to Fc-Fc interaction. In order to determine the effect of concentration on cryoprecipitation, a set of experiments were performed. All the experiments were performed at physiological pH. Cryoglobulins were dissolved in PBS pH 7.2 and incubated at 37°C to completely solubilize the cryoprecipitate. Optical density change at 600 nm due to light scattering was measured in a spectrophotometer, while reducing the temperature of the cuvette from 37°C to 4°C at an interval of 0.1°C and then allowing the temperature to rise to 37°C to resolubilize the precipitate.

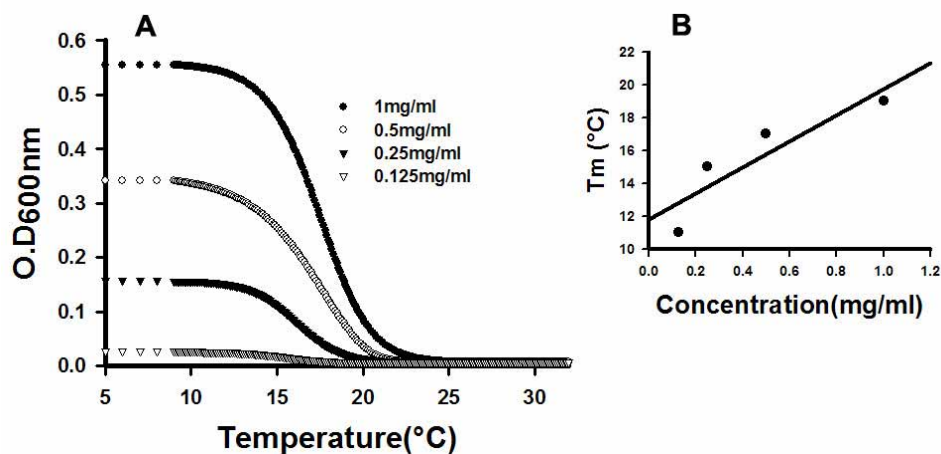


**Figure 32.** Effect of cryoglobulin KCR concentration on cold induced precipitation. Change in  $O.D_{600nm}$  as a function of temperature (A). Threshold temperature ( $T_m$ ) versus concentration (B).

The cryoglobulin KCR was prepared at four different concentrations (1mg/ml, 0.5 mg/ml, 0.25 mg/ml and 0.125 mg/ml) for cryoprecipitation study. There was steady

increase in the level of cryoprecipitation with the increase in the concentration of the cryoglobulin (Figure 32 A). Threshold temperature ( $T_m$ ) is the one at which the cryoprecipitation initiated while lowering the temperature from 37°C to 4°C. The  $T_m$  value also changed with the increase in concentration of cryoglobulin KCR. The  $T_m$  at concentrations 0.125 mg/ml, 0.25mg/ml, 0.5 mg/ml and 1.0 mg/ml were 11°C, 15°C, 17°C and 19°C respectively (Figure 32 B).

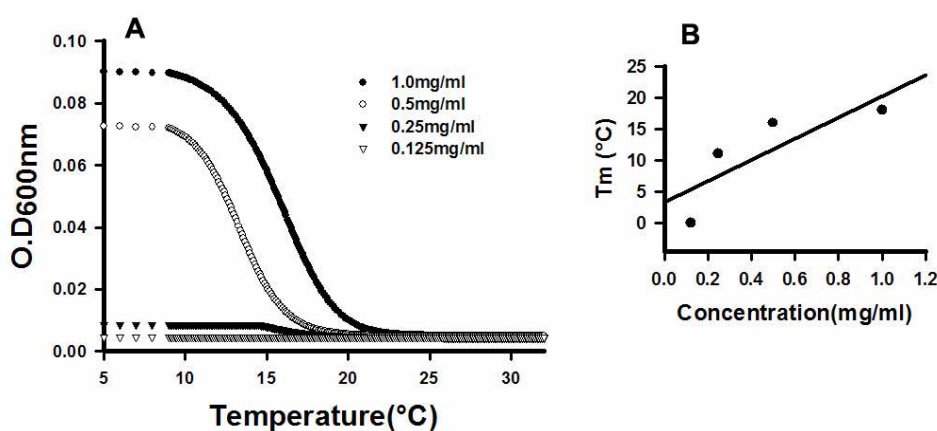


**Figure 33.** Effect of cryoglobulin NCR concentration on cold induced precipitation. Change in  $O.D_{600nm}$  as a function of temperature (A). Threshold temperature ( $T_m$ ) versus concentration (B).

The cryoglobulin NCR showed concentration dependent cryoprecipitation, the level being the highest at 1 mg/ml concentration. Cryoprecipitation level was much less at lower concentrations (Figure 33 A). The  $T_m$  value at concentrations of 0.125 mg/ml, 0.25mg/ml, 0.5 mg/ml and 1.0 mg/ml of cryoglobulin KCR were 0°C, 11°C, 16°C and 18°C respectively (Figure 33 B).

These results suggest that beyond a critical concentration the cryoprecipitation is much faster and below this concentration the cryoprecipitation is significant. So there seems

to be a critical threshold temperature determined by the concentration of the cryoglobulin. So the concentration of pathogenic antibodies in the sera of patients is important. At high concentrations cryoglobulins precipitate even at a moderate drop in temperature. Therefore vasculitis and glomerulonephritis patients may be treated with immunosuppressive drugs to keep the concentration of IgGs at a lower level.

### **3.2.7. Osmolytes lower the threshold Temperature for Cryoprecipitation**

An important element of protein aggregation in diseases such as cryoglobulinemia is the reduced capacity of the protein to retain or maintain its native structure. The thermodynamic forces responsible for protein folding and stability are hydrogen bonding, electrostatic, van der Waals and hydrophobic interactions. Molecules that stabilize or facilitate formation of or maintenance of native state might play a role in modulating abnormal conformational changes. Osmolytes are a group of small naturally occurring molecules, which protect proteins from chemically induced or thermally induced denaturation (Anjum et al., 2000; Santoro et al., 1992; Wang and Bolen, 1997) and also facilitate the correct folding of some proteins (Baskakov and Bolen, 1998; Baskakov et al., 1999; Brown et al., 1997). During the evolutionary process plants, animals and certain microorganisms have adapted to harsh environments by accumulating osmolytes in intracellular medium (Somero, 1986; Yancey et al., 1982).

The possible role of osmolytes in stabilizing the cryoglobulins was studied. Cryoprecipitation was studied in the presence of osmolytes such as Sarcosine and trimethylamine N-oxide (TMAO). Cryoglobulins were incubated at various molar

---

concentrations of the osmolytes at 37°C and subsequently the cryoprecipitation was recorded in a spectrophotometer.

### 3.2.7.1. Effect of Sarcosine on Cryoprecipitation

The cryoglobulin KCR at a concentration of 1mg/ml was incubated with 1M, 2M and 3 M sarcosine at 37°C. Samples were then added to the cuvette at 37°C and gradually the cuvette temperature was lowered to 4°C. Spectral changes due to turbidity were measured at 600 nm.

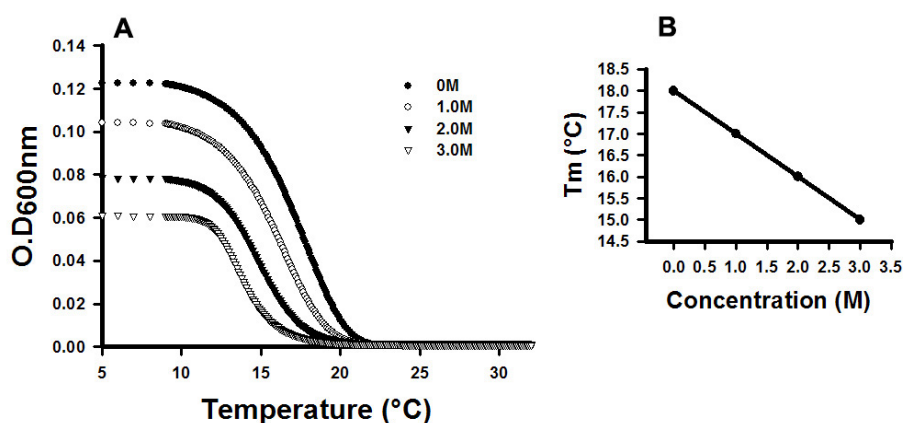


**Figure 34.** Effect of Sarcosine on Cryoprecipitation. Change in  $O.D_{600nm}$  of Cryoglobulin KCR at increasing concentrations of Sarcosine (A). Threshold temperature ( $T_m$ ) as function of sarcosine concentration (B)

In the absence of sarcosine, highest turbidity was noticed in case of cryoglobulin KCR and the threshold temperature ( $T_m$ ) for cryoprecipitation was 18°C. A decrease in turbidity as well as  $T_m$  was observed with the increase in sarcosine concentration (Figure 34 A, B). The  $T_m$  at 1 M, 2M and 3M sarcosine were 17°C, 16°C and 15°C respectively.

Quite similar results were obtained for cryoglobulin NCR. Increasing sarcosine concentrations resulted in a decrease in turbidity as well as  $T_m$ . The  $T_m$  for 1 mg/ml cryoglobulin NCR without sarcosine was 18°C and it decreased to 16°C at 1M, to 14°C at 2M and finally to 13°C at 3M sarcosine (Figure 35 A, B)

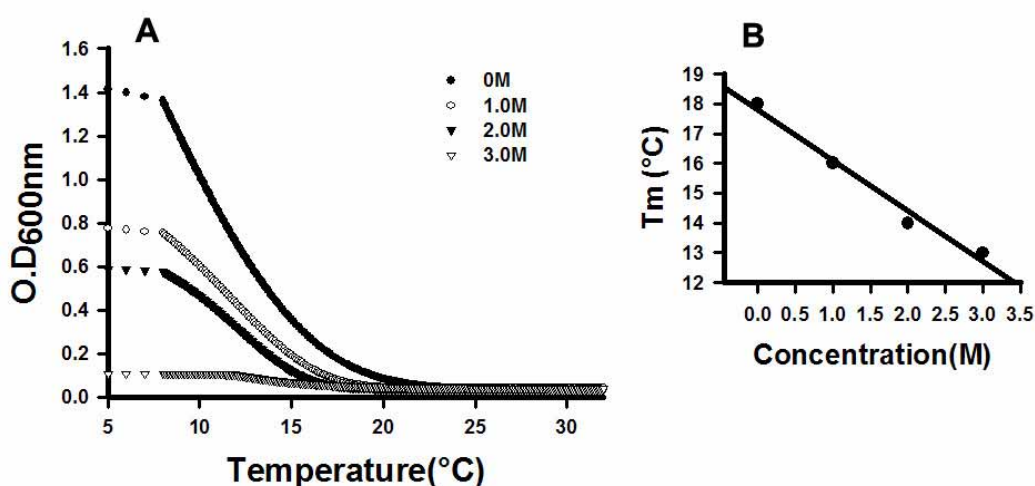


**Figure 35.** Effect of Sarcosine on Cryoprecipitation. Change in  $O.D_{600nm}$  of Cryoglobulin (NCR) at increasing concentrations of Sarcosine (A). Threshold temperature ( $T_m$ ) as function of sarcosine concentration (B)

### 3.2.7.2. Effect of TMAO on Cryoprecipitation

TMAO considerably protected the cryoglobulins from cold induced precipitation at higher concentration. Both the cryoglobulins were taken at a concentration of 1 mg/ml and incubated with varying molar concentrations of TMAO (1M, 1.5M, and 2M). In case of cryoglobulin KCR, the  $T_m$  without TMAO was 18°C and it decreased to 16°C at 1M TMAO, to 13°C at 1.5M TMAO and finally to 10°C at 2M TMAO (Figure 36 A, B).

Similarly for cryoglobulin NCR, the  $T_m$  without TMAO was 18°C. This  $T_m$  value decreased to 15°C at 1M TMAO, to 10°C at 1.5M TMAO and finally to 8°C 2M TMAO (Figure 37 A, B).

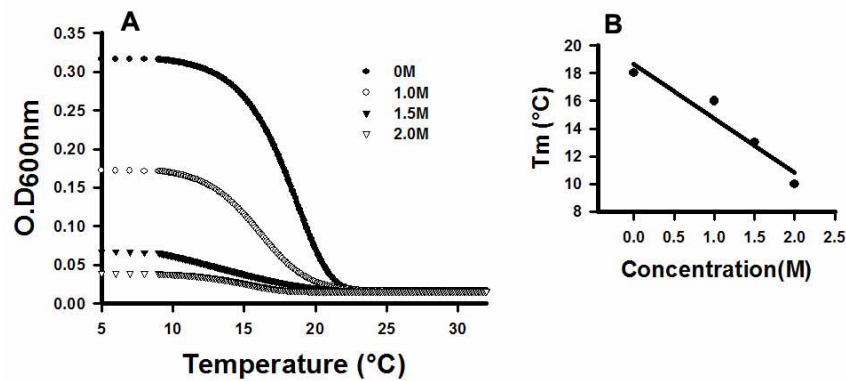


**Figure 36.** Effect of TMAO on Cryoprecipitation. Change in  $O.D_{600nm}$  of Cryoglobulin KCR at increasing concentrations of TMAO (A). Threshold temperature ( $T_m$ ) as function of TMAO concentration (B)

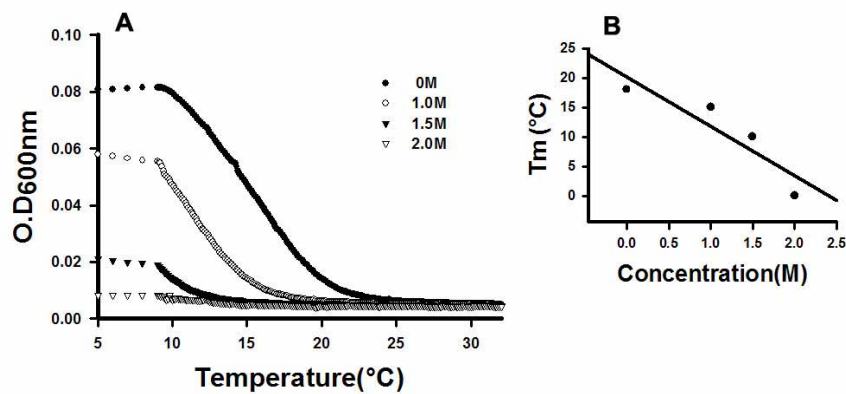


**Figure 37.** Effect of TMAO on Cryoprecipitation. Change in  $O.D_{600nm}$  of Cryoglobulin NCR at increasing concentrations of TMAO (A). Threshold temperature ( $T_m$ ) as function of TMAO concentration (B)

---

### **3.2.8. Chemical Chaperone “Cyclodextrin” protects Immunoglobulins from Cryoprecipitation**

Molecular events underlying the cryoprecipitation are poorly understood. In the study discussed in section 3.2.6, a considerable precipitation was observed at 4°C for a cryoglobulin concentration of 1mg/ml. So in order to understand the kinetics at the initiation phase of the reaction, a temperature jump experiment was performed. Cryoglobulin NCR was used for the study at different concentrations (2mg/ml, 3 mg/ml and 4 mg/ml). Samples were incubated at 37°C to completely solubilize the cryoglobulins. Then the cuvette temperature was set to 4°C with constant stirring at the bottom with the help of a magnetic bead. The samples were added to the cuvette (4°C) with the help of a syringe without disturbing the temperature of the cuvette. Once the thermal equilibrium was reached, light scattering was measured at 600 nm as a function of time.

It was observed that there was a monotonic increase in the absorbance at 600nm due cryoprecipitation with time (Figure 38). A short initial lag phase was observed, which decreased with increase in concentration of cryoglobulin. The initial rate of the reaction also showed concentration dependence. The rate was slower at 2 mg/ml compared to 3 and 4 mg/ml. Quite interestingly it was found out that after an initial burst phase there was a slow but steady state process of polymer build up. At lower concentrations (2mg/ml) the initial burst phase lasted for about 20 minutes, and then slow phase was noticed displaying a slow increase in the absorbance (Figure 38). In higher concentrations the initial burst phase was shorter. At a concentration of 3 mg/ml the initial burst phase lasted for only 5 minute and at a concentration of 4 mg/ml, this phase accounted for only 1 minute.

Again with time polymer building increased steadily and finally reached a jelly state at which absorbance at 600nm could not be determined (Figure 38). At a cryoglobulin concentration of 4 mg/ml, there was decay in the absorbance after about 10 minutes of initiation of the reaction. A clear mass of jelly was observed in the cuvette.

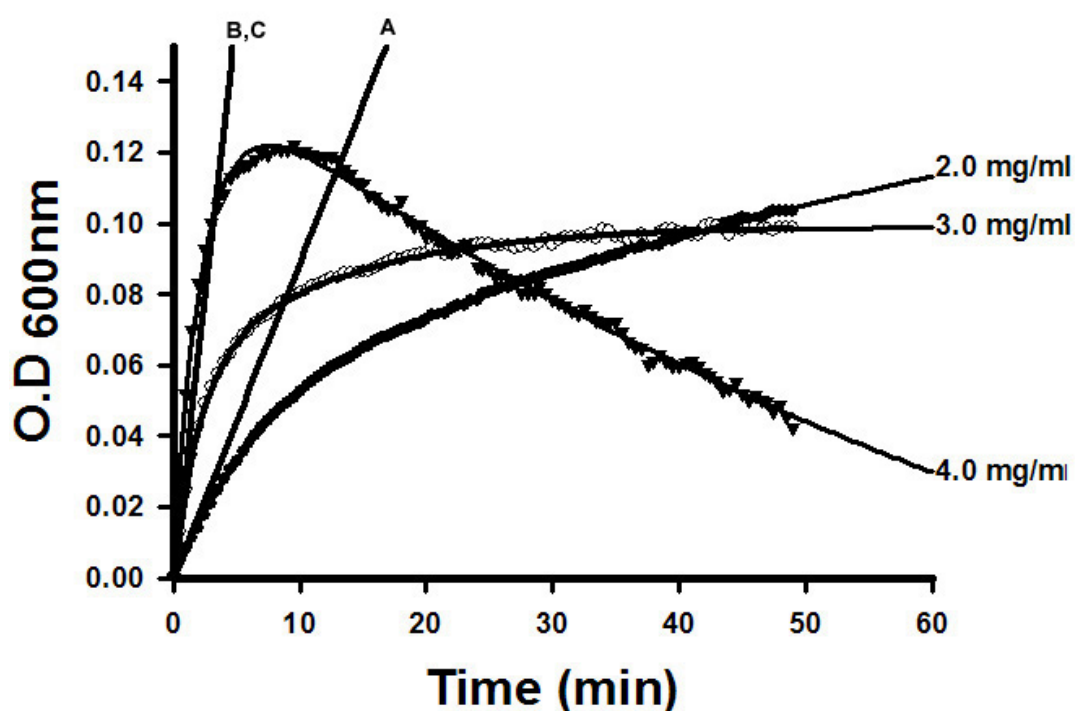


**Figure 38.** Kinetics of cold-induced precipitation of cryoglobulin. A change in absorbance at 600<sub>nm</sub> as a function of time for various concentrations of cryoglobulin NCR. Straight lines at the origin of the graph indicates observed initial rates of reaction at 2mg/ml (A), 3mg/ml (B) and 4mg/ml (C) of Cryoglobulin NCR. Observed initial rates at 3mg/ml (B) and at 4 mg/ml (C) of cryoglobulin are identical.

These results suggest that during cryoprecipitation, there is an initial phase of self-association of cryoglobulins. This initial self-nucleation process eventually results in polymer formation.

To further investigate the initial nucleation event, cryoprecipitation was performed in the presence of a molecular chaperon  $\beta$ -cyclodextrin. Artificial chaperon-assisted refolding of proteins have been reported before (Daugherty et al., 1998; Rozema and Gellman, 1996).

Cryoglobulin NCR at a concentration of 3 mg/ml was incubated at 37°C in the presence of various concentrations of cyclodextrin (0.25mM, 0.5mM, 1.0mM, 1.3mM, 1.5mM, 2.0mM and 2.5mM). Then the samples were taken for cold-induced precipitation studies in a temperature jump experiment as discussed above.

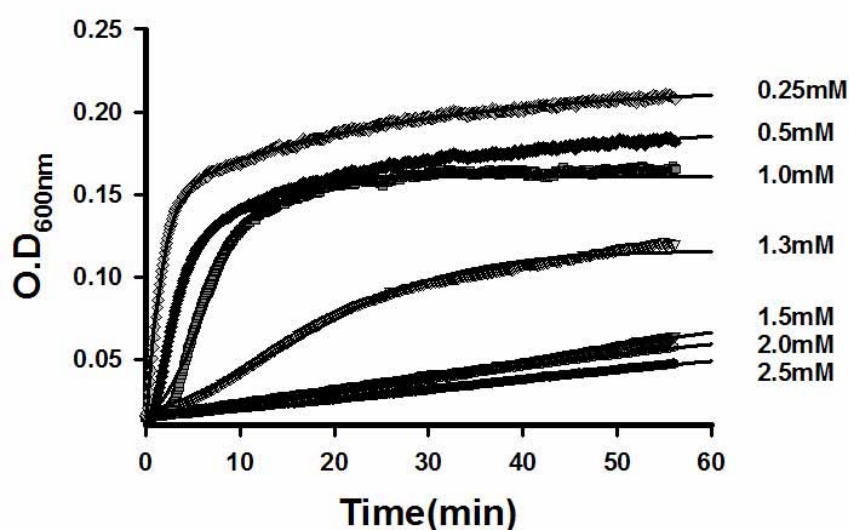


**Figure 39.** Kinetics of cold-induced precipitation of cryoglobulin NCR at various concentrations of cyclodextrin. A change in absorbance at 600<sub>nm</sub> as a function of time.

The chemical chaperon prevented the cold-induced precipitation of cryoglobulin NCR. The initial burst phase kinetics changed in the presence of cyclodextrin (Figure 39).

The initial lag phase of the reaction was increased with increasing cyclodextrin concentrations. At 0.5mM and 1.0mM cyclodextrin increased the initial lag phase from 1 to 2 minute and then the burst phase occurred. Again the absorbance did not reach the maximum level at the saturation phase. Hence there was partial rescue of immunoglobulin molecules undergoing self-association. The initial lag phase was considerably increased at 1.3mM cyclodextrin and a slow burst phase was observed thereafter (Figure 38). At higher concentrations (1.5mM, 2.0mM and 2.5mM), the initial burst phase was completely prevented.

Again to establish the fact, the initial rates of the reactions were determined graphically. The observed initial rate of the reaction decreased significantly in the presence of the cyclodextrin.

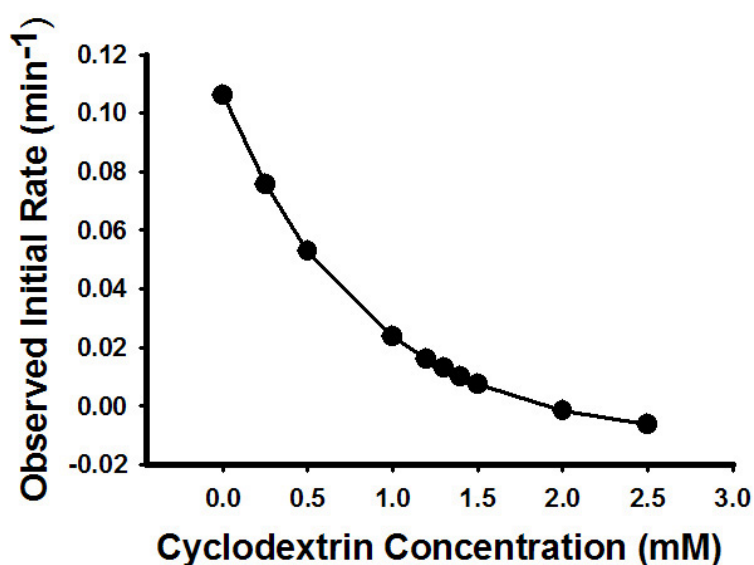


*Figure 40. Observed Initial rate of the cryoprecipitation as function of cyclodextrin concentration.*

Nucleation is the important event in the cold-induced precipitation. It is thought that the initial association of IgG molecules takes place due to hydrophobic interactions.

Probably there are sticky hydrophobic patches on the surface of cryoglobulins. Cyclodextrin may occupy these hydrophobic patches, thereby preventing self-association of cryoglobulins. So nucleation is the rate-limiting step in cold-induced precipitation of cryoglobulins.

---

## CHAPTER IV

### DISCUSSION

#### **4.1. Emergence of Auto reactive T cells in the Periphery of K/BxN and Cr2<sup>-/-</sup>K/BxN Mice**

Several examples of transgenic mouse lines carrying genes specifying auto reactive TCRs have been reported (Miller and Morahan, 1992). In most of the cases T lymphocytes carrying the transgene encoded TCRs are tolerized by means of one or more mechanisms such as clonal deletion, receptor or coreceptor down-modulation or anergy induction. The auto reactive T cells carrying the KRN-TCR emerge to periphery of the arthritic mice in our colonies at the second week after birth. The reduced cell numbers (CD4+Vβ6+clones) in the youngest animals show signs of clonal deletion until the second week after birth. Subsequently the profile normalized and the animal became susceptible to the arthritis development. The auto reactive T cells may escape clonal deletion due to incomplete allelic exclusion (Kouskoff et al). The KRN-TCR positive T cells and the NOD MHC II molecule are most important in arthritis development in Cr2<sup>-/-</sup>K/BxN mice, because the litter mate mice which lack the KRN-TCR remained unaffected. The specific requirement of the A<sup>g7</sup> molecule has been shown previously by (Korganow et al., 1999). The T cells expressing KRN-TCR recognize the GPI peptides in the context of A<sup>g7</sup> molecule (Matsumoto et al., 1999) and get activated. The activated KRN-TCR positive T cells interact with B cells through TCR: A<sup>g7</sup> and CD40L:CD40 engagement thereby promoting further T cell stimulation, polyclonal B cell activation and T cell help dependent Ig production. Antibodies thus

---

produced bind to the soluble antigen in the serum or bind to the antigen localized on the cartilage surface. There are Ab/Ag complexes in the circulation, which may lead to further complication of the disease such as vasculitis. Immune complexes activate the complement cascade, leading to cell lysis and release of inflammatory mediators, engagement of Fc receptors and activation of the local cell types such as macrophages and fibroblasts in the synovial membrane.

### **4.2. Lack of or Incomplete Tolerance Results in High Levels of GPI Specific Auto antibodies in $Cr2^{-/-}$ K/BxN Mice Serum**

The B cells secreting Igs in K/BxN and  $Cr2^{-/-}$ K/BxN mice must depend on a number of factors. Only the engagement of TCR:MHC and CD40L:CD40 interaction are not sufficient to push the B cells to produce Igs in vivo (Cooke et al., 1994). There must be involvement of BCR. Only those B cells that have specificities for the self-antigen (GPI) can become Igs secretors. Once the potentially auto reactive B cells are produced, they must face the antigen in circulation and might undergo tolerization. An important factor for the self reactive B cells is whether and how they are tolerized. The exact cause of incomplete tolerance or lack of tolerance in these models of rheumatoid arthritis is still not known. The biochemistry of the potential antigen GPI might be playing a crucial role.

High levels of autoantibodies in the sera of  $Cr2^{-/-}$ K/BxN mice draw attention towards the role of CD21/CD19 coreceptor complex in the selection of auto reactive B cells.

A definitive role for CD21/CD35 in the humoral response to T dependent antigens was first identified by characterization of  $Cr2^{-/-}$  mice (Ahearn et al., 1996; Molina et al., 1990). The  $Cr2^{-/-}$  mice have impaired secondary antibody responses and a reduced

---

number and size of germinal center (GC) following immunization with antigens (Ahearn et al., 1996). However the defect in GC formation depends on the type of the antigen. The impaired response in the *Cr2*<sup>-/-</sup> mice is due to reduced coreceptor signaling and antigen retention.

The elimination of self-reactive B cells was best studied in the Hen Egg lysozyme (HEL) double transgenic model. In this model the HEL-specific B cells are eliminated in the bone marrow in mice expressing a membrane form of the lysozyme (Hartley et al., 1991). In contrast, the self-reactive B cells are not eliminated but functionally inactivated in double transgenic mice expressing a soluble form of HEL (sHEL) (Goodnow et al., 1989). In transgenic model of anti-dsDNA, the self-reactive B cells are eliminated either in bone marrow (Chen et al., 1995) or anergized in the periphery (Mandik-Nayak et al., 1997; Santulli-Marotto et al., 1998). In the models dealing with soluble self antigens, it is not known how the antigens are localized in BM and periphery for exposure to immature (Norvell et al., 1996; Norvell et al., 1995; Norvell and Monroe, 1996) and transitional (Carsetti et al., 1995) B cells that are sensitive to negative selection. The strength of signal induced via the BCR is critical in determining the fate of self-reactive B cells whether eliminated, anergized or ignored (Goodnow, 1996).

In the lysozyme-anti-lysozyme transgenic model of peripheral tolerance the self-reactive B cells are not eliminated but anergized on encounter with above threshold level of sHEL-self-antigen. Using lysozyme double transgenic mice and *Cr2*<sup>-/-</sup> mice, Prodeus et al have shown that HEL-binding B cells escape tolerance in mice deficient in CD21/CD35. There was apparent absence of anergy, as indicated by CD86 and sIgM expressing B cells (Prodeus et al., 1998).

Similarly in  $Cr2^{-/}$ -K/BxN mice, there is poor selection of auto-reactive B cells recognizing the auto-antigen GPI. This leads to high levels of anti-GPI antibodies in the sera of these mice at about day 16 after birth compared to K/BxN mice. High levels of autoantibodies result in the formation of immune complexes that initiates the complement activation and release of inflammatory molecules resulting in tissue damage. However complement activation is tightly regulated in humans and mice by different molecules such as DAF, MCP, factor-H, factor-I and CD35.

In the context of our model, the role of CD35 needs to be addressed. Administration of CR1 (CD35) suppresses tissue damage in rat models of post-ischemic myocardial injury and immune complex-mediated vasculitis (Mulligan and Ward, 1992). Furthermore decreased expression of CR1 on B cells and neutrophils has been reported in patients with SLE and other autoimmune diseases (Fyfe et al., 1987; Walport and Lachmann, 1988; Wilson et al., 1986). The role of CR1 in mice tissues has not been so well characterized. However, CR1 expressed on erythrocytes of humans play a crucial role in clearance of immune complexes. It seems that earlier onset of disease in  $Cr2^{-/}$ -K/BxN compared to K/BxN mice is due to the high levels of anti-GPI antibodies and poor clearance of GPI-anti-GPI Ab immune complexes. This could have lead to the secondary effects such as vasculitis. This may be one of the factors responsible for the high mortality rate in case of  $Cr2^{-/}$ -K/BxN mice in the chronic phase of the disease.

### **4.3. Rapid and Aggressive destruction of Joints in $Cr2^{-/}$ -K/BxN Mice**

Occurrence of pathogenic autoantibodies in the serum of K/BxN mice is the most important and crucial factor for RA pathogenesis (Korganow et al., 1999; Kouskoff et al., 1996; Matsumoto et al., 1999). Transfer of serum from arthritic mice to C57BL/6,

---

Balb/c or  $Cr2^{-/-}$  mice leads to development of arthritis (Solomon et al., 2002). In our model of  $Cr2^{-/-}$  K/BxN mice, anti-GPI antibodies appear at about 16 days after birth. This leads to the formation of immune complexes on the cartilage surface and activation of complement system. Joint specific inflammation leads to the formation of a series of inflammatory molecules and attraction of a variety of inflammatory cell types. A series of events takes place in the joint including the activation of macrophages and fibroblasts. The early onset of joint swelling in  $Cr2^{-/-}$  K/BxN mice indicates quick recruitment of neutrophils to the joint cavity and accumulation of synovial fluid.

The activated synovial neutrophils release elastase that degrades the glycoprotein forming the protective layer on cartilage. At the same time neutrophil enzymes begin to degrade the proteoglycans within the type II collagen molecules. Cytokines particularly IL1, produced by activated macrophages and fibroblasts diffuse into the accessible cartilage matrix and activate the chondrocytes to produce collagenase and stromelysin. Both the enzymes initiate the process of destruction of cartilage from within. Slowly the macrophages and synovial cells find attachment sites on the collagen in the exposed matrix to build the pannus tissue and begin to destroy the joint architecture. The synovial macrophages phagocytose cartilage bound immune complexes, renewing the activation.

#### **4.4. Growth Retardation in $Cr2^{-/-}$ K/BxN Mice**

Bone erosion in  $Cr2^{-/-}$  K/BxN mice was more rapid compared to K/BxN mice. There is a slow but persistent remodeling of bone in case of K/BxN mice (Korganow et al., 1999). In case of the  $Cr2^{-/-}$  K/BxN mice there was apparently no bone remodeling as the mice

showed extensive damage to the subchondral bone leading to stunted growth. Erosion of cortical and trabecular bone is seen in case of K/BxN mice (Kouskoff et al., 1996; Pettit et al., 2001; Solomon et al., 2002). The bone erosion is mainly done by the osteoclasts, specialized cells derived from monocyte lineage. The osteoclasts are formed through a combination of effects of a cytokine (M-CSF) differentiation factor generated by stromal cells in response to PGE<sub>2</sub>, parathyroid hormone and inflammatory cytokines such as IL6 and IL11. Bradykinin produced by neutrophils may stimulate osteoclast bone degradation by enhancing endogenous prostaglandin formation in the local areas adjacent to the bone (Lerner et al., 1987). Osteoclasts pump protons into the extracellular pocket decreasing pH. The metalloproteases (MMP1, MMP3 and MMP9) as well as cathepsin B and L are predominantly involved in degradation of organic matrix of the bone (Higuchi et al., 1999; Hummel et al., 1998). Our histological analysis suggests that excessive osteoclast activity in the absence of bone remodeling during chronic phase of the disease results in severe joint destruction in Cr2<sup>-/-</sup>K/BxN mice. The destruction of joints in K/BxN mice is moderate in comparison to the Cr2<sup>-/-</sup>K/BxN mice and periodic remodeling of the bone does not lead to growth retardation in K/BxN mice.

The elongation of long bones takes place by proliferation and maturation of the chondrocytes in the epiphyseal growth plate region. The rapid destruction of chondrocytes in the epiphyseal growth plate region resulted in poor growth and mineralization of bone. In pathological conditions (Dyschondroplasia) there is accumulation of undifferentiated chondrocytes in the growth plate. The joint erosion in RA is due to an imbalance in RANKL signaling pathway. RANKL was originally identified as a T cell product, which acted as a receptor activator of nuclear factor-κB

---

ligand. It is also known as tumor necrosis factor-related activation induced cytokine (TRANCE), which can regulate dendritic cell function and survival. TRANCE/RANKL serves as ligand for osteoclast differentiation factor osteoprotegerin (OPG). The endogenous osteoprotegerin levels are inadequate to neutralize the excessive RANKL level during RA pathogenesis (Itonaga et al., 2000; Takayanagi et al., 2000).

### **4.5. Sympathetic Nervous System and Antibody Induced Arthritis**

Importance of nervous system in immune regulation is clearly suggested by innervations of lymphoid tissue by sympathetic nerve fibers. Neuroendocrine regulation of rheumatic diseases is evident from the effects of glucocorticoids, gender, pregnancy, hemiparalysis and stress on clinical aspects of the disease (Bijlsma et al., 1999). In a disease like arthritis, there is a persistent inflammation characterized by micro vascular permeability and neutrophil influx to the knee joints. In the antibody-induced model of arthritis, the onset of disease is marked by joint swelling within 24 hours of pathogenic antibody injection in Balb/c mice. This strain is highly susceptible to antibody-induced arthritis. In this model of arthritis, the alternative pathway of the complement system is involved (Ji et al., 2002; Solomon et al., 2002). Development of disease requires Fc $\gamma$ RIII and C5aR as well as neutrophils (Wipke and Allen, 2001), mast cells (Lee et al., 2002) inflammatory cytokines. These requirements closely resemble the Arthus reaction (Kohl and Gessner, 1999; Ravetch and Bolland, 2001). Here GPI-antiGPI antibody immune complexes may engage the FcRs onto the synovial tissue and like in the Arthus reaction (Ramos et al., 1992; Sylvestre et al., 1996), Fc $\gamma$ RIII engagement on mast cells leads to degranulation and instantaneous release of proteases.

In this context, the role of the neuropeptides at the site of inflammation is very crucial. The anaphylatoxin like role of C5a is very important in the Arthus reaction. Joints are supplied with nerves containing myelinated and unmyelinated primary afferent fibers. About 80% of nerves in the joints are nociceptive. About half the unmyelinated fibers in the joint are sympathetic efferents, which disappear upon sympathectomy. Almost all the nerve endings show immunoreactivity for the neuropeptide substance P and calcitonin-gene-related peptide (CGRP) or Neuropeptide Y, which are present in the sympathetic nerve endings (Mapp et al., 1990). Substance P is a powerful mediator of vascular permeability. Substance P is released from the unmyelinated C fibers in joint. Besides joints and mucosal epithelium, immunoreactive substance P, substance P mRNA and NK-1R are found on the macrophages and mast cells where they can stimulate the release of the TNF $\alpha$  (Ansel et al., 1993; Luber-Narod et al., 1994; Pascual and Bost, 1990). Substance P receptor, NK-1R is also present on the post capillary venular endothelium (Baluk et al., 1996). The release of substance P is an early event in immune-complex-mediated injury and it acts as an amplifier of the subsequent inflammatory changes. Substance P acts on the vascular endothelium to cause leakage of plasma proteins and there by increasing the concentration of more and more complement components to the site of inflammation. Complement components are fixed by the immune complexes and ultimately release C5a.

The relevant question, how substance P release from the sensory nerve endings is induced. One possible mechanism is that thrombin cleaves proteinase-activated receptor-1 (PAR-1) on sensory neurons to release substance P, which binds with NK-1R on endothelial cells to cause plasma extravasations. PAR1, which mediates proinflammatory actions of thrombin is known to be expressed by platelets, endothelial

---

cells, fibroblasts, smooth muscle cells, mast cells, neurons and astrocytes (Dery et al., 1998). Additionally substance P can cause degranulation of mast cells to release other mediators of inflammation (Otsuka et al., 1993). Tryptase released from the degranulated mast cells in the vicinity of sensory nerves may cleave PAR2 on sensory nerves to release substance P and CGRP, which also cause plasma extravasations and edema (Steinhoff et al., 2000).

In our model of antibody-induced arthritis we observed complete protection in permanently sympathectomised mice. However, the substance P knockout mice showed partial protection. This is in agreement with the observations reported earlier that release of intraneuronal substance P in joints contributes to severity of the arthritis (Levine et al., 1984).

#### **4.6. IgG1/IgG3 Cryoglobulin Suggesting Lack of Allelic Exclusion**

Isolation and purification of IgG1/IgG3 and Ig $\kappa$  immunoglobulin molecules from the serum of a vasculitis patient resulted in a new subclass of Type I cryoglobulins. The uniqueness in this subclass is the occurrence of Ig $\kappa$  light chain and two IgG heavy chains. The complex did not resolve under SDS-treatment and boiling as revealed by non-reducing SDS-PAGE analysis. Reduction of the complex in the presence of  $\beta$ -mercaptoethanol readily showed that the complex contained two Ig-HC isotypes and one LC isotype. The most likely composition of the cryoglobulin according to our data is the presence of two IgG3-HC, two Ig $\kappa$ -LC and a single IgG1-HC. The Ig chains are most likely covalently attached to each other because their interaction is resistant even to treatment with 6 M guanidium hydrochloride. Covalent bonds between Ig chains are introduced by the cytoplasmic enzyme disulphide-isomerase. Three Ig-H chains

---

comprising the cryoglobulin might have been synthesized within a single plasma B cell clone. The other possibility would be that IgG1, which gives a low intensity band in SDS PAGE might have been added to the IgG3 molecule post synthetically. Expression of IgG1-HC requires class switch recombination. This recombination takes place in the germinal center and depends on antigen-specific cellular interactions and is directed towards specific isotypes through particular cytokines. In the N-terminal part of the  $V_{\kappa 3}$  gene we found 7 out of 51 amino acids, which do not match the germ line sequences known. Most likely this is evidence for somatic hyper mutation driven by antigen. Therefore the B cell must have undergone several rounds of proliferation and checks for affinity maturation using membrane bound immunoglobulin in order to survive selection in the germinal center. Thus the cryoglobulin-producing B cell was selected on specific antigen. We have no experimental evidence that the IgG3/IgG1 cryoglobulin was expressed as a membrane bound molecule, but it would be rather unlikely that the membrane exons would not have been expressed in the cryoglobulin molecule. Notably cryoglobulin complexes from Hepatitis-C-virus-infected patients contain virus particles, suggesting that the virus particles are the antigens stimulating the production of the cryoglobulin. In the case of the cryoglobulin analyzed here, the cryoprecipitation did not depend on antigen and no proteins other than the Ig-chains have been detected in the precipitate. Thus the elusive antigen might not be present in the serum. Alternatively the antigen could have been an infectious agent occurring long ago and the resulting plasma cells are long-lived and produce Ig in the absence of antigen (Manz et al., 1999). Bone marrow analysis of the patient over a period of 8 years did not show any signs of malignant transformation. Moreover, the patients' cryoglobulin producing cells were refractory to treatment with steroids and cytotoxic

---

drugs (Nambiar et al., 2001). In fact treatment resulted in lower  $\gamma$ -globulin titers while the cryoglobulins persisted with the consequence of ongoing complement activation. In such a scenario, the phenotype of the cryoglobulin producing B cell would be most likely a long-lived plasma cell (Manz et al., 1999).

So far, antigens recognized by type I monoclonal cryoglobulins have not been described. Type I cryoglobulinemic patients with non-malignant B-cell clones may suffer from complications involving immune-complex deposition of the cryoglobulins in the kidney and vessels walls. This may lead to renal failure and cutaneous vasculitis (as has been observed in this case). Therefore it will be of importance to define the antigens, which trigger non-malignant B-cell clones. The expression of two antibodies, or like in this case, possibly a trimeric cryoglobulin molecule might lead to B cell clones recognizing two antigens. This may result in autoimmunity and cryoglobulinemia. Lack of allelic exclusion in B cells has been shown before in a fraction of patients suffering from CLL (Rassenti and Kipps, 1997), but it was not shown whether these cells produce any significant amount of antibody. In the murine system a hybridoma derived from autoimmune (NZBxNZB) f1 mice lacked allelic exclusion (Payelle-Brogard et al., 1998). In T cells it is a well-established fact that allelic exclusion in the TCR-locus does not take place all the time (Padovan et al., 1995).

Most probably the B cell producing IgG1/IgG3 cryoglobulin has undergone differentiation without allelic exclusion. Moreover, the plasma B cell has undergone differentiation to the plasma cell stage. The cell in all likely hoods passed all kinds of immunological selections including somatic hypermutation and class switching. We do not know which form of the Ig was expressed on the cell surface in order to

---

differentiate in the bone marrow and which form was recognizing antigen, a prerequisite for entrance and the selection process in the germinal center. Therefore it would be of interest to analyze which antigen is recognized by the cryoglobulin.

#### **4.7. Cryoprecipitation is the Outcome of a Cooperative Intermolecular Interaction**

Cold-induced precipitation of cryoglobulins takes place in two steps. In the first step there is association of molecules leading to dimerization. This step is highly concentration-dependent and there is a critical concentration below which cryoprecipitation does not occur. These features are characteristics of proteins that require a nucleation event.

In the second phase, only dimers but not monomers can undergo a reversible conformation change when the temperature is lowered. The low temperature conformer can precipitate reversibly at low temperature. This process may involve a series of polymeric intermediates.

Cryoprecipitation is clearly dependent on intact interchain disulfide bonds (Scoville et al., 1979). Cleavage of disulfide bonds in the hinge region gives flexibility to the molecule and thus the cryoprecipitation is inhibited.

#### **4.8. Osmolytes and the Chemical Chaperon Cyclodextrin Prevent Cryoprecipitation**

The extraordinary ability of the osmolytes to fold proteins into their native structures both in vitro and tissue-cultured cells suggests that the mechanism involved does not

seriously alter the common forces involved in folding such as electrostatic, hydrogen bonding, hydrophobic interactions and van der Waals interactions (Baskakov and Bolen, 1998; Brown et al., 1997; Welch and Brown, 1996). Osmolytes focus on the peptide backbone and contribute hydrophobic forces necessary for protein folding in dilute aqueous solution. Osmolytes also provide a favorable protein-folding environment in whole cells. It has been shown in tissue culture that the protein folding defects seen in cystic fibrosis can be avoided by addition of osmolytes like TMAO to the culture medium (Welch and Brown, 1996).

The role of cyclodextrin in preventing cryoprecipitation is far more important. The cyclodextrin, a small chemical chaperon prevents cryoprecipitation at mM concentrations, while the cryoglobulin concentration was 3 mg/ml. The relatively small quantity of cyclodextrin preventing large aggregation process taking place during cryoprecipitation, clearly indicates that cyclodextrin acts quite early in the event. Initial nucleation process of cryoglobulin dimerization is prevented by cyclodextrin by binding to apparent hydrophobic patches on the surface of the cryoglobulins. Since, crucial step of dimerization in cryoprecipitation is prevented, no further cold-induced conformational change takes place. It is known that the cryoglobulins do not undergo conformational changes in the monomer form. Hence, results obtained from experiments with the osmolytes and chemical chaperones show that the nucleation kinetics is altered and the cryoglobulin precipitation is completely blocked. In conclusion our experiments show ways to inhibit the cryoglobulin precipitation and to open up new vistas for pharmacological investigations.

## CHAPTER V

### SUMMARY

The pathogenesis of autoimmune diseases is a complex process. Organ specific autoimmune diseases may be caused by the dysregulated reactivity of T lymphocytes with MHC-bound self peptide. In a recent model of murine autoimmune arthritis the transgenic KRN-TCR recognizes a NOD derived MHC class II A<sup>g7</sup> molecule together with a peptide derived from glucose-6-phosphate-isomerase (GPI) leading to inflammatory joint specific tissue destruction. Here we have asked the question what role(s) complement receptors (CR1 and CR2) may play in the pathogenesis of murine autoimmune arthritis. KRN-TCR transgenic mice were bred into the  $Cr2^{-/-}$  mice in order to generate the  $Cr2^{-/-}$ KRN mouse line. Similarly the  $Cr2^{-/-}$  strain was bred into the NOD strain to generate the  $Cr2^{-/-}$ NOD mouse line. Then  $Cr2^{-/-}$ KRN mice were bred to  $Cr2^{-/-}$  NOD mouse line to generate the desired model  $Cr2^{-/-}$ K/BxN. KRN-TCR being heterozygous essentially produced two different phenotypes, sick  $Cr2^{-/-}$ K/BxN (carrier of KRN-TCR) and healthy  $Cr2^{-/-}$ BxN (without KRN-TCR). Analysis of the  $Cr2^{-/-}$  K/BxN in comparison to the original arthritogenic model (K/BxN) revealed a striking result. The onset of the disease in case of the  $Cr2^{-/-}$ K/BxN was earlier compared to K/BxN.

$Cr2^{-/-}$ K/BxN mice lost their climbing ability and showed reduced motility. Loss of *Cr2* resulted in early onset of autoantibody production in  $Cr2^{-/-}$ K/BxN mice, which is in agreement with previous findings (Immunity 1998 Nov; 9(5): 721-31) for a role of *Cr2* in protection against auto reactive B cells. The growth of the  $Cr2^{-/-}$ KBxN mice was retarded due to the severity of the disease compared to the KBxN mice and their

---

littermate controls. In the acute phase of the disease, the Cr2<sup>-/-</sup>K/BxN mice showed high mortality compared to the K/BxN mice and healthy control mice. Hence the pathophysiological consequences of the disease are quite different in Cr2<sup>-/-</sup>K/BxN mice compared to K/BxN mice.

Importance of the nervous system in immune regulation is clearly suggested by innervations of lymphoid tissues by sympathetic nerve fibers. Neuroendocrine regulation of rheumatic diseases is evident from the effects of glucocorticoids, gender, pregnancy, hemiparalysis and stress on clinical aspects of the disease (Bijlsma JWJ, 1999, *Immunol today*). In arthritis, there is a persistent inflammation characterized by micro vascular permeability and neutrophil influx to the joints. In the antibody-induced model of arthritis, the onset of the disease is marked by joint swelling within 24 hours after pathogenic antibody injection in Balb/c mice. Here GPI-antiGPI antibody immune complexes may engage the FcRs onto the synovial tissue and like in the Arthus reaction (Ramos et al., 1992; Sylvestre and Ravetch, 1996) FcγRIII engagement on mast cells leads to degranulation and instantaneous release of proteases.

About 80% of nerves in the joints are nociceptive. About half of the unmyelinated fibers in the joint are sympathetic efferents, which disappear upon sympathectomy. Almost all the nerve endings show immunoreactivity for the neuropeptide substance P (Iwasaki et al., 1995; Mapp et al., 1990). Substance P is a powerful mediator of vascular permeability and is released from the unmyelinated C fibers in the joint. The release of substance P is an early event in immune-complex –mediated injury and could act as an amplifier of the subsequent inflammatory changes. Substance P acts on the vascular endothelium to cause leakage of plasma proteins and thereby increasing the concentration of complement components at the site of inflammation. Complement

---

components are fixed by the immune complexes and ultimately release C5a. In our antibody-induced arthritis, it was observed that transiently sympathectomised mice showed partial protection from disease whereas permanently sympathectomised mice showed complete protection from disease. Similarly the substance P knockout mice showed partial protection from antibody-induced arthritis.

Isolation and purification of IgG1/IgG3 and Ig $\kappa$  immunoglobulin molecules from the serum of a vasculitis patient resulted in a new subclass of Type I cryoglobulins. The uniqueness in this subclass is the occurrence of Ig $\kappa$  light chain and two IgG heavy chains. The cryoglobulin purified from the plasmapheresis samples of a plasmacytoma patient was found to be a type I cryoglobulin of IgG3 isotype.

The biophysical and molecular basis for the reversible precipitation underlying the disease was investigated. Precipitation analysis at different concentrations indicated concentration dependence in the formation of precipitate. Nucleation seemed to be the critical factor for the cryoprecipitation. It was observed that the threshold temperature of cryoglobulin precipitation was lowered by the addition of osmolytes implying a role for hydrophobic patches of the cryoglobulins in nucleation. The results with the osmolytes and chemical chaperone cyclodextrin showed that the nucleation kinetics was altered and the cryoglobulin precipitation was completely blocked.

## CHAPTER VI

### ZUSAMMENFASSUNG

Die Pathogenese von Autoimmunkrankheiten ist ein komplexer Prozess. Organ spezifische Autoimmunerkrankungen können durch T-Lymphozyten, die MHC-gebundene Selbstantigene erkennen, ausgelöst werden. In einem vor kurzem entwickelten Mausmodell für Autoimmune Arthritis, erkennt ein transgener KRN-TCR einen von der Mauslinie NOD stammendes MHC Klasse II A<sup>g7</sup> Molekül zusammen mit einem Peptid das von der Glukose-6-Phosphatisomerase (GPI) stammt, was zu einer gewebsspezifischen Gelenkzerstörung führt. In dieser Arbeit wollten wir die Frage klären, welche Rolle die Komplementrezeptoren CR1 und CR2 bei der Pathogenese der Arthritis spielen. Hierzu wurden KRN-TCR spezifische transgene Mäuse mit Cr2<sup>-/-</sup> Mäuse gekreuzt, um eine Cr2<sup>-/-</sup>KRN Mauslinie zu erzeugen. Außerdem wurde die Cr2<sup>-/-</sup> Linie noch mit der NOD Mauslinie gekreuzt, um in diesem Fall Cr2<sup>-/-</sup>NOD Linie zu erzeugen. Danach wurden diese beiden Mauslinien miteinander gekreuzt, um das gewünschte Cr2<sup>-/-</sup>K/BxN Maus-Modell zu erhalten. Der heterozygote KRN-TCR dieser Mäuse erzeugte zwei verschiedene Phänotypen, kranke Cr2<sup>-/-</sup> K/BxN und gesunde Cr2<sup>-/-</sup>BxN. Die Vergleich der Cr2<sup>-/-</sup>K/BxN Mäuse mit dem Original arthritogenen Mausmodell (K/BxN) zeigte deutliche Unterschiede. Der Beginn der Krankheitssymptome der Cr2<sup>-/-</sup>K/BxN Mäuse war früher, im Vergleich zu K/BxN. Zudem verloren sie ihre Fähigkeit zu klettern und hatten eine reduzierte Beweglichkeit. Der Verlust des Cr2 Genes führte zu einer früheren Autoantikörperproduktion, und spricht für eine protektive Rolle von CD21 bei der Entstehung von autoreaktiven B-Zellen. Weiterhin zeigten die Cr2<sup>-/-</sup>K/BxN Mäuse ein

verzögertes Wachstum, was auf die Schwere der Krankheit zurückzuführen ist. Auch war während der akuten Phase der Krankheit eine erhöhte Mortalität im Vergleich zu K/BxN Mäusen und gesunden Kontrollmäusen zu beobachten. Daher sind die pathophysiologischen Konsequenzen der Krankheit, bei Cr2<sup>-/-</sup>K/BxN Mäusen im Vergleich zu K/BxN Mäusen deutlich verschieden.

Die Innervation von lymphoiden Geweben mit sympathischen Nervenfasern ist ein Zeichen für die Bedeutung des Nervensystems in der Immunregulation. Die neuroendokrine Regulation von rheumatischen Erkrankungen zeigt sich durch die Einflüsse von Glukokortikoiden, Geschlecht, Schwangerschaft, halbseitige Lähmungen und Stress auf die klinischen Parameter der Krankheit (Bijlsma et al., 1999). Rheumatoide Arthritis ist gekennzeichnet durch eine persistierende Entzündungsreaktion, die durch eine erhöhte mikrovaskuläre Permeabilität und das Einwandern von neutrophilen Granulozyten in Gelenke charakterisiert ist. Im dem von uns untersuchten Mausmodell, indem Antikörper Arthritis induzieren, ist die Krankheit durch eine deutliche Schwellung der Gelenke innerhalb von 24 Stunden nach Injektion von Autoantikörpern in gesunde Balb/c Mäuse gekennzeichnet. In diesem Fall könnten GPI-/Anti-GPI Antikörperkomplexe mit FcRezeptoren auf Synovialgewebe interagieren, wie bei der Arthus Reaktion (Ramos et al., 1992; Sylvestre and Ravetch, 1996) bei der die Bindung von Immunkomplexen an Fc $\gamma$ -Rezeptor III zu einer Degranulation von Mastzellen und einer sofortigen Freisetzung von Proteasen führt.

Ungefähr 80% aller Nerven in Gelenken sind hitzesensitiv. Auch sind die Hälfte der nichtmyelinhaltigen Nervenfasern im Gelenk sympathische Fasern, welche nach einer Symphektomie verschwinden. Beinahe alle Nervenendigungen enthalten das Neuropeptid, Substanz P (Iwasaki et al., 1995; Mapp et al., 1990). Substanz P ist ein

---

wirkungsvoller Mediator für erhöhte Gefäßpermeabilität und wird von nichtmyelinhaltigen Typ C Nervenfasern im Gelenk freigesetzt. Die Freisetzung von Substanz P ist ein frühes Ereignis bei der durch Immunkomplexe vermittelten Verletzung der Gelenkoberfläche und kann zu einer Verstärkung von nachfolgenden Entzündungsprozessen führen. Substanz P wirkt auf das Gefäßendothel und führt Komplementaktivierung am Entzündungsherd. Komplementkomponenten werden von Immunkomplexen gebunden und führen dann zur Freisetzung von C5a. Im Mausmodell der Antikörper induzierten Arthritis, machten sich die Beobachtung das transient symphatektomierte Mäuse eine teilweise Protektion gegen Arthritis zeigten, während permanent symphatektomierte Mäuse vollständig vor der Krankheit geschützt waren. In Übereinstimmung mit diesen Beobachtungen zeigten auch Substanz P Knockout Mäuse eine teilweise Protektion gegen Antikörper induzierte Arthritis.

Die Isolierung und Reinigung eines aus IgG1/IgG3 und Igκ Immunoglobulinmolekülen bestehenden Kryoglobulins vom Serum eines Patienten führte zur Entdeckung einer neuen Subklasse von Kryoglobulinen. Das Molekül war durch das Vorhandensein einer Igκ leichten Kette und zwei IgG schweren Ketten gekennzeichnet. Eine Plasmaphorese Probe eines weiteren Patienten der an einem Plasmazytom litt, führte zur Entdeckung eines Typ I IgG3 Kryoglobulins.

In dieser Arbeit untersuchte ich die biophysikalische und molekulare Basis für die reversible Präzipitation, die das zugrundeliegende Merkmal der Krankheit ist. Die Präzipitationsanalyse mit verschiedenen Konzentrationen der Immunoglobulinmoleküle zeigte eine Konzentrationsabhängigkeit für die Formation des Präzipitats. Nukleation ist der kritische Faktor für die Präzipitation. Es konnte gezeigt werden das die kritische Temperaturschwelle für die Kryoglobulinpräzipitation durch Hinzugabe von

---

Osmolyten erniedrigt werden konnte, was für hydrophobe Regionen im Molekülkomplex während des Prozesses der Nukleations spricht. Die Ergebnisse mit den Osmolyten und dem chemischen Chaperon Cyclodextrin zeigten, daß die Nukleationskinetiken sich verändern und der Kryoglobulinpräzipitationsprozess komplett blockiert werden kann.

---

## CHAPTER VII

### REFERENCES

- Acha-Orbea H. and McDevitt H. O. (1987) The first external domain of the nonobese diabetic mouse class II I-A beta chain is unique. *Proc Natl Acad Sci U S A* **84**, 2435-9.
- Ahearn J. M., Fischer M. B., Croix D., Goerg S., Ma M., Xia J., Zhou X., Howard R. G., Rothstein T. L. and Carroll M. C. (1996) Disruption of the Cr2 locus results in a reduction in B-1a cells and in an impaired B cell response to T-dependent antigen. *Immunity* **4**, 251-62.
- Anderson A. C., Nicholson L. B., Legge K. L., Turchin V., Zaghouani H. and Kuchroo V. K. (2000) High frequency of autoreactive myelin proteolipid protein-specific T cells in the periphery of naive mice: mechanisms of selection of the self-reactive repertoire. *J Exp Med* **191**, 761-70.
- Anjum F., Rishi V. and Ahmad F. (2000) Compatibility of osmolytes with Gibbs energy of stabilization of proteins. *Biochim Biophys Acta* **1476**, 75-84.
- Ansel J. C., Brown J. R., Payan D. G. and Brown M. A. (1993) Substance P selectively activates TNF-alpha gene expression in murine mast cells. *J Immunol* **150**, 4478-85.
- Arnett F. C., Edworthy S. M., Bloch D. A., McShane D. J., Fries J. F., Cooper N. S., Healey L. A., Kaplan S. R., Liang M. H., Luthra H. S. and et al. (1988) The American Rheumatism Association 1987 revised criteria for the classification of rheumatoid arthritis. *Arthritis Rheum* **31**, 315-24.
- Baluk P., Bertrand C., Geppetti P., McDonald D. M. and Nadel J. A. (1996) NK1 receptor antagonist CP-99,994 inhibits cigarette smoke-induced neutrophil and eosinophil adhesion in rat tracheal venules. *Exp Lung Res* **22**, 409-18.
- Baskakov I. and Bolen D. W. (1998) Forcing thermodynamically unfolded proteins to fold. *J Biol Chem* **273**, 4831-4.
- Baskakov I. V., Kumar R., Srinivasan G., Ji Y. S., Bolen D. W. and Thompson E. B. (1999) Trimethylamine N-oxide-induced cooperative folding of an intrinsically unfolded transcription-activating fragment of human glucocorticoid receptor. *J Biol Chem* **274**, 10693-6.
- Basu D., Horvath S., O'Mara L., Donermeyer D. and Allen P. M. (2001) Two MHC surface amino acid differences distinguish foreign peptide recognition from autoantigen specificity. *J Immunol* **166**, 4005-11.
- Bijlsma J. W., Cutolo M., Masi A. T. and Chikanza I. C. (1999) The neuroendocrine immune basis of rheumatic diseases. *Immunol Today* **20**, 298-301.
- Bilkei-Gorzo A., Racz I., Michel K. and Zimmer A. (2002) Diminished anxiety- and depression-related behaviors in mice with selective deletion of the Tac1 gene. *J Neurosci* **22**, 10046-52.
- Bohnsack J. F. and Cooper N. R. (1988) CR2 ligands modulate human B cell activation. *J Immunol* **141**, 2569-76.
- Bradbury L. E., Kansas G. S., Levy S., Evans R. L. and Tedder T. F. (1992) The CD19/CD21 signal transducing complex of human B lymphocytes includes the target of antiproliferative antibody-1 and Leu-13 molecules. *J Immunol* **149**, 2841-50.
-

- 
- Brouet J. C., Clauvel J. P., Danon F., Klein M., Seligmann M., Applequist S. E., Dahlstrom J., Jiang N., Molina H. and Heyman B. (1974) Biologic and clinical significance of cryoglobulins. A report of 86 cases. *Am J Med* **57**, 775-88.
- Brown C. R., Hong-Brown L. Q. and Welch W. J. (1997) Correcting temperature-sensitive protein folding defects. *J Clin Invest* **99**, 1432-44.
- Carsetti R., Kohler G. and Lamers M. C. (1995) Transitional B cells are the target of negative selection in the B cell compartment. *J Exp Med* **181**, 2129-40.
- Carson C. W., Beall L. D., Hunder G. G., Johnson C. M. and Newman W. (1993) Serum ELAM-1 is increased in vasculitis, scleroderma, and systemic lupus erythematosus. *J Rheumatol* **20**, 809-14.
- Chen C., Nagy Z., Radic M. Z., Hardy R. R., Huszar D., Camper S. A. and Weigert M. (1995) The site and stage of anti-DNA B-cell deletion. *Nature* **373**, 252-5.
- Choo Q. L., Kuo G., Weiner A. J., Overby L. R., Bradley D. W. and Houghton M. (1989) Isolation of a cDNA clone derived from a blood-borne non-A, non-B viral hepatitis genome. *Science* **244**, 359-62.
- Cooke M. P., Heath A. W., Shokat K. M., Zeng Y., Finkelman F. D., Linsley P. S., Howard M. and Goodnow C. C. (1994) Immunoglobulin signal transduction guides the specificity of B cell-T cell interactions and is blocked in tolerant self-reactive B cells. *J Exp Med* **179**, 425-38.
- D'Amico G. (1998) Renal involvement in hepatitis C infection: cryoglobulinemic glomerulonephritis. *Kidney Int* **54**, 650-71.
- Daugherty D. L., Rozema D., Hanson P. E. and Gellman S. H. (1998) Artificial chaperone-assisted refolding of citrate synthase. *J Biol Chem* **273**, 33961-71.
- Dery O., Corvera C. U., Steinhoff M. and Bunnett N. W. (1998) Proteinase-activated receptors: novel mechanisms of signaling by serine proteases. *Am J Physiol* **274**, C1429-52.
- Edwards J. C., Blades S. and Cambridge G. (1997) Restricted expression of Fc gammaRIII (CD16) in synovium and dermis: implications for tissue targeting in rheumatoid arthritis (RA). *Clin Exp Immunol* **108**, 401-6.
- Edwards J. C. and Cambridge G. (1998) Rheumatoid arthritis: the predictable effect of small immune complexes in which antibody is also antigen. *Br J Rheumatol* **37**, 126-30.
- Ellis M., Rathaus M., Amiel A., Manor Y., Klein A. and Lishner M. (1995) Monoclonal lymphocyte proliferation and bcl-2 rearrangement in essential mixed cryoglobulinaemia. *Eur J Clin Invest* **25**, 833-7.
- Fearon D. T. and Austen K. F. (1977) Activation of the alternative complement pathway due to resistance of zymosan-bound. *Proc Natl Acad Sci U S A* **74**, 1683-7.
- Feldmann M., Brennan F. M. and Maini R. N. (1996a) Rheumatoid arthritis. *Cell* **85**, 307-10.
- Feldmann M., Brennan F. M. and Maini R. N. (1996b) Role of cytokines in rheumatoid arthritis. *Annu Rev Immunol* **14**, 397-440.
- Ferri C., Monti M., La Civita L., Longombardo G., Greco F., Pasero G., Gentilini P., Bombardieri S. and Zignego A. L. (1993) Infection of peripheral blood mononuclear cells by hepatitis C virus in mixed cryoglobulinemia. *Blood* **82**, 3701-4.
- Fingeroth J. D., Heath M. E. and Ambrosino D. M. (1989) Proliferation of resting B cells is modulated by CR2 and CR1. *Immunol Lett* **21**, 291-301.
-

- 
- Firestein G. S., Alvaro-Gracia J. M., Maki R. and Alvaro-Garcia J. M. (1990) Quantitative analysis of cytokine gene expression in rheumatoid arthritis. *J Immunol* **144**, 3347-53.
- Fitzgerald M. (1989) Arthritis and the nervous system. *Trends Neurosci* **12**, 86-7.
- Fyfe A., Holme E. R., Zoma A. and Whaley K. (1987) C3b receptor (CR1) expression on the polymorphonuclear leukocytes from patients with systemic lupus erythematosus. *Clin Exp Immunol* **67**, 300-8.
- Genereau T., Martin A., Lortholary O., Noel V. and Guillevin L. (1998) Temporal arteritis symptoms in a patient with hepatitis C virus associated type II cryoglobulinemia and small vessel vasculitis. *J Rheumatol* **25**, 183-5.
- Gonzalez-Quintal R., Baccala R., Pope R. M. and Theofilopoulos A. N. (1996) Identification of clonally expanded T cells in rheumatoid arthritis using a sequence enrichment nuclease assay. *J Clin Invest* **97**, 1335-43.
- Goodnow C. C. (1996) Balancing immunity and tolerance: deleting and tuning lymphocyte repertoires. *Proc Natl Acad Sci U S A* **93**, 2264-71.
- Goodnow C. C., Crosbie J., Jorgensen H., Brink R. A. and Basten A. (1989) Induction of self-tolerance in mature peripheral B lymphocytes. *Nature* **342**, 385-91.
- Goronzy J. J., Bartz-Bazzanella P., Hu W., Jendro M. C., Walser-Kuntz D. R. and Weyand C. M. (1994) Dominant clonotypes in the repertoire of peripheral CD4+ T cells in rheumatoid arthritis. *J Clin Invest* **94**, 2068-76.
- Guillevin L., Lhote F. and Gherardi R. (1997) The spectrum and treatment of virus-associated vasculitides. *Curr Opin Rheumatol* **9**, 31-6.
- Harrington C. J., Paez A., Hunkapiller T., Mannikko V., Brabb T., Ahearn M., Beeson C. and Goverman J. (1998) Differential tolerance is induced in T cells recognizing distinct epitopes of myelin basic protein. *Immunity* **8**, 571-80.
- Hartley S. B., Crosbie J., Brink R., Kantor A. B., Basten A. and Goodnow C. C. (1991) Elimination from peripheral lymphoid tissues of self-reactive B lymphocytes recognizing membrane-bound antigens. *Nature* **353**, 765-9.
- Hartmann H., Schott P., Polzien F., Mihm S., Uy A., Kaboth U., Pardowitz I. and Ramadori G. (1995) Cryoglobulinemia in chronic hepatitis C virus infection: prevalence, clinical manifestations, response to interferon treatment and analysis of cryoprecipitates. *Z Gastroenterol* **33**, 643-50.
- Hattori M., Buse J. B., Jackson R. A., Glimcher L., Dorf M. E., Minami M., Makino S., Moriwaki K., Kuzuya H., Imura H. and et al. (1986) The NOD mouse: recessive diabetogenic gene in the major histocompatibility complex. *Science* **231**, 733-5.
- Higuchi Y., Ito M., Tajima M., Higuchi S., Miyamoto N., Nishio M., Kawano M., Kusagawa S., Tsurudome M., Sudo A., Katou K., Uchida A. and Ito Y. (1999) Gene expression during osteoclast-like cell formation induced by antifusion regulatory protein-1/CD98/4F2 monoclonal antibodies (MAbs): c-src is selectively induced by anti-FRP-1 MAb. *Bone* **25**, 17-24.
- Hingorani R., Monteiro J., Furie R., Chartash E., Navarrete C., Pergolizzi R. and Gregersen P. K. (1996) Oligoclonality of V beta 3 TCR chains in the CD8+ T cell population of rheumatoid arthritis patients. *J Immunol* **156**, 852-8.
- Hourcade D. E., Mitchell L. M. and Oglesby T. J. (1998) A conserved element in the serine protease domain of complement factor B. *J Biol Chem* **273**, 25996-6000.
- Hummel K. M., Petrow P. K., Franz J. K., Muller-Ladner U., Aicher W. K., Gay R. E., Bromme D. and Gay S. (1998) Cysteine proteinase cathepsin K mRNA is
-

- expressed in synovium of patients with rheumatoid arthritis and is detected at sites of synovial bone destruction. *J Rheumatol* **25**, 1887-94.
- Ikegami H., Makino S., Harada M., Eisenbarth G. S. and Hattori M. (1988) The cataract Shionogi mouse, a sister strain of the non-obese diabetic mouse: similar class II but different class I gene products. *Diabetologia* **31**, 254-8.
- Itonaga I., Fujikawa Y., Sabokbar A., Murray D. W. and Athanasou N. A. (2000) Rheumatoid arthritis synovial macrophage-osteoclast differentiation is osteoprotegerin ligand-dependent. *J Pathol* **192**, 97-104.
- Iwasaki A., Inoue K. and Hukuda S. (1995) Distribution of neuropeptide-containing nerve fibers in the synovium and adjacent bone of the rat knee joint. *Clin Exp Rheumatol* **13**, 173-8.
- Janossy G., Panayi G., Duke O., Bofill M., Poulter L. W. and Goldstein G. (1981) Rheumatoid arthritis: a disease of T-lymphocyte/macrophage immunoregulation. *Lancet* **2**, 839-42.
- Jennette J. C., Falk R. J., Andrassy K., Bacon P. A., Churg J., Gross W. L., Hagen E. C., Hoffman G. S., Hunder G. G., Kallenberg C. G. and et al. (1994) Nomenclature of systemic vasculitides. Proposal of an international consensus conference. *Arthritis Rheum* **37**, 187-92.
- Ji H., Ohmura K., Mahmood U., Lee D. M., Hofhuis F. M., Boackle S. A., Takahashi K., Holers V. M., Walport M., Gerard C., Ezekowitz A., Carroll M. C., Brenner M., Weissleder R., Verbeek J. S., Duchatelle V., Degott C., Benoist C. and Mathis D. (2002) Arthritis critically dependent on innate immune system players. *Immunity* **16**, 157-68.
- Kinoshita T., Lavoie S. and Nussenzweig V. (1985) Regulatory proteins for the activated third and fourth components of complement (C3b and C4b) in mice. II. Identification and properties of complement receptor type 1 (CR1). *J Immunol* **134**, 2564-70.
- Klein L., Klugmann M., Nave K. A., Tuohy V. K. and Kyewski B. (2000) Shaping of the autoreactive T-cell repertoire by a splice variant of self protein expressed in thymic epithelial cells. *Nat Med* **6**, 56-61.
- Kohl J. and Gessner J. E. (1999) On the role of complement and Fc gamma-receptors in the Arthus reaction. *Mol Immunol* **36**, 893-903.
- Korganow A. S., Ji H., Mangialaio S., Duchatelle V., Pelanda R., Martin T., Degott C., Kikutani H., Rajewsky K., Pasquali J. L., Benoist C. and Mathis D. (1999) From systemic T cell self-reactivity to organ-specific autoimmune disease via immunoglobulins. *Immunity* **10**, 451-61.
- Kouskoff V., Korganow A. S., Duchatelle V., Degott C., Benoist C. and Mathis D. (1996) Organ-specific disease provoked by systemic autoimmunity. *Cell* **87**, 811-22.
- Kozono H., Kinoshita T., Kim Y. U., Takata-Kozono Y., Tsunasawa S., Sakiyama F., Takeda J., Hong K. and Inoue K. (1990) Localization of the covalent C3b-binding site on C4b within the complement classical pathway C5 convertase, C4b2a3b. *J Biol Chem* **265**, 14444-9.
- Kumar V., Bhardwaj V., Soares L., Alexander J., Sette A. and Sercarz E. (1995) Major histocompatibility complex binding affinity of an antigenic determinant is crucial for the differential secretion of interleukin 4/5 or interferon gamma by T cells. *Proc Natl Acad Sci U S A* **92**, 9510-4.

- 
- Kurtz C. B., O'Toole E., Christensen S. M. and Weis J. H. (1990) The murine complement receptor gene family. IV. Alternative splicing of Cr2 gene transcripts predicts two distinct gene products that share homologous domains with both human CR2 and CR1. *J Immunol* **144**, 3581-91.
- Lee D. M., Friend D. S., Gurish M. F., Benoist C., Mathis D. and Brenner M. B. (2002) Mast cells: a cellular link between autoantibodies and inflammatory arthritis. *Science* **297**, 1689-92.
- Lerner A. B. and Watson C. J. (1947) Studies of Cryoglobulins: I. Unusual purpura associated with the presence of high concentration of cryoglobulin (cold precipitable serum globulin). *Am J Med Sci* **314**, 410-415.
- Lerner U. H., Jones I. L. and Gustafson G. T. (1987) Bradykinin, a new potential mediator of inflammation-induced bone resorption. Studies of the effects on mouse calvarial bones and articular cartilage in vitro. *Arthritis Rheum* **30**, 530-40.
- Levine J. D., Clark R., Devor M., Helms C., Moskowitz M. A. and Basbaum A. I. (1984) Intraneuronal substance P contributes to the severity of experimental arthritis. *Science* **226**, 547-9.
- Levine J. D., Coderre T. J., Helms C. and Basbaum A. I. (1988) Beta 2-adrenergic mechanisms in experimental arthritis. *Proc Natl Acad Sci USA* **85**, 4553-6.
- Levine J. D., Dardick S. J., Roizen M. F., Helms C. and Basbaum A. I. (1986) Contribution of sensory afferents and sympathetic efferents to joint injury in experimental arthritis. *J Neurosci* **6**, 3423-9.
- Liu G. Y., Fairchild P. J., Smith R. M., Prowle J. R., Kioussis D. and Wraith D. C. (1995) Low avidity recognition of self-antigen by T cells permits escape from central tolerance. *Immunity* **3**, 407-15.
- Luber-Narod J., Kage R. and Leeman S. E. (1994) Substance P enhances the secretion of tumor necrosis factor-alpha from neuroglial cells stimulated with lipopolysaccharide. *J Immunol* **152**, 819-24.
- Luxembourg A. T. and Cooper N. R. (1994a) Modulation of signaling via the B cell antigen receptor by CD21, the receptor for C3dg and EBV. *J Immunol* **153**, 4448-57.
- Luxembourg A. T. and Cooper N. R. (1994b) T cell-dependent, B cell-activating properties of antibody-coated small latex beads. A new model for B cell activation. *J Immunol* **153**, 604-14.
- Maccioni M., Zeder-Lutz G., Huang H., Ebel C., Gerber P., Hergueux J., Marchal P., Duchatelle V., Degott C., van Regenmortel M., Benoist C. and Mathis D. (2002) Arthritogenic monoclonal antibodies from K/BxN mice. *J Exp Med* **195**, 1071-7.
- Mandik-Nayak L., Bui A., Noorchashm H., Eaton A. and Erikson J. (1997) Regulation of anti-double-stranded DNA B cells in nonautoimmune mice: localization to the T-B interface of the splenic follicle. *J Exp Med* **186**, 1257-67.
- Manz R. A., Cassese G., Thiel A., Radbruch A., Alexander A., Steinmetz M., Barritault D., Frangione B., Franklin E. C., Hood L. and Buxbaum J. N. (1999) Long-lived plasma cells survive independent of antigen. *Curr Top Microbiol Immunol* **246**, 71-4.
- Mapp P. I., Kidd B. L., Gibson S. J., Terry J. M., Revell P. A., Ibrahim N. B., Blake D. R. and Polak J. M. (1990) Substance P-, calcitonin gene-related peptide- and C-flanking peptide of neuropeptide Y-immunoreactive fibres are present in normal
-

- synovium but depleted in patients with rheumatoid arthritis. *Neuroscience* **37**, 143-53.
- Matsumoto A. K., Kopicky-Burd J., Carter R. H., Tuveson D. A., Tedder T. F. and Fearon D. T. (1991) Intersection of the complement and immune systems: a signal transduction complex of the B lymphocyte-containing complement receptor type 2 and CD19. *J Exp Med* **173**, 55-64.
- Matsumoto A. K., Martin D. R., Carter R. H., Klickstein L. B., Ahearn J. M. and Fearon D. T. (1993) Functional dissection of the CD21/CD19/TAPA-1/Leu-13 complex of B lymphocytes. *J Exp Med* **178**, 1407-17.
- Matsumoto I., Staub A., Benoist C. and Mathis D. (1999) Arthritis provoked by linked T and B cell recognition of a glycolytic enzyme. *Science* **286**, 1732-5.
- Miller J. F. and Morahan G. (1992) Peripheral T cell tolerance. *Annu Rev Immunol* **10**, 51-69.
- Mitchell D. M. and Fries J. F. (1982) An analysis of the American Rheumatism Association criteria for rheumatoid arthritis. *Arthritis Rheum* **25**, 481-7.
- Molina H., Kinoshita T., Inoue K., Carel J. C. and Holers V. M. (1990) A molecular and immunochemical characterization of mouse CR2. Evidence for a single gene model of mouse complement receptors 1 and 2. *J Immunol* **145**, 2974-83.
- Molina H., Kinoshita T., Webster C. B. and Holers V. M. (1994) Analysis of C3b/C3d binding sites and factor I cofactor regions within mouse complement receptors 1 and 2. *J Immunol* **153**, 789-95.
- Monti G., Galli M., Invernizzi F., Pioltelli P., Saccardo F., Monteverde A., Pietrogrande M., Renoldi P., Bombardieri S., Bordin G. and et al. (1995) Cryoglobulinaemias: a multi-centre study of the early clinical and laboratory manifestations of primary and secondary disease. GISC. Italian Group for the Study of Cryoglobulinaemias. *Qjm* **88**, 115-26.
- Mulligan M. S. and Ward P. A. (1992) Immune complex-induced lung and dermal vascular injury. Differing requirements for tumor necrosis factor-alpha and IL-1. *J Immunol* **149**, 331-9.
- Musset L., Diemert M. C., Taibi F., Thi Huong Du L., Cacoub P., Leger J. M., Boissy G., Gaillard O. and Galli J. (1992) Characterization of cryoglobulins by immunoblotting. *Clin Chem* **38**, 798-802.
- Musset L., Duarte F., Gaillard O., Du L. T., Bilala J., Galli J. and Preud'homme J. L. (1994) Immunochemical characterization of monoclonal IgG containing mixed cryoglobulins. *Clin Immunol Immunopathol* **70**, 166-70.
- Nakamura M. and Ferreira S. H. (1987) A peripheral sympathetic component in inflammatory hyperalgesia. *Eur J Pharmacol* **135**, 145-53.
- Nambiar M. P., Enyedy E. J., Fisher C. U., Warke V. G., Juang Y. T. and Tsokos G. C. (2001) Dexamethasone modulates TCR zeta chain expression and antigen receptor-mediated early signaling events in human T lymphocytes. *Cell Immunol* **208**, 62-71.
- Nemerow G. R., McNaughton M. E. and Cooper N. R. (1985) Binding of monoclonal antibody to the Epstein Barr virus (EBV)/CR2 receptor induces activation and differentiation of human B lymphocytes. *J Immunol* **135**, 3068-73.
- Norvell A., Birkeland M. L., Carman J., Sillman A. L., Wechsler-Reva R. and Monroe J. G. (1996) Use of isolated immature-stage B cells to understand negative selection and tolerance induction at the molecular level. *Immunol Res* **15**, 191-207.

- 
- Norvell A., Mandik L. and Monroe J. G. (1995) Engagement of the antigen-receptor on immature murine B lymphocytes results in death by apoptosis. *J Immunol* **154**, 4404-13.
- Norvell A. and Monroe J. G. (1996) Acquisition of surface IgD fails to protect from tolerance-induction. Both surface IgM- and surface IgD-mediated signals induce apoptosis of immature murine B lymphocytes. *J Immunol* **156**, 1328-32.
- Nossal G. J. (1994) Negative selection of lymphocytes. *Cell* **76**, 229-39.
- Otsuka H., Ohkubo K., Seki H., Ohnishi M. and Fujikura T. (1993) Mast cell quantitation in nasal polyps, sinus mucosa and nasal turbinate mucosa. *J Laryngol Otol* **107**, 418-22.
- Padovan E., Giachino C., Cella M., Valitutti S., Acuto O. and Lanzavecchia A. (1995) Normal T lymphocytes can express two different T cell receptor beta chains: implications for the mechanism of allelic exclusion. *J Exp Med* **181**, 1587-91.
- Pascual D. W. and Bost K. L. (1990) Substance P production by P388D1 macrophages: a possible autocrine function for this neuropeptide. *Immunology* **71**, 52-6.
- Payelle-Brogard B., Ragimbeau J., Avrameas S. and Christodoulou C. (1998) Immunoglobulin double isotype-producing hybridomas isolated from an autoimmune (NZB x NZW)F1 mouse. *Hybridoma* **17**, 289-97.
- Peccoud J., Dellabona P., Allen P., Benoist C. and Mathis D. (1990) Delineation of antigen contact residues on an MHC class II molecule. *Embo J* **9**, 4215-23.
- Pettit A. R., Ji H., von Stechow D., Muller R., Goldring S. R., Choi Y., Benoist C. and Gravallese E. M. (2001) TRANCE/RANKL knockout mice are protected from bone erosion in a serum transfer model of arthritis. *Am J Pathol* **159**, 1689-99.
- Prodeus A. P., Goerg S., Shen L. M., Pozdnyakova O. O., Chu L., Alicot E. M., Goodnow C. C. and Carroll M. C. (1998) A critical role for complement in maintenance of self-tolerance. *Immunity* **9**, 721-31.
- Ramos B. F., Zhang Y., Angkachatchai V. and Jakschik B. A. (1992) Mast cell mediators regulate vascular permeability changes in Arthus reaction. *J Pharmacol Exp Ther* **262**, 559-65.
- Rassenti L. Z. and Kipps T. J. (1997) Lack of allelic exclusion in B cell chronic lymphocytic leukemia. *J Exp Med* **185**, 1435-45.
- Ravetch J. V. and Bolland S. (2001) IgG Fc receptors. *Annu Rev Immunol* **19**, 275-90.
- Ridgway W. M., Fasso M. and Fathman C. G. (1999) A new look at MHC and autoimmune disease. *Science* **284**, 749, 751.
- Rozema D. and Gellman S. H. (1996) Artificial chaperone-assisted refolding of carbonic anhydrase B. *J Biol Chem* **271**, 3478-87.
- Santoro M. M., Liu Y., Khan S. M., Hou L. X. and Bolen D. W. (1992) Increased thermal stability of proteins in the presence of naturally occurring osmolytes. *Biochemistry* **31**, 5278-83.
- Santulli-Marotto S., Retter M. W., Gee R., Mamula M. J. and Clarke S. H. (1998) Autoreactive B cell regulation: peripheral induction of developmental arrest by lupus-associated autoantigens. *Immunity* **8**, 209-19.
- Scoville C. D., Abraham G. N. and Turner D. H. (1979) Spectroscopic and kinetic analysis of a monoclonal IgG cryoglobulin. Effect of mild reduction on cryoprecipitation. *Biochemistry* **18**, 2610-5.
- Solomon S., Kolb C., Mohanty S., Jeisy-Walder E., Preyer R., Schollhorn V. and Illges H. (2002) Transmission of antibody-induced arthritis is independent of
-

- complement component 4 (C4) and the complement receptors 1 and 2 (CD21/35). *Eur J Immunol* **32**, 644-51.
- Somer T. and Finegold S. M. (1995) Vasculitides associated with infections, immunization, and antimicrobial drugs. *Clin Infect Dis* **20**, 1010-36.
- Somero G. N. (1986) Protons, osmolytes, and fitness of internal milieu for protein function. *Am J Physiol* **251**, R197-213.
- Steinhoff M., Vergnolle N., Young S. H., Tognetto M., Amadesi S., Ennes H. S., Trevisani M., Hollenberg M. D., Wallace J. L., Caughey G. H., Mitchell S. E., Williams L. M., Geppetti P., Mayer E. A. and Bunnett N. W. (2000) Agonists of proteinase-activated receptor 2 induce inflammation by a neurogenic mechanism. *Nat Med* **6**, 151-8.
- Struyk L., Hawes G. E., Dolhain R. J., van Scherpenzeel A., Godthelp B., Breedveld F. C. and van den Elsen P. J. (1995) Evidence for selective usage of amino acids within CDR3 regions of T cell receptor V genes derived from synovial tissue-infiltrating CD4+CD45RO+ T-lymphocytes. *Scand J Rheumatol Suppl* **101**, 147-52.
- Sylvestre D., Clynes R., Ma M., Warren H., Carroll M. C. and Ravetch J. V. (1996) Immunoglobulin G-mediated inflammatory responses develop normally in complement-deficient mice. *J Exp Med* **184**, 2385-92.
- Sylvestre D. L. and Ravetch J. V. (1996) A dominant role for mast cell Fc receptors in the Arthus reaction. *Immunity* **5**, 387-90.
- Takayanagi H., Iizuka H., Juji T., Nakagawa T., Yamamoto A., Miyazaki T., Koshihara Y., Oda H., Nakamura K. and Tanaka S. (2000) Involvement of receptor activator of nuclear factor kappaB ligand/osteoclast differentiation factor in osteoclastogenesis from synoviocytes in rheumatoid arthritis. *Arthritis Rheum* **43**, 259-69.
- Targoni O. S. and Lehmann P. V. (1998) Endogenous myelin basic protein inactivates the high avidity T cell repertoire. *J Exp Med* **187**, 2055-63.
- Theofilopoulos A. N. and Dixon F. J. (1980) Immune complexes in human diseases: a review. *Am J Pathol* **100**, 529-94.
- Thomas R. and Lipsky P. E. (1996a) Could endogenous self-peptides presented by dendritic cells initiate rheumatoid arthritis? *Immunol Today* **17**, 559-64.
- Thomas R. and Lipsky P. E. (1996b) Dendritic cells: origin and differentiation. *Stem Cells* **14**, 196-206.
- van den Berg W. B. and van Lent P. L. (1996) The role of macrophages in chronic arthritis. *Immunobiology* **195**, 614-23.
- von Boehmer H. (1994) Positive selection of lymphocytes. *Cell* **76**, 219-28.
- Walport M. J. and Lachmann P. J. (1988) Erythrocyte complement receptor type 1, immune complexes, and the rheumatic diseases. *Arthritis Rheum* **31**, 153-8.
- Wang A. and Bolen D. W. (1997) A naturally occurring protective system in urea-rich cells: mechanism of osmolyte protection of proteins against urea denaturation. *Biochemistry* **36**, 9101-8.
- Welch W. J. and Brown C. R. (1996) Influence of molecular and chemical chaperones on protein folding. *Cell Stress Chaperones* **1**, 109-15.
- Wilson B. S., Platt J. L. and Kay N. E. (1985) Monoclonal antibodies to the 140,000 mol wt glycoprotein of B lymphocyte membranes (CR2 receptor) initiates proliferation of B cells in vitro. *Blood* **66**, 824-9.

- Wilson J. G., Ratnoff W. D., Schur P. H. and Fearon D. T. (1986) Decreased expression of the C3b/C4b receptor (CR1) and the C3d receptor (CR2) on B lymphocytes and of CR1 on neutrophils of patients with systemic lupus erythematosus. *Arthritis Rheum* **29**, 739-47.
- Wintrobe M. M. and Buell M. V. (1933) Hyperproteinemia associated with multiple myeloma. *Bulletin of the John Hopkins Hospital* **52**.
- Wipke B. T. and Allen P. M. (2001) Essential role of neutrophils in the initiation and progression of a murine model of rheumatoid arthritis. *J Immunol* **167**, 1601-8.
- Woessner J. F., Jr. and Gunja-Smith Z. (1991) Role of metalloproteinases in human osteoarthritis. *J Rheumatol Suppl* **27**, 99-101.
- Wong V. S., Egner W., Eley T., Brown D. and Alexander G. J. (1996) Incidence, character and clinical relevance of mixed cryoglobulinaemia in patients with chronic hepatitis C virus infection. *Clin Exp Immunol* **104**, 25-31.
- Yancey P. H., Clark M. E., Hand S. C., Bowlus R. D. and Somero G. N. (1982) Living with water stress: evolution of osmolyte systems. *Science* **217**, 1214-22.
- Zvaifler N. J., Steinman R. M., Kaplan G., Lau L. L. and Rivelis M. (1985) Identification of immunostimulatory dendritic cells in the synovial effusions of patients with rheumatoid arthritis. *J Clin Invest* **76**, 789-800.